The immunogenic effects of a potentially allergenic protein of *Acer negundo*

Marta Alexandra Correia de Sousa

Mestrado em Biologia Celular e Molecular

Departamento de Biologia

2017

Orientador
Susana Pereira, Professora associada, Faculdade de Ciências da Universidade do Porto

Coorientador
Ilda Noronha, Professora associada convidada, Faculdade de Ciências da Universidade do Porto

Coorientador
Paula Veríssimo, Professora auxiliar, Faculdade de Ciências e Tecnologia da Universidade de Coimbra

Declaração de autoria

Eu, Marta Alexandra Correia de Sousa, aluna com o número mecanográfico 201102799 do mestrado de Biologia Celular e Molecular da edição de 2016/2017, declaro por minha honra que sou a autora da totalidade do texto apresentado, não apresentando texto plagiado, e tomei conhecimento das consequências de uma situação de plágio.

Porto, 30 de outubro de 2017

Marta Sousa

Agradecimentos

Sendo este o último passo de um projeto que se revelou bastante desafiante, gostaria de agradecer às minhas orientadoras, professora Susana, professora Ilda e professora Paula, e ao professor Pissarra por terem apoiado e acreditado neste projeto e por terem disponibilizado todos os recursos possíveis e impossíveis para a realização do mesmo apesar do esforço que requereu. Muito obrigada pelo voto de confiança e por terem permitido que evoluísse para além das minhas expectativas!

Gostaria de agradecer em especial à professora Paula por ter aceite este projeto ambicioso; por todo o conhecimento que me passou, pelo apoio, cuidado e disponibilidade que sempre demonstrou, principalmente no período que estive em Coimbra. Obrigada pelo positivismo constante, foi uma força extra para ultrapassar os momentos mais desafiantes!

Gostaria de agradecer também a todos que me acolheram no CNC, mas principalmente à Isabel Nunes por tudo o que me ensinou e pelo apoio incansável que me deu (e às minhas meninas)! Obrigada também à Dra Rosário pela companhia e pelo apoio dado nas minhas últimas semanas em Coimbra.

Obrigada a todas as pessoas (caros vizinhos do 2.62 e do 2.60 principalmente) que partilharam comigo o dia-a-dia no piso 2 do Departamento de Biologia no último ano e que contribuíram para dias, e principalmente almoços, mais animados.

Ao Bruno, obrigada por todo o apoio desde o meu primeiro no 2.61! Foste (e ainda és) incansável! Obrigada por tudo, não só pelo que me ensinaste e ensinas (apesar da distância!) mas pela amizade e pela paciência! E por puxares sempre mais por mim!

Por último, mas não menos importante gostaria de agradecer à minha família pelo apoio e compreensão neste período tão intenso.

Ao João, obrigada por me fazeres rir… Principalmente quando não me apetece! Obrigada por me apoiares em todas as fases ao longo dos últimos anos, mas principalmente pela tua paciência! E pelos miminhos em forma de comida!!

Gostaria de agradecer e dedicar este trabalho à pessoa que sempre mais exigiu de mim, mas que sempre me apoiou incondicionalmente. Sem ti este meu sonho não se teria realizado certamente, obrigada Mãe! Obrigada por tudo o que me ensinas, pela mulher que és e pela pessoa que me tornaste!

Obrigada também a Coimbra, por tudo o que essa cidade representa na minha vida académica e pessoal. Foi sem dúvida uma experiência que fez valer a pena todos os sacrifícios.

Resumo

As doenças respiratórias como a asma e a rinite alérgica estão a aumentar mundialmente. O pólen, apesar do seu baixo potencial alergénico, é conhecido como um dos maiores elicitadores de reações inflamatórias nas vias respiratórias devido ao seu potencial proteolítico. Nas últimas décadas tem aumentado o interesse em identificar as proteínas do pólen de forma a perceber os mecanismos moleculares que estão na base da reação alérgica e desenvolver novas terapias com melhores resultados terapêuticos. Dentro dessa linha de pensamento, este projeto teve como objetivo explorar a imunogenicidade de uma proteína potencialmente alergénica do pólen de *Acer negundo* – a Calreticulina. Resultados preliminares revelaram que esta proteína pode induzir uma resposta alérgica típica mediada por imunoglobulinas E, no entanto, neste trabalho quisemos verificar se esta proteína poderia provocar o mesmo efeito através de outros mecanismos não mediados por estas imunoglobulinas e não dependentes de atividades proteolíticas do extrato de pólen dado a função da sua homóloga animal na resposta imune.

Para testar esta hipótese foi produzida uma proteína recombinante parcial. Adicionalmente, o extrato proteico do pólen de *A. negundo* foi também caracterizado relativamente à sua potencial atividade proteolítica e, consequentemente, os seus efeitos imunogénicos. O potencial proteolítico e conteúdo proteico foram caracterizados através de zimografia, ensaios de proteólise específica de péptidos sintéticos e SDS-PAGE, determinando que após hidratação o pólen de *A. negundo* liberta protéases de alto peso molecular pertencentes à família das metaloproteases e outras aminopeptidades dependentes de zinco.

Os efeitos imunogénicos foram determinados em culturas de epitélio pulmonar da linhagem celular A549, tendo sido verificado que o destacamento celular se correlacionava com a concentração dos extratos polínicos e com os períodos de incubação. Foi também verificado que, contrariamente ao expectado, a Calreticulina recombinante por si só não afetou significativamente as culturas celulares. No entanto, esta aumentou os efeitos prejudiciais dos extratos polínicos nas culturas epiteliais, uma vez que foi verificado um aumento de citocinas libertadas e de destacamento celular em células expostas a extratos combinados comparativamente às células expostas a extratos polínicos isolados.

Os resultados obtidos neste trabalho indicam que a Calreticulina de *A. negundo* tem um papel adjuvante nas respostas pro-inflamatórias em contexto de dano epitelial, no entanto estudos adicionais devem ser realizados para confirmar se se trata de consequências de interações da proteína com recetores celulares e quais os recetores e mecanismos especificamente envolvidos.

Abstract

Respiratory diseases such as asthma and allergic rhinitis are increasing worldwide. Despite their low allergenic potential, pollen grains are known to be one of the major elicitors of inflammatory reactions in the airway mainly due to their proteolytic potential. In the past decades, there has been an increasing interest in identifying potentially allergenic single proteins of pollen total protein extracts to better understand the molecular mechanisms behind an allergic reaction and develop new improved therapies that might have better outcomes. In that line of thought, this project proposed to explore the immunogenicity of a potential allergenic protein of *Acer negundo*'s pollen grains - Calreticulin. Preliminary results revealed that calreticulin can induce an allergic response through IgE-mediated mechanisms; however, we wanted to explore if this protein could provoke an allergic reaction through non-IgE mediated, non-proteolytic mechanisms given the role of its mammalian homologue in the immune response.

To test this hypothesis a partial recombinant protein was produced. Moreover, *A. negundo*'s pollen protein extract was characterized relatively to its potential proteolytic activity and immunogenic effects. The proteolytic potential and protein content of *A. negundo*'s pollen was characterized through zymography, peptide proteolysis assays and SDS-PAGE. It was determined that after being hydrated *A. negundo*'s pollen releases high molecular weight proteases, particularly of the metalloprotease family and other zinc-dependent aminopeptidases.

Immunogenic effects were assessed in the lung epithelial cell line A549, and we verified that cellular detachment correlated with pollen protein extract concentration and incubation periods. We also verified that, contrarily to what was expected, recombinant calreticulin by itself did not affect the epithelial cell culture significantly. However, it increased the damaging effects of pollen extracts in lung epithelial cells since an increase in cellular detachment and released cytokines in combined extracts was verified comparatively to isolated pollen extracts stimuli.

The outcome of this project indicates that *A. negundo*'s calreticulin plays an adjuvant role in pro-inflammatory responses in context of epithelial damage; however further studies should be performed to confirm if it was a consequence of protein's interactions with cell receptors and which receptors and mechanism are specifically involved.

Key-words

Allergy; *Acer negundo*; Calreticulin; pollen proteases; lung epithelium; pro-inflammatory cytokines; inflammation; alveolar barrier disruption.

Index

List of tables

List of figures

List of abbreviations

2D- PAGE	Two-Dimensional Polyacrylamide Gel Electrophoresis
AJ	Adherens junctions
Akt	Protein kinase B
AMC	7-amino-4-methylcoumarin
*An*CRT	*Acer negundo*'s Calreticulin
AP	Alkaline Phosphatase
APC	Antigen-presenting cell
ASL	Airway surface liquid
*At*CRT1a	*Arabidopsis thaliana*'s Calreticulin isoform 1a
*At*CRT1b	*Arabidopsis thaliana*'s Calreticulin isoform 1b
BALT	Bronchus-associated lymphoid tissue
BOC	Butyloxycarbonyl
bp	Base-pair
BLASTN	Nucleotide Basic Local Alignment Search Tool
BLASTX	Protein Basic Local Alignment Search Tool
BSA	Bovine serum albumin
Bz	Benzoyl
CBA	Cytometric bead array
CCL20	Chemokine (C-C motif) ligand 20
CD3	Cluster of differentiation 3
CD4	Cluster of differentiation 4
CD47	Cluster of differentiation 47
CD8	Cluster of differentiation 8
cDNA	Complementary DNA
CIAP	Calf intestine alkaline phosphatase
CLAP	Chymostatin, leupeptin, antipain and pepstatin
CRT(1a/1b/3)	Calreticulin 1a/1b/3
DAMPs	Damage- associated molecular patterns
DC	Dendritic cell
DNA	Deoxyribonucleic acid
DTT	Dithiothreitol
E-64	N-[N-(L-3-trans-carboxyirane-2-carbonyl)-L-leucyl]-agmatine

ECM	Extracellular matrix
EDTA	Ethylenediamine tetra acetic acid
EFR	Elf18 responsive EF-Tu receptor
EGFR	Epithelial growth factor receptor
EMT	Epithelial-to-mesenchymal transition
ER	Endoplasmic reticulum
ERK	Extracellular signal-regulated kinase
FBS	Fetal bovine serum
FCξR	Fragment crystallisable region ξ receptor
gDNA	Genomic DNA
GM-CSF	Granulocyte-macrophage colony-stimulating factor
HC	High concentration
IFN-γ	Interferon γ
IgA	Immunoglobulin A
IgE	Immunoglobulin E
IL-1β	Interleukin 1 β
IL-1R	Interleukin 1 receptor
IL-4	Interleukin 4
IL-5	Interleukin 5
IL-6	Interleukin 6
IL-8	Interleukin 8
IL-9	Interleukin 9
IL-10	Interleukin 10
IL-13	Interleukin 13
IMAC	Immobilized Metal Affinity Chromatography
IPTG	Isopropyl-β-D-thiogalactoside
IRF	Interferon-regulatory factor
Kan	Kanamycin
kDa	Kilodaltons
LB	Luria Broth
LC	Low concentration
LIC	Ligation independent cloning
LRP1/CD91	Lipoprotein receptor- related protein/ Cluster of differentiation 91
MALDI	Matrix-assisted laser desorption/ ionization

MAPK	Mitogen activated protein kinase
MCL	Maximum composite likelihood
MCP i	Monocyte-chemotactic protein i
MEM	Eagle's minimum essential medium
MHC	Major histocompatibility complex
MLH	Maximum-likelihood
mRNA	Messenger RNA
MS	Mass spectrometry
MW	Molecular weight
NF-κB	Nuclear factor kappa-light-chain-enhancer of activated B cells
Ni-NTA	Nickel- nitrilotriacetic acid
NJ	Neighbour-joining
NO	Nitric oxide
OD	Optical density
PAMPs	Pathogen- associated molecular patterns
PBS	Phosphate saline buffer
PCR	Polymerase chain reaction
PDB	Protein Data Bank
PFA	Paraformaldehyde
PfCRT	Partial form Calreticulin
pI	Point isoelectric
PI3k	Phosphoinositide 3-kinase
PMF	Peptide mass fingerprinting
PMSF	Phenylmethanesulfonyl fluoride
PRR	Pathogen recognition receptor
PVDF	Polyvinylidene fluoride
qRT-PCR	Quantitative reverse transcription-polymerase chain reaction
RAR	Rapidly adapting receptor
rCRT	Recombinant Calreticulin
RFU	Relative fluorescence unit
RIG-I	Retinoic acid-inducible gene I
RLM-RACE	RNA ligase mediated-rapid amplification of cDNA ends
RNA	Ribonucleic acid
RppH	RNA-Pyrophosphohydrolase

RT	Room temperature
Rpm	Rotations per minute
SAR	Slowly adapting receptor
SB	Sodium borate
SDS	Sodium dodecyl sulphate
SDS-PAGE	Sodium dodecyl sulphate polyacrylamide gel electrophoresis
SLP1	Secretory leukoprotease inhibitor 1
SP	Surfactant protein
SRA	Scavenger receptor A
ssDNA	Single-stranded DNA
TBS	Tris-buffered saline
TBS-T	TBS-Tween
T_C	Cytotoxic T cells
TCR	T-cell receptor
TGF-β	Transforming growth factor type β
T_H	Helper T cells
T_H1	Type 1 helper T cells
T_H2	Type 2 helper T cells
TJ	Tight junction
TLCK	Tosyl-L-lysis-chloromethane hydrochloride
TLR-4	Toll-like receptor-4
TNF-α	Tumour necrosis factor α
TPCK	Tosyl phenylalanyl chloromethyl ketone
tRNA	Transfer RNA
TSP-1	Thrombospondin-1
UV	Ultra-violet
VEGF	Vascular endothelial growth factor
ZO-1	Zonula occludens-1

Nucleotide Abbreviations	
Nucleotides	**One-letter Code**
Adenosine	A
Cytosine	C
Guanine	G
Thymine	T

Amino-acid Abbreviations		
Amino-acid	**Three-letter Code**	**One-letter Code**
Alanine	Ala	A
Arginine	Arg	R
Asparagine	Asn	N
Aspartic acid	Asp	D
Glutamic acid	Glu	E
Glutamine	Gln	Q
Glycine	Gly	G
Histidine	His	H
Isoleucine	Ile	I
Leucine	Leu	L
Lysine	Lys	K
Methionine	Met	M
Phenylalanine	Phe	F
Proline	Pro	P
Serine	Ser	S
Threonine	Thr	T
Tryptophan	Trp	W
Tyrosine	Tyr	Y
Valine	Val	V

Chapter I – Introduction

The respiratory system

The respiratory apparatus

The respiratory apparatus is composed by several organs mainly responsible for oxygen absorption and carbon dioxide elimination. It can be distinguished by lungs and respiratory airways, which are constituted by the nasal cavities, pharynx, larynx, trachea and bronchioles. The respiratory airway is subdivided in upper and lower respiratory tract that correspond to structures between the nose - larynx (upper) and larynx – visceral pleura (lower). The lower part is a branched system of airways that act as conductive (trachea and bronchial tree subdivided in bronchioles) or respiratory tracts (bronchi and alveolar ducts composed by alveolar sacs), depending if they conduct air or execute gas exchanges with circulating blood. The last of purely conductive airways are known as terminal bronchioles, beyond which are further branches of transitional bronchioles that can perform both functions.

The inhaled air harbours several damaging agents such as irritants, infectious organisms and allergenic substances, which increase the damage susceptibility of the delicate respiratory epithelium. As one of the first barriers of defence against exogenous substances, the respiratory airway performs many functions other than gas conduction, *e.g.* humidification and elimination of injurious substances from circulating air; although, these functions are dependent on branching patterns, integrity and composition of structural components and interaction between them and neural and immunocompetent elements of the airways. The more distal respiratory area is protected from these agents by defence mechanisms that are a result of a coordinated response of the different constituents of the airway wall. The nervous elements produce nervous signals that result in bronchoconstriction and involuntary cough to eliminate secreted substances (*i.e.* mucus, lysozyme, lactoferrin and IgA) with the aid of ciliary activity. Additionally, epithelial cells can recruit and modulate immune cells activity through the release of chemotactic substance that consequently results in immune reactions, another defence mechanism of respiratory tracts (Canning *et al*., 2014; Ganesan *et al*., 2013; Georas and Rezaee, 2014; Jones, 2012).

The airway wall and its components – epithelial elements

The airway wall is generally composed by a coating mucosa of surface epithelium, basement membrane and supporting elastic lamina propria; a submucosa containing glands, muscle and cartilage; and a thin adventitial coat. Although, the composition of

the surface epithelium differs depending on the structure. The upper respiratory part has a pseudostratified epithelium constituted by ciliated, columnar cells and sporadic mucus-secreting (Goblet) cells, except in the anterior nares which has stratified epithelium constituted by keratinising squamous cells. The lower portion is also pseudostratified composed by columnar ciliated cells as well, becoming simple cuboidal in peripheral airways. Contrarily, the larynx is composed by stratified squamous epithelium either keratinized or not (Jeffery, 1983).

Despite the similar organization between upper and lower part of the airways, the epithelial cells that compose the epithelium vary. The epithelium of conducting airways can be composed by distinct epithelial cells with specific functions, *i.e.* basal, ciliated, mucous (Goblet), serous, Clara or neuroendocrine cells. The basal cells contribute to the pseudostratified appearance of epithelium in the large bronchi and trachea; however, some authors also considered them as major stem cells for mucous and ciliated cells, highlighting their proliferative and reparative role in the lung epithelium (Ayers and Jeffery, 1988). Mucous cells are responsible for mucus production and secretion with optimum viscoelastic profile to maintain the mucociliary clearance performed by ciliated cells (Saetta *et al*., 2000). The function of serous cells is yet to be fully defined, but previous studies performed suggested a key role in mucosal defences due to their secretion of anti-fungi and anti-bacterial compounds (Wine, 1999). It was also evidenced that these cells differentiate into mucous cells after damage (Jeffery and Reid, 1981). Clara cells are usually restricted to human's terminal bronchioles and are considered as major stem cells of ciliated and mucous cells in small airways (Ayers and Jeffery, 1988). Additionally, it was suggested that Clara cells play a key role in the production of an hypophase component of surfactant and an antiprotease (De Water *et al*., 1986; Gil and Weibel, 1971). The neuroendocrine cells respond to stimuli of airway's nervous elements, possibly contain biogenic peptides that could influence vascular and bronchial smooth muscle tone, mucus secretion and ciliary activity (Wharton *et al*., 1978).

The epithelium of alveolar walls is mainly composed by other cells denominated as Type I or squamous cells and Type II or granular cells. Type I cells thinly cover the alveolar wall, thus preventing fluid loss while facilitating rapid gas exchange; however, they are extremely sensitive to injury. Type II cells are taller and twice as numerous as the Type I, despite only covering 7% of the alveolar surface due to their cuboidal shape (Crapo *et al*., 1982). These cells have an extremely significant role in pulmonary surfactant production and secretion, but also function as substitutes of damaged Type I cells after proliferation and differentiation (Evans *et al*., 1973).

- The airway wall and its components – epithelial barrier

Besides the skin, the respiratory tract comprises the only tissue that is directly exposed to environmental factors. Given this, the lung epithelium is composed by multi-layered physical-chemical barriers to prevent pathogen-crossing into the bloodstream. The barrier function of the respiratory epithelium is influenced by cell's secreted products, ciliary movements and intercellular junctional complexes.

As well as fluids and mucines, airway epithelial cells also secrete a series of antimicrobial substances and peptides – enzymes, protease inhibitors and oxidants (nitric oxide (NO) and hydrogen peroxide) – which are accumulated in the airway surface liquid (ASL) and help eliminate inhaled pathogens. The produced protease inhibitors, *e.g.* secretory leukoprotease inhibitor (SLP1), elastase inhibitor, α1-antiprotease and anti-chymotrypsin, reduce the effects of proteases expressed by pathogens and recruited innate immune cells maintaining the protease/anti-protease balance. This balance is crucial to prevent lung inflammation and preserve tissue homeostasis (Ganesan *et al*., 2013; Whitsett and Alenghat, 2015). While ASL holds and eliminates inhaled pathogens or particles, the ciliary activity is responsible for movement of retained substances from the lungs to the pharynx to be ingested or expelled by coughing. The efficiency of this process, which is crucial to ensure the airway's clearance, depends on coordinated movements of cilia and ASL's composition. The intercellular junctional complexes allow paracellular selective permeability to ions, macromolecules and water. Moreover, these complexes also promote differentiation of lung epithelial cells by separating basolateral surface's proteins from apical surface's ones (Ganesan *et al*., 2013; Shin *et al*., 2006).

Apical junctional complexes include tight (TJ) and adherens (AJ) junctions; although there are also basal junctional complexes composed by desmosomes, gap junctions and hemidesmosomes (Ganesan *et al*., 2013; Whitsett and Alenghat, 2015). Tight and adherens junctions are formed by homo- and heterotypic binding between several claudins expressed by lung epithelial cells and their cooperation is essential to maintain the paracellular permeability of the epithelium and tissue integrity (Ganesan *et al*., 2013; Pohl *et al*., 2009). While TJ function as barrier to molecule-diffusion from lumen to parenchyma and regulate the paracellular transport of molecules and ions, AJs mediate cell-to-cell adhesion and promote TJ formation (Hartsock and Nelson, 2008). Tight junctions are the most apical junctions of every junctional complex which possibly explains the consequent increase in epithelial permeability and airway inflammation after their disruption (Bhattacharya and Matthay, 2013; Georas and Rezaee, 2014; Grainge

and Davies, 2013; Koval, 2013a; Koval, 2013b; LaFemina *et al*., 2014). They are composed by several transmembrane and cytoplasmic scaffolding proteins – *e.g.* Occludin and Zonula Occludens-1 (ZO-1), respectively. The first are responsible for tightly connect adjacent cells while the others form protein networks between transmembrane proteins and cell's actin cytoskeleton (Schneeberger and Lynch, 2004). Moreover, the transmembrane protein Occludin was previously indicated as essential for *de novo* assembly of TJs (Ganesan *et al*., 2013; Rao, 2009). Adherens junctions are more basal than tight junctions and are responsible for the initiation and maturation of intercellular contacts. Their main proteins are type I transmembrane glycoproteins, epithelial cadherin (E-cadherin), α- and β- catenin. The extracellular domains of E-cadherin are responsible for the formation of homotypic, calcium-dependent adhesions between adjacent epithelial cells. Moreover, previous studies indicated the role of E-cadherin in regulation of cell proliferation and differentiation by modulation of Epidermal Growth Factor Receptor (EGFR) and β- catenin activities (Casalino-Matsuda *et al*., 2006; Ganesan *et al*., 2013; Wendt *et al*., 2010). The remaining basal junctional complexes also have important roles in cell-to-cell communication and in cell-cell and cell-extracellular matrix adhesion processes.

- The airway wall and its components – nervous elements

The afferent nerves innervating the respiratory airway that regulate reflexes such as bronchoconstriction and coughing have terminations largely infiltrated within the epithelial basement membrane, being surrounded by epithelial cells. Bronchopulmonary vagal afferent nerves are mostly unmyelinated C-fibers, which are sensitive to bradykinin, ion channels activators (*e.g.* capsaicin, protons, ozone, allyl isothiocyanate), inflammatory mediators (*e.g.* prostaglandin E2) and environmental irritants (*e.g.* ozone, nicotine) contrarily to other afferent nerves (Canning *et al*., 2014). There is also a set of mechanically sensitive myelinated vagal afferent nerves, known for decades as Widdicombe Cough Receptors. These Cough Receptors are exclusive to extrapulmonary airways with terminations between the smooth muscle layer and the epithelial layer of the mucosa. Finally, the afferent nerves of airways can also be Lung Stretch Receptors categorised according to their responses to sustained inflation – rapidly and slowly adapting receptors (RARs and SARs, respectively). Terminal structures of RARs are yet to be defined in the airway, but some functional studies indicate that possibly these nervous fibers terminate within or beneath the epithelium of intrapulmonary structures. The terminal location of SARs is believed to be primarily

associated to the peripheral intrapulmonary airways, although it was described at other locations in distinct species (Canning *et al*., 2014).

- The airway wall and its components – lymphoid elements

Due to the constant exposure to damaging agents, the respiratory tract should respond rapidly to return to a homeostatic state. Therefore, the airway is also composed by lymphoid elements, which include lymph nodes, bronchus-associated lymphoid tissue (BALTs), lymphoreticular aggregates and dispersed lymphocytes, dendritic cells, macrophages and mast cells. Mast cells present in airways are morphologically and functionally distinct from the ones present in deep connective tissues, but release several inflammatory mediators that affect epithelial and vascular permeability, smooth muscle function and other functional responses (Enerback, 1986). Lymphocytes may be either B or T cells, specifically T cells CD3+, CD4+ (T helper) and CD8+ (T cytotoxic); however, T-cell immunity is regulated by balancing signals of resident Ia+ dendritic cells and macrophages. Alveolar macrophages are mainly located in the alveoli and are avidly phagocytic (Brody *et al*., 1981). They also have the ability to interact with pulmonary lymphocytes to present antigens via surface immunoglobulins and complement receptors, highlighting their importance in eliciting immune responses against exogenous agents (Kaltreider, 1982). Although, lysosomal enzymes released during phagocytosis (*e.g.* elastases, collagenases) and other substances released independently of phagocytic activities (*e.g.* matrix metalloproteinases, interferon and fibroblast-stimulating factor) may damage the lung tissue if the normal anti-protease screen α1-antiprotease is compromised.

- The airway wall and its regulation mechanisms

Contrarily to what was initially thought, the respiratory epithelium is more than just a physical barrier to exogenous agents. The lung epithelial cells have a crucial role in tissue remodelling processes and in modulation of immune responses – either innate or adaptive (Grainge and Davies, 2013; Whitsett and Alenghat, 2015). The expression of several receptors (*e.g.* pattern recognition receptors (PRRs), Toll-like receptors (TLRs), retinoic acid-inducible gene I-like receptor (RIG-I-like receptor), C-type lectins and inflammasome components) on epithelial cell's surface indicates that these cells contribute for early detection of pathogens or other damaging agents (Weitnauer *et al*., 2016). Although, cell receptor's interactions with molecules present in ASL or expressed during airway epithelium damage greatly contribute to the maintenance of the

hyporesponsive state of lung epithelium or to initiation of immune responses, thus highlighting the complexity of airway's regulation mechanisms.

The immune response can be regulated by epithelial cells in two distinct mechanisms: one responsible for maintaining pulmonary homeostatic state and other responsible for immune response initiation. These two processes are modulated by airway's distinct components interactions and by expression of chemical mediators and other molecules. As previously referred, the airway epithelial tissue secretes a series of proteins to constitute ASL such as mucins, which are glycoproteins with high potential for post-translational modifications. Besides forming a physical barrier between antigens and microbes and epithelial cells, mucins also have anti- oxidant/ proteolytic/ microbial activities that contribute to unspecific innate defences. Although, previous studies indicated that mucins also had immunoregulatory effects by inhibiting TLR signalling, possibly contributing to its actively suppression in airway's and alveolar epithelial cells in homeostatic states (Weitnauer *et al*., 2016). On the alveolar level, the ASL is replaced by pulmonary surfactant constituted by surfactant proteins (SP) with immunoregulatory mechanisms as well. Previous studies highlighted the role of SP in limiting the contact between alveolar epithelial cells and pathogens or their pathogen-associated molecular patterns (PAMPs). It was verified that SP-A and SP-D and phosphatidyl glycerol-containing surfactant vesicles directly bound to TLR2, TLR-4, MD2 and CD14 resulting in receptor's blockage to PAMPs. Additionally, it was proved SP-C binds to LPS thus eliminating their damaging potential (Weitnauer *et al*., 2016). In parallel, the alteration of expressed mucins by airway epithelial cells and the suppression SP expression by alveolar epithelial cells caused by exogenous agents revealed to be crucial for initiation of inflammatory responses. Moreover, these alterations could be an immediate effect of pathogen's activities or caused by perturbations in mucociliary elimination and incomplete clearance of airways. Additionally to epithelial surface's protection by ASL or pulmonary surfactant, the intercellular tight junctions also play a crucial part in modulation of immune response - possibly due to the fact that some of the receptors are limited to the basolateral side off cells, which is inaccessible in healthy homeostatic epithelium. Although several studies indicated that TJ and AJ disruption induced the expression and secretion of cytokines and chemokines that elicited immune responses.

When both biochemical and physical barriers of airway's tissue are compromised, epithelial cells express chemotactic substances, cell-surface molecules and cytokines to recruit inflammatory cells to the injured site and modulate their activity (Mayer *et al*., 2008). Several molecules and chemotactic factors (*e.g.* nitric oxide (NO), Leukotriene B4) are involved in activation of neutrophils, macrophages, eosinophils and lymphocytes

(Marcet *et al*., 2007); however, there are other molecules (*e.g.* Chemokine (C-C motif) ligand 20 – CCL20) capable of recruiting dendritic cells (DCs) into the epithelial tissue which consequently initiates more specific immune responses of B and T cells (Kato and Schleimer, 2007; Pichavant *et al*., 2005; Pichavant *et al*., 2006; Reibman *et al*., 2003). The released molecules could have pro- or anti-inflammatory effects in order to ensure that inflammatory reactions do not escalate to chronic inflammation of the tissue. Previous studies revealed the role of epithelial cells in negative regulation of inflammatory cells in certain context (Mayer *et al*., 2008; Weitnauer *et al*., 2016). For example, Mayer *et al*. (2008) indicated inhibition of lymphocyte proliferation and T-cell differentiation through synthesis of Transforming Growth Factor type β (TGF- β) by epithelial cells.

After elimination of the damaging agent, the epithelial tissue must repair and regenerate its normal structure in order to return to homeostatic state. Tissue repair and remodelling mechanisms are also initiated by the expression of chemical mediators and cytokines. In coordination with basal fibroblasts, the epithelial cells strictly regulate the airway microenvironment in such processes. After injury, epithelial cells dedifferentiate and suffer epithelial-to-mesenchymal transition (EMT) to repair the injured area. To perform their reparative functions, epithelial cells migrate to cover the area and restore the affected barrier protection; however, these cells remain in their epithelial compartment without surpassing the basement membrane. It was previously evidenced that cell's migration and proliferation is regulated by upregulation of epithelial growth factor receptor (EGFR) (Grainge and Davies, 2013). Simultaneously to epithelial cell's migration, the underlying fibroblasts proliferate and differentiate to synthesize a temporary fibrotic matrix to support the migrating mesenchymal-like cells. Subsequently to barrier restorage, myofibroblasts suffer apoptosis to reinstate normal tissue structure and the basal epithelial cells differentiate into the different epithelial components of the airway wall. Although, the restored epithelium first differentiates in mucous cells followed by ciliated cells to re-establish the mucociliary escalator. Previous studies indicated that the airway can also initiate EMT and repair mechanisms (fibroblast proliferation and increased expression of fibronectin and type III and V collagen) in response to increased expression of TGF-β2 triggered by methacholine-induced bronchoconstriction (Grainge and Davies, 2013).

The molecular basis of allergy

The immune system is defined by several biological structures, *i.e.* cells and tissues, and mechanisms that protect an organism against disease or environmental

aggressions. The immune response is classified as innate or adaptive depending on the activated mechanisms. Innate immune response is defined as non-specific cellular and humoral mechanisms that culminate in inflammatory and phagocytic reactions to an unknown agent – this is the first response to a new damaging molecule. The adaptive immune response is defined by complex reactions – also cellular and humoral – that adapt specifically to a certain antigen to respond to subsequent exposures more quickly. However, the immune system also has the capacity of damaging an organism when its regulatory mechanisms are somehow affected. This is commonly known as hypersensitivity of the immune system.

Currently, four types of hypersensitivity are defined, according to their origin and consequences. Respiratory allergy is classified as type 1 hypersensitivity and generally there is a genetic predisposition to such condition. It is a well-known inflammatory process which involves several immune cell types, molecules and signalling pathways. The allergic reaction is initiated by a sensitization process that occurs during the first exposure to an allergen which begins with allergen uptake by antigen- presenting cells (APC). Consequently, APCs migrate to lymph nodes while the allergen is digested in their lysosomes and fragments are loaded onto the major histocompatibility complex (MHC) class II. Once loaded, the MHC class II molecule migrates to the cell surface and is recognized by a specific T-cell subpopulation – the Type 2 helper T (T_H2) cells. The activation of this T_H2 subpopulation results in the expression of chemical mediators that are responsible for the class-switching process necessary for immunoglobulin E (IgE) production, *i.e*. interleukin 4 (IL-4); and for the activation and recruitment of other immune cells – eosinophils, mast cells, macrophages, B cells –, *e.g.* IL-4, IL-5, IL-9, IL-13. IgE synthesis and eosinophilia distinguish the allergic inflammation from other forms of inflammation and are important components of the allergic process (Bacharier and Geha, 2000; Broide, 2001; Stone *et al*., 2010).

In subsequent exposures, IgE-allergen specifically binds to granulocytes through the FCξR receptor. Consequently, the granulocyte degranulates releasing a series of pro-inflammatory mediators involved in early- and late-phase symptoms of the allergic reaction. The early phase of allergy is characterized by dyspnea, edema, swelling and protein degradation caused by bronchiole's smooth muscle contraction, blood vessels dilation and eosinophil's activation. The late phase is characterized by an increased inflammation and aggravated symptoms of the early phase due to constant recruitment of immune cells, *e.g.* eosinophils, T_H2 cells, basophils, neutrophils, mastocytes, etc.

The common symptoms associated with this condition are sneezing, itchiness, rhinorrhea and nasal congestion in the upper respiratory apparatus and chronic

inflammation and bronchioles tightness in the lower respiratory apparatus, also known as allergic asthma (Calderon *et al*., 2015). Although, allergic symptoms could also be a consequence of cytokine production and tissue inflammation elicited by non-IgE mediated processes. Specifically, the pathological eosinophilia characteristic of asthma, rhinitis and other respiratory diseases could be elicited by non-IgE mediated stimuli such as the proteolytic and non-proteolytic effects of allergen extracts of inhaled environmental substances, *e.g.* pollen grains or dust mites (Atkinson and Strachan, 2004; Pinto and Todo-Bom, 2009; Robinson *et al*., 2008; Runswick *et al*., 2007; Schleh and Hohlfeld, 2009; Tomee *et al*., 1998). Moreover, several studies performed to classify types of asthma indicated that there are asthmatic patients with atypical elevated levels of neutrophils instead of T_H2 cells (Carr *et al*., 2017; Ray and Kolls, 2017). This asthmatic subtype, highlights a non-IgE mediated alternative mechanism that results in similar symptoms of the allergic asthma subtype.

Pollen as an allergy elicitor

Pollen-related allergic symptoms affect a wide amount of world's population and tend to be aggravated in overdeveloped areas. Despite the well-recognized pollen allergenicity, the sensitization is often silent and only detected when a symptom develops in the affected individual (Calderon *et al*., 2015). Throughout the years several plant species were identified as producers of allergenic pollen, however the allergenic potential of pollen grains varies according to the geographical area and the environmental factors surrounding the studied population – *e.g.* air pollution, climate changes, etc (Asam *et al*., 2015; Atkinson and Strachan, 2004; Chapman, 1986; Ribeiro *et al*., 2013; Ribeiro *et al*., 2014; Robinson *et al*., 2008; Schleh and Hohlfeld, 2009; Silva *et al*., 2015; Sousa *et al*., 2012).

As previously referred, for antigen presentation to occur the antigen must cross the epithelial barrier to access immune cells and elicit an immune response. Several studies performed in the last decades revealed that the allergenic potential of air allergens, including pollen grains, was dependent of intercellular junctional complexes' disruption with consequent lung epithelial damage caused by amplified inflammatory responses (Runswick *et al*., 2007; Tomee *et al*., 1998; Wan *et al*., 1999). These studies have proved the ability of certain enzymatically active proteins from air allergens – *e.g.,* fungi allergens of *Alternaria* and *Aspergillus* and specifically Pen ch 13 (*Penicillium chrysogenum*); Der p1 (*Dermatophagoides pteronyssinus*); pollen proteases of four distinct plant species – to induce expression of cytokines and other mediators in epithelial cells, *in vitro* cell detachment and Occludin's degradation with consequent increase of epithelial

permeability (Kauffman *et al*., 2000; McKenna *et al*., 2017; Runswick *et al*., 2007; Tai *et al*., 2006; Vinhas *et al*., 2011).

Some authors defend a "protease hypothesis" where apical junctional complexes disruption is directly caused by proteolytic potential of pollen protein extracts (Hollbacher *et al*., 2017; McKenna *et al*., 2017; Runswick *et al*., 2007; Vinhas *et al*., 2011). Despite being difficult to predict bioactivity of pollen extracts based on biochemical properties, the proteolytic activity has in fact an adjuvant role in the development of allergic diseases since it is involved in the first step of allergen sensitization.

Acer negundo as a potential allergenic tree

The urban land-use planning of a certain area also has a significant impact in public health. Specifically in Porto (Portugal), a previous study performed by Ribeiro *et al*. (2009) revealed correlation between production peaks of potentially allergenic pollen and maximum hospital emergency admissions for asthma- or dyspnea-related respiratory diseases. One of the identified potential allergenic pollen was produced by *A. negundo* tree, which is an ornamental tree predominant on the streets of the city. Subsequent studies revealed that the exposure of these trees to urban pollutants can aggravate the pollen allergy on predisposed individuals and affect plant reproduction (Sousa *et al*., 2012).

A. negundo is commonly known as box-elder and it is a native species from North America that belongs to the Sapindaceae (Aceraceae) family. It is identified has a potential allergenic tree, since it has been verified a hypersensitization to *A. negundo*'s pollen in the areas where it occurs. This maple tree was introduced in Europe in the 17th century as a park tree, but is now considered an invasive species in Central Europe. This tree is primarily wind pollinated and has subprolate or spheroidal pollen – depending on the hydration levels – which has a striated ornamentation and three elongated apertures (Pehlivan *et al*., 2003). Due to its short living period it is a fast-growing tree and, unlike other maple trees, *A. negundo* is dioecious. Its seeds have a winged structure that helps dissemination.

To characterize the potentially allergenic proteins present in total protein content of *A. negundo*'s pollen grains, a two-dimensional polyacrylamide gel electrophoresis (2D-PAGE) was performed followed by a Western Blot analysis using sera of patients with allergenic susceptibility to *A. negundo*'s pollen proteins. The immunoreactive proteins were identified by Mass Spectrometry (MS) analysis using matrix-assisted laser desorption/ionization (MALDI) and peptide mass fingerprinting (PMF) and one of the potential allergenic proteins identified was Calreticulin (CRT).

Calreticulin – a well-known unknown protein

Calreticulin is a highly conserved multifunctional protein of 46-60 kDa involved in protein folding and Ca^{2+} homeostasis predominant in the endoplasmic reticulum (ER) of eukaryotic cells due to its ER retention sequence – K/HDEL (Jia *et al*., 2009; Michalak *et al*., 2009; Opas *et al*., 1996). Several studies on the animal CRT over the past decade suggested other subcellular localizations, *e.g*. nucleus, cytoplasm and extracellular membrane, as well as other CRT functions such as integrin's regulation, cell to cell interactions and gene expression modulation in addition to molecular chaperoning and calcium sequestration, mobilization and signalling (Lenartowska *et al*., 2002; Li and Komatsu, 2000; Navazio *et al*., 1998). The significant structural similarity of the protein across eukaryotes, particularly in parts of the protein crucial for functionality, suggests important biological functions (Coppolino and Dedhar, 1998; Jia *et al*., 2009).

The protein is subdivided into three distinct domains: the globular N- and the proline-rich P- domains both responsible for the chaperone activity; and the C- domain with a wide range of acidic residues involved in calcium buffering. Also, it has a signal peptide sequence previous to the N-domain and an ER-retention signal (KDEL or HDEL in mammals or plants, respectively) at the C-terminus. Relatively to its three-dimensional structure CRT presents a globular shape composed by N- and C- domains with an extended arm-like hairpin (P- domain). The N-domain is extremely conserved and two signature motifs were identified in plant CRTs (KHEQKLDCGGGYVKLL and IMFGPDICG). This N-terminal domain also contains consensus sites for N-glycosylation through most plant species; however the glycosylation potential varies according to the protein isoform, which is a possible explanation for CRT redistribution in the cell described elsewhere (Thelin *et al*., 2011). The P- domain comprises two proline-rich motifs repeated three times – PxxIxDPKxxKKPExWDD (motif A) followed by GxWxAxxIxNPxYK (motif B) – subsequent to a putative nuclear targeting sequence (PPKxIKDPx). In animal CRTs, the P-domain contains repeated motifs which are also noted as letters A and B. Despite the similarity with plant CRT segments, these repeated motifs correspond to different amino-acidic sequences – PxxIxDPDAxKPEDWDE (motif A) and GxWxxPxIxNPxYK (motif B). Repeats A and B are essential for the lectin-like activity of CRT but are also responsible for the high-affinity Ca^{2+} binding capacity of the P-domain. This domain also contains 4 amino-acid residues crucial for chaperone interaction: Glu, Asp, Glu and Trp. The C-domain is highly acidic and negatively charged to bind high concentrations of Ca^{2+} despite having low calcium affinity. The calcium binding function is mainly associated to the C-terminal domain, regardless of the high

affinity of the P-domain which binds low concentrations of Ca^{2+}. The C-domain is the least conserved domain of this protein and contains several putative phosphorylation sites, which some authors defend as extremely important for regulation of CRT's role in signal transduction in various cellular processes (Droillard *et al*., 1997; Li and Komatsu, 2000; Thelin *et al*., 2011).

The increasing studies on plant CRTs revealed that there is at least 3 isoforms functional divergent (Christensen *et al*., 2010; Jia *et al*., 2009; Thelin *et al*., 2011). However, there are only two groups distinguished: CRT1/ CRT2 - also referred as CRT1a/ CRT1b respectively - and CRT3. Phylogenetic studies using plant CRTs showed that CRT1a and CRT1b have higher sequence homology between them than with CRT3, subsequently confirmed by expression studies (Jia *et al*., 2009; Persson *et al*., 2003). CRT3 isoform is pointed out as the most divergent isoform; although according to some works it is the ancestral isoform, despite having very specific functions in plants as previously described (Persson *et al*., 2003).

Phylogenetic analyses based on coding sequences and deduced amino-acidic sequences of animal CRT using as out-group *Arabidopsis thaliana* suggested purifying selection over the protein's primary structure with periodic positive selection which resulted in fixated polymorphisms (Bakiu, 2014). The found polymorphisms might be responsible for some specific functions of CRT found in both animal and plant cells, as well as the conserved primary structure being responsible for shared functions between them. Consequently, some mammalian CRT functions were transposed to its plants homologues since there is no complete functional characterization of plants CRTs. However, there is increasing proof that CRT has acquired special functions in plants throughout evolution. In plants, it has been suggested CRT participation in several reproductive processes due to detection of enhanced expression levels in specific reproductive structures, *e.g.* whole ovaries of barley, sperm cells of maize and in tobacco anthers and pollen tubes (Chen *et al*., 1994; Chen *et al*., 2016; Jia *et al*., 2009; Nardi *et al*., 2006; Navazio *et al*., 1998; Williams *et al*., 1997). Jin *et al*. (2009) reported that CRT3 is crucial and exclusive for retention of misfolded brassinosteroid receptor in the ER. Other studies revealed that this isoform was also responsible for the correct folding of a specific receptor, which has a key role in plant immunity since it recognizes Pathogen Associated Molecular Patterns (PAMPs) – the elf18 responsive EF-Tu receptor (EFR) – and was not capable to balance the phenotype resulting from double mutant organisms lacking the other two isoforms (CRT1a/1b) (Christensen *et al*., 2010; Thelin *et al*., 2011).

- Calreticulin as a cell adhesiveness modulator

As previously noted, calreticulin is an ER protein with well characterized main functions. However, throughout the years emerging evidences suggested unexpected functions for this protein. A previously published work reviewed the interactions and pathways where animal calreticulin is involved (Michalak *et al*., 2009). The crucial role of this protein in cell differentiation and in several processes of the embryonic development was highlighted, *e.g.* cardiac and central nervous system development. Moreover, in the same review it was noted the importance of this protein in other processes essential to maintain tissue integrity, *i.e.* the role of CRT in wound healing (Michalak *et al*., 2009).

Previous studies proved that the re-epithelialization of a wounded tissue was accelerated by CRT protein since it chemoattracted and stimulated the proliferation of epithelial cells (keratinocytes and fibroblasts), both *in vivo* and *in vitro* (Gold *et al*., 2010; Michalak *et al*., 2009). Additionally, there are evidences that CRTs also plays important roles in cellular adhesiveness, mobility and proliferation by regulating the expression of specific growth factors or certain proteins crucial for adhesive structures formation and maintenance commonly known as extracellular matrix (ECM) proteins (*e.g.* vinculin, fibronectin, collagen α1, N-cadherin) (Bedard *et al*., 2005; Fadel *et al*., 1999; Fadel *et al*., 2001; Papp *et al*., 2007; Villagomez *et al*., 2009). These effects are opposite depending on protein's location. For example, the overexpression of intracellular CRT was correlated with augmented cell adhesiveness; however cell-surfaced or extracellular CRT activated signalling cascades (PI3 kinase, ERK and Gi-protein systems) that led to focal contact disassembly and consequently decreased cell adhesiveness (Goicoechea *et al*., 2002; Villagomez *et al*., 2009).

The regulation of ECM proteins occurs consequently to intracellular signalling cascades that may be modulated by CRT expression levels (Bedard *et al*., 2005; Fadel *et al*., 1999; Fadel *et al*., 2001; Papp *et al*., 2007; Villagomez *et al*., 2009); or by CRT interaction with transmembrane proteins, *e.g*. integrins, lipoprotein receptor- related protein (LRP1, also known as CD91 receptor) (Coppolino and Dedhar, 1998, 1999; Coppolino *et al*., 1997; Raghavan *et al*., 2013). Specifically, in mammalian systems a correlation between increased secreted calreticulin and detachment of cancer cells during initiation of metastasis was suggested, which indicates interactions between secreted CRT and cell-membrane receptors that are involved in adhesion processes (Chiang *et al*., 2013; Shi *et al*., 2014). Regardless of the accumulating evidences in the past years that corroborate the potential role of CRT as a cell-adhesion modulator, the intrinsic mechanisms are still to be fully understood and described.

- Calreticulin as an immune system activator

It was previously reviewed elsewhere (Wiersma *et al*., 2015) that the immune system can be activated by ER chaperones through interactions with LRP1 receptor, even though the mechanisms behind that activation are still to be fully understood. In fact, some studies proved that ER chaperones are autoimmunity targets since their displacement to the extracellular environment is more likely to occur in dying cells or cells exposed to stressing stimuli (Eggleton *et al*., 2000). Consequently, ER chaperones can act as Damage-associated molecular patterns (DAMPs) and activate the immune system through a series of cascade reactions that can lead to immune-complex clearance, anti-tumour immunologic response or even autoimmunity (Wiersma *et al*., 2015).

Given the fact that ER chaperones are proteins naturally located in the ER due to the presence of specific retention motifs, they can suffer post-translational modifications or interact with other proteins that relocate them to unexpected locations. For instance, in joints of patients suffering from rheumatoid arthritis there is higher prevalence of a post-translationally modified CRT isoform that potentiates the activating signals of innate immune cells (Ling *et al*., 2013; Wiersma *et al*., 2015). There is also evidence for LRP1 involvement in immunogenicity regulation of some ER chaperones (calreticulin, gp96, HSP90 and HSP70), since the non-transmembrane CRT binds to the LRP1 receptor and is relocated to the cell surface (Basu *et al*., 2001; Wiersma *et al*., 2015). This relocation can occur in apoptotic cells and acts as an “eat-me” signal by competing with the inhibitory signal provided by CD47 (Gardai *et al*., 2005), confirming the important role of this protein in phagocytosis. Furthermore, it was previously evidenced that membrane exposure of calreticulin – either by stimulation with anthracycline treatment or by exogenous supplementation of recombinant CRT after mitomycin C treatment – lead to tumour cells phagocytosis and immunogenic cell death (Chaput *et al*., 2007). It was also proven in the past few years that surface CRT interacts with proteins (*e.g.* collectins) that are involved in the initiation and modulation of several immune processes (phagocytosis, inflammatory or immunogenic responses). As stated by Gardai *et al*. (2003), lung collectins behave like a bifunctional sensor in order to enhance or repress inflammatory response depending on their collagenous tail domain orientation, which alters according to certain ligands, *e.g.* Pathogen-associated molecular patterns (PAMPs), apoptotic cells or cell debris. In the presence of those ligands, the collagenous tails of collectins suffer reorientation and interact with surface CRT/LRP1 – characteristic of apoptotic cells – stimulating the expression of proinflammatory mediators.

Additionally, extracellular CRT is known to have a significant role in the progression of autoimmune diseases, since it affects immune complex clearance. This occurs due to the inhibition of the C1q-dependent antibody hemolysis caused by the C1q-binding competition between extracellular CRT and antibodies (Schwab, 2008).

Project's Goals:

A recent review stated that identified allergenic proteins are most likely to maintain their allergenicity since they are proteins under purifying selection due to their biologically important roles (Chen *et al*., 2016). Given this, it is important not only to characterize the identified proteins but to understand the effects on the exposed epithelial cells to describe the inflammatory response that consequently develops. Knowing the processes and molecules involved helps to better understand the allergic reaction and consequently, to discover potential unknown targets that can alleviate the uncomfortable symptoms of an allergic reaction.

Since there are evidences in the current literature of immunogenic effects specifically addressed to CRT isolated from parasites (Kasper *et al*., 2001), and there is proof of its involvement in several cell processes that in specific conditions develop an inflammatory or an immune response (Gardai *et al*., 2005; Martins *et al*., 2010; Trautmann *et al*., 2005), we raised the hypothesis that plant CRTs – being structurally and functionally similar to mammalian calreticulin and capable of restoring some of its main functions – could have similar immunogenic effects and induce the expression of proinflammatory molecules resulting in an inflammatory response; or interact as the secreted mammalian protein, compromise cell adhesion resulting in epithelium detachment and consequently induce an inflammatory response due to tissue damaging. Given this, we also raised the question if the allergenic potential of *Acer negundo*'s calreticulin (*An*CRT) could be a consequence of specific interactions with cell-membrane receptors, as evidenced by several studies that highlighted the immunostimulatory effects of extracellular CRT – *e.g.* LRP1 in phagocytes, Toll-like receptor 4 (TLR-4) in dendritic cells (DC), Scavenger receptor A (SRA) in macrophages (Chaput *et al*., 2007; Gardai *et al*., 2005; Gold *et al*., 2010; Martins *et al*., 2010; Obeid *et al*., 2007; Raghavan *et al*., 2013; Schwab, 2008; Wiersma *et al*., 2015); or a cumulative effect of the inflammatory reaction initiated from the pollen- epithelium contact that results in production of CRT-specific IgE.

Chapter II – Materials and Methods

RNA Extraction from pollen samples

Pollen of *Acer negundo* (100 mg) was frozen in liquid nitrogen and homogenized "in tube" with a pestle. Total RNA was extracted using Trizol® reagent (Invitrogen) according to the manufacturer's protocol with some modifications relatively to isopropanol precipitation and ethanol washing steps. RNA molecules were precipitated by incubation with ice-cold isopropanol at -20ºC for 30 minutes. The resulting pellet was washed with ethanol (80%), air-dried on ice and eluted in nuclease-free water.

RNA retrieval from enzymatic treatments

Treated RNA was retrieved with Trizol® reagent (Invitrogen) with modifications on manufacturer's protocol in accordance to mixture volumes. Trizol® reagent was added to reaction mixture (1:1). After centrifugation at 10000 *g* for 5 minutes, the upper phase was transferred to a sterile nuclease-free tube and phase separation was repeated with addition of chlorophorm (1:1). The upper phase was again transferred to a sterile nuclease-free tube and RNA precipitation was performed as previously described. Subsequently, the mixture was centrifuged at 4ºC in maximum speed for 20 minutes (Eppendorf 5427 R). Pellet was washed with ethanol (80%), air-dried on ice and eluted in nuclease-free water.

Determination of RNA quality and yield

Total and treated RNA molecules were quantified using µDrop™ plate (Thermo Fisher Scientific). RNA concentration was determined by the following equation:

$$\mathbf{1)\ RNA\ concentration\ = RNA\ Extinction\ coefficient\ \times\ OD_{260}\ \times\ dilution\ factor}$$

Where RNA Extinction coefficient is pre-determined as 40 µg RNA/mL when OD_{260}=1. Since samples were not diluted prior to quantification, the dilution factor corresponds to the path length (10/0.51 mm) of the µDrop™ plate (Thermo Fisher Scientific). RNA quality was evaluated by OD_{260}/OD_{230} and OD_{260}/OD_{280} ratio as indicated in µDrop™ plate (Thermo Fisher Scientific) User Manual and by visual analysis of agarose gels.

Agarose gel electrophoresis

RNA molecules were analysed in a 1% (w/v) agarose gel prepared with 1x Sodium Borate (SB) buffer [50 mM Sodium Hydroxide, 40 mM Boric acid] supplemented with 1%

(v/v) bleach as described by Aranda *et al*. (2012) and pre-stained with 0.5 µg/mL ethidium bromide.

DNA molecules resulting from RLM-RACE reactions were analysed in a 1% (w/v) agarose gel prepared with 1x SB buffer and pre-stained with 0.5 µg/mL ethidium bromide. DNA molecules resulting from SemiNested Polymerase Chain Reaction (PCR) and Minipreps were analysed in a 0.8% (w/v) agarose gel prepared as described. All electrophoreses were performed at 200 V in 1x SB buffer using DNA Ladder Mix GeneRuler (Fermentas) as molecular weight marker. RNA and DNA bands were visualized in a UV transilluminator (302-365 nm) and gels were photographed with compatible systems.

RNA Ligase-Mediated – Rapid Amplification of cDNA ends (RLM-RACE)

The following methods were based on previously described protocols used to increase the probability of retrieving full transcripts from a total RNA pool (Suzuki *et al*., 1997).

- RNA Enzymatic treatments

Total RNA extracted was submitted to enzymatic treatments as previously described (Suzuki *et al*., 1997) (Figure 1). The total RNA was treated with 2U of Calf Intestine Alkaline Phosphatase (CIAP – Thermo Fisher Scientific) at 37ºC for 1 hour. To prevent RNA degradation, the reaction mixture was supplemented with Ribolock (1.08 U/µL). The reaction was terminated with ammonium acetate (100 mM) and the treated RNA was retrieved as previously described in *RNA retrieval from enzymatic treatments*. Subsequently, the CIAP-treated RNA was treated with 25U of RNA-Pyrophosphohydrolase (RppH - NEB) at 37ºC for 1 hour to remove the CAP structure of full transcripts. To prevent RNA degradation, the reaction mixture was supplemented with Ribolock (1.08 U/µL). The reaction was terminated with addition of EDTA (10 mM) and incubation at 65ºC for 5 minutes.

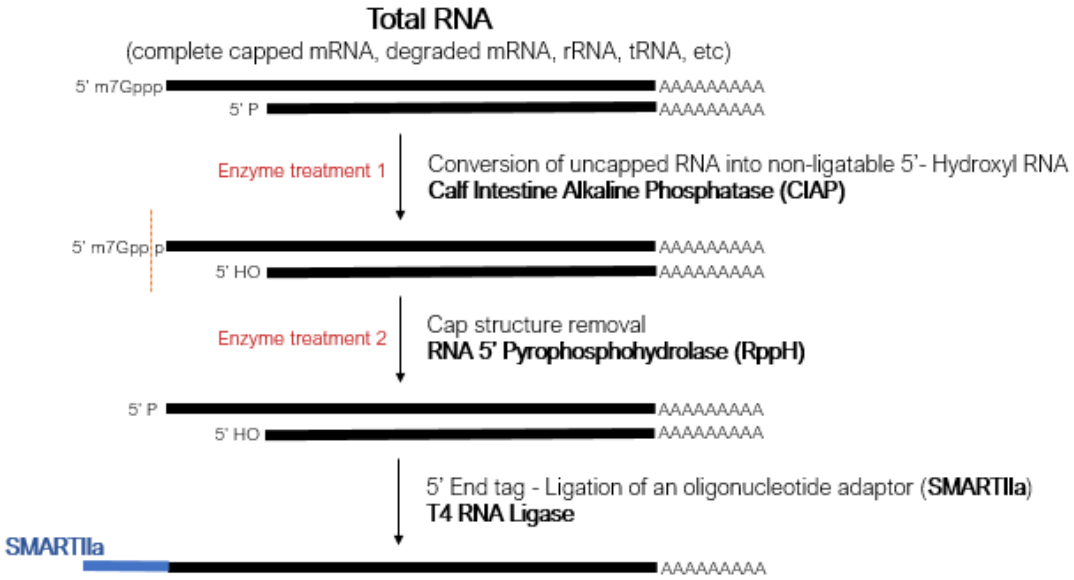

Figure 1 – Schematic representation of RNA enzymatic treatment prior to 5' Rapid Amplification of cDNA ends. Uncapped, i.e. 5' monophosphate, RNA was converted to non-ligatable 5' hydroxyl (HO) RNA by Calf Intestine Alkaline Phosphatase. Cap structure of complete mRNA molecules was removed by RNA 5' Pyrophosphohydrolase resulting in a 5' monophosphate end capable of binding to a free 3' HO end. Subsequently, resulting RNA was ligated by T4 RNA Ligase to an oligonucleotide adaptor (SMARTIIa) with free 3' HO end.

- 5' Rapid Amplification of cDNA ends (5' RACE)

The uncapped RNA was bound to the SMARTIIa 5' – oligonucleotide adaptor (Figure 2 - 30 pmol; custom order, 5' - AAG CAG TGG TAT CAA CGC AGA GTA CGC GGG - 3') recurring to a ligation reaction performed with 7.5 U of T4 RNA ligase (TaKaRa) according to manufacturer's protocol specified for intermolecular ligations. To prevent RNA degradation, the reaction mixture was supplemented with Ribolock (1.08 U/µL).

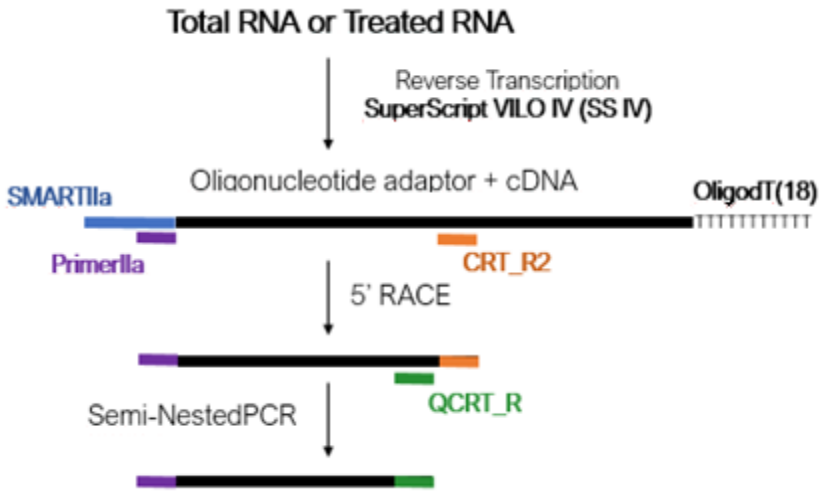

Figure 2 – Schematic representation of 5' Rapid Amplification of cDNA ends (5'RACE). Subsequently to reverse transcription of total and enzymatically-treated RNA, cDNA molecules were submitted to 5' RACE using as primer forward an oligonucleotide (PrimerIIa) that annealed in a specific region of the oligonucleotide adaptor (SMARTIIa) and a gene-

specific inner primer (CRT_R2 or QCRT_R) as primer reverse. Afterwards, the RACE products were amplified in a Semi-Nested PCR in order to increase the number of desired cDNA molecules using the same primer forward and another, or the same, gene-specific inner primer as in RACE reaction.

Subsequently, the adaptor-ligated RNA was reverse transcribed for cDNA synthesis recurring to Super Script IV VILO Master Mix (Invitrogen) according to manufacturer's protocol. As control reaction, untreated RNA was also used for cDNA synthesis using Super Script IV VILO Master Mix (Invitrogen). In this reaction, SMARTIIa 5' oligonucleotide adaptor (20 pmol) was added to the cDNA synthesis reaction. First-strand cDNA products were used as template for 5'- end amplification (5' RACE) with proofreading *Pfu* DNA polymerase (Thermo Scientific) and specific primers, according to the intended reaction (Table 1).

Table 1 – Specifications of used primers in all amplification reactions performed. Melting temperatures and respective primer sequence are indicated.

Primer	Melting temperature (ºC)	Sequence (5' → 3')
CRT_F	59.3	ATK TGG TGG TGA TAC CCT TAC
CRT_R2	60.3	CAG GAT CTG CTA TCT CCT TTG G
QCRT_F	55.3	CTA CCT ACA GCA TCC TTA TC
QCRT_R	51.2	TTC TTT GTC ATC CCA ATC TT
A_ACT_F	59.0	GAT TCT GGT GAT GGT GTG TCT C
A_ACT_R	57.9	ACG GAC AAT TTC CCG TTC
PrimerIIa	60.6	AAG CAG TGG TAT CAA CGC AGA GT
M13 (-20) Forward	59.0	GTA AAA CGA CGG CCA G
M13 Reverse	58.0	CAG GAA ACA GCT ATG AC

To assess genomic DNA contamination, PCR reactions were performed in the same conditions with untreated RNA not submitted to reverse transcription reaction as template (Table 2 – Reaction 5: Non- RT untreated RNA). Actin primers were also used to assess cDNA quality. Moreover, PCR components were tested for heterologous contamination through amplification reaction using nuclease-free water as template.

Table 2 - Templates and primers used for 5' Rapid Amplification of cDNA ends (5' RACE) reactions and respective positive and negative controls. RACE reactions (A and C) are highlighted with a light-grey background. Their correspondent control reactions (B and D, white background) were performed with gene-specific inner primers chosen depending on the reverse primer selected for RACE reaction to assess the presence of the desired transcript and to determine the ideal template volume. Actin primers (A_ACT_F and A_ACT_R) were used to assess complementary DNA (cDNA) quality. Non-reverse transcribed untreated RNA was used as template to assess genomic DNA contamination in each reaction and nuclease-free water was used to check cross-contamination of PCR components.

		Template					
Primer forward	**Primer reverse**	cDNA from treated RNA 1	cDNA from treated RNA 2	cDNA from treated RNA 3	cDNA from untreated RNA	Non-RT untreated RNA	Water
PrimerIIa	CRT_R2	A1	A2	A3	A4	A5	**C-** (A)
CRT_F		B1	B2	B3	B4	B5	**C-** (B)
PrimerIIa	QCRT_R	C1	C2	C3	C4	C5	**C-** (C)
QCRT_F		D1	D2	D3	D4	D5	**C-** (D)
A_ACT_F	A_ACT_R	E1	E2	E3	E4	E5	**C-** (E)

All amplifications were performed in a MJ Mini Thermal Cycler (Bio-Rad) using Touchdown PCR program (Korbie and Mattick, 2008) and analysed by agarose gel electrophoresis as previously specified. Annealing temperature of each amplification reaction had variations according to used primer-pairs melting temperatures specified in Table 1. Primer binding sites in known sequence of *An*CRT coding sequence are also schematized in Figure 3.

Figure 3 – Graphical representation of used primers binding sites. The limits of each primer binding site are also indicated but correspond to a specific position in the sequenced region. The unknown region is also represented bound to the SMARTIIa oligonucleotide adaptor used.

SemiNested Polymerase Chain Reaction (PCR)

The PCR products obtained from 5' RACE were diluted and used as template for SemiNested PCR with *Pfu* DNA Polymerase (Thermo Fisher Scientific) and specific primers, according to the intended reaction (Table 3). The PCR primers used are specified in Table 1 and amplifications were performed as previously specified in *5' Rapid Amplification of cDNA ends (5' RACE)*. SemiNested PCR products were analysed by agarose gel electrophoresis as previously specified.

Table 3 - Templates and primers used for SemiNested PCR reactions and respective positive and negative controls. SemiNested PCR reactions are represented by letters A and C according to the RACE products used as template and highlighted with a light-grey background. Intern gene-specific primers (QCRT_F and QCRT_R) were used to assess the presence of the desired transcript and to determine the ideal template volume. Nuclease-free water was used as template to assess cross-contamination of PCR components in each reaction. All SemiNested PCR reactions were performed in triplicates.

		Template				
Primer forward	**Primer reverse**	RACE products from A1/C1	RACE products from A2/C2	RACE products from A3/C3	RACE products from A4/C4	Water
PrimerIIa	QCRT_R	A1/C1	A2/C2	A3/C3	A4/C4	**C-**
QCRT_F		A1/C1*	A2/C2*	A3/C3*	A4/C4*	**C-***

PCR products purification

After agarose gel electrophoresis analysis, SemiNested PCR products with estimated size higher than 900 base pairs (bps) were selected and purified from gel using PCR & Gel Purification kit (Grisp) according to manufacturer's protocol. The purified molecules were quantified with both µDrop™ plate (Thermo Fisher Scientific) and "in-gel" comparison to the used DNA ruler.

Insert: Vector Ligation Reaction

Purified products were ligated to pCR®-Blunt vector (Thermo Scientific) in a 10 :1 (insert: vector) proportion with Anza T4 DNA ligase (Invitrogen) according to manufacturer's protocol. A no-insert ligation was also performed to confirm the possibility of vector religation. It was used 2µL of each ligation product for transformation protocols.

Preparing electrocompetent *E. coli* cells

A glycerol-stock of *Escherichia coli* DH5α strain was pre-cultured in 5 mL of Luria-Bertani broth (LB broth) and incubated overnight at 37ºC with constant agitation (160 rpm). Subsequently, the pre-culture was used to inoculate 50 mL of LB broth and the primary culture was incubated at 37ºC with constant agitation (160 rpm) until it reached the desired optical density (OD_{600} = 0.6-0.8). The cell culture was collected by centrifugation at 6000 g (Eppendorf 5427 R) for 15 minutes at 4ºC. Subsequently, pelleted cells were resuspended in ice-cold milliQ water. Centrifugation and resuspension steps were repeated three times. Electrocompetent cells were stored at -80ºC until use after addition of 10% (v/v) sterile ice-cold glycerol and freezing in liquid nitrogen.

Transformation of *E. coli* DH5α by Electroporation

Ligation products were incubated on ice with a 50 µL aliquot of electrocompetent cells. After homogenization, the mixture was transferred to a 0.1 cm-gap Electroporation Cuvette (Bio-Rad) and incubated at room temperature for 5 minutes before applying the electric pulse in Micropulser™ (Bio-Rad). Cells were gently resuspended in 250 µL of LB broth and removed from the cuvette for regeneration. The regeneration step was performed by incubating the cells at 37ºC for 1 hour without agitation. Subsequently, the mixture was plated in a LB – 1.5% (w/v) agar plate supplemented with 50 µg/mL kanamycin. Plates were incubated at 37ºC overnight.

Colony PCR

Potential positive clones were selected and inoculated in 2 mL of LB broth supplemented with 50 µg/mL kanamycin (LB+Kan). The inoculums were incubated at 37ºC for 1h-2h with constant agitation (180 rpm). Subsequently, a 200 µL aliquot was collected and centrifuged at maximum velocity for 30 seconds (Eppendorf Minispin®) for media removal. The pellet was resuspended in 100 µL of water and 2 µL were used as template for Colony PCR.

The amplification reactions were performed with *Taq* DNA Polymerase (Fermentas) according to manufacturer's protocol and using gene-specific inner primers QCRT_F and QCRT_R, as previously described. Control reactions were prepared in the same conditions with different templates. As positive control, it was used a *E. coli* DH5α cell culture harbouring the partial coding sequence of Calreticulin. To assess possible contaminations a negative reaction was performed using nuclease-free water as template. Amplified products were analysed by agarose gel electrophoresis in a 2% (w/v) agarose gel prepared as previously specified.

Miniprep & Endonuclease Restriction Mapping reactions

Plasmid DNA of positive clones was extracted with GeneJET Plasmid Miniprep Kit (Thermo Fisher Scientific) according to manufacturer's protocol. Subsequently, the extracted plasmid DNA was submitted to endonuclease digestions using Anza *Eco*RI (Invitrogen), *Eco*RI Fast Digest (Thermo Fisher Scientific) and Speedy *Eco*RI (Nzytech) according to each manufacturer's protocol. All digested products were analysed by agarose gel electrophoresis as previously specified.

Ligation PCR for ligation reaction analysis

Ligation reaction products were diluted (1:10) in nuclease-free water. The diluted products were used as template for amplification with M13F (-20) and M13R universal primers using illustra™ PuReTaq Ready-To-Go PCR beads (GE Healthcare) according to manufacturer's protocol. As control reaction PCR reactions were performed using "re-ligated" and linear pCR®-Blunt vector as template. The amplified products were analysed by agarose gel electrophoresis as previously described.

Recombinant Protein Expression studies

A glycerol-stock of *Escherichia coli* BL21 (DE3) strain harbouring the recombinant plasmid pET-30a (+)::partial form Calreticulin (PfCRT) was pre-cultured in 10 mL LB + Kan and incubated overnight at 37ºC with constant agitation (160 rpm). Subsequently, the pre-culture was used to inoculate 50 mL LB + Kan and the primary culture was incubated at 37ºC with constant agitation (160 rpm) until it reached the desired optical density (OD_{600}= 0.6-0.8). An aliquot of the primary culture was collected for subsequent procedures. The primary culture was subdivided previously to induction with 300 µM (IPTG) and incubated in different temperature conditions: 1) Room temperature; 2) 28ºC; 3) 37ºC. The subdivided cultures were induced overnight with constant agitation (160 rpm). In parallel, a glycerol-stock of *E. coli* BL21 (DE3) without pET-30a (+) plasmid was grown in LB media and induced in the same conditions as cell growth control.

Cell cultures were collected by centrifugation at 6000 g (Eppendorf 5810 R) for 15 minutes at 4ºC. Pelleted cells were either stored at -20ºC until protein extraction (frozen) or immediately processed for protein extraction (fresh). Pelleted cells were resuspended in phosphate- buffered saline buffer (PBS – 1x: 137 mM NaCl, 2.7 mM KCl, 10 mM Na_2HPO_4, 1.8 mM KH_2PO_4, pH 7.4) and lysed by sonication – 5 pulses of 30 seconds with 30 seconds rest. After incubation on ice for 30 minutes, lysates were centrifuged at 14 000 g (Eppendorf 5810 R) for 15 minutes at 4ºC. The supernatant was collected and pellet was resuspended in the same volume of PBS (1x) that was used to resuspend pelleted cells. The resulting products were denominated as soluble fraction and insoluble fraction, respectively. Both fractions were analysed by SDS-PAGE.

Recombinant Protein Purification

E. coli BL21 (DE3) cultures were induced for protein expression and their total protein content was obtained as previously specified. Soluble fractions from frozen and fresh

cell pellets were diluted in Binding buffer (50 mM Tris, 300 mM NaCl, 5 mM Imidazole, pH 8.0) and incubated with Profinity™ IMAC Resin, Ni-charged (Bio-Rad) for 2 hours at room temperature with constant agitation. The resin was loaded on an Econo-Pac® Chromatography column (Bio-Rad) and the unbound fraction was collected. Resin incubated with soluble fractions obtained from frozen pellets was washed with 5 bed volumes of Washing buffer 1 (50 mM Tris, 300 mM NaCl, 100 mM Imidazole, pH 8.0). The washing step was repeated with Washing buffer 2 (50 mM Tris, 300 mM NaCl, 200 mM Imidazole, pH 8.0). Purified protein was eluted with 5 bed volumes of Elution buffer (50 mM Tris, 300 mM NaCl, 500 mM Imidazole, pH 8.0). Resin incubated with soluble fractions obtained from fresh cell pellets was washed with 5 bed volumes of Washing buffer 1 (50 mM Tris, 300 mM NaCl, 20 mM Imidazole, pH 8.0) followed by additional washes with Washing buffer 2 (50 mM Tris, 300 mM NaCl, 60 mM Imidazole, pH 8.0). Purified protein was eluted with 5 bed volumes of Elution buffer (50 mM Tris, 300 mM NaCl, 300 mM Imidazole, pH 8.0). Washing flow throughs were collected for further analysis by SDS-PAGE, as well as the unbound fraction.

Protein Extraction from pollen samples

Pollen protein content was obtained by pollen hydration suspended in 5% (w/v) PBS (1x) and incubated at 4ºC for 4 hours with constant stirring. Subsequently, the pollen suspension was centrifuged at 12250 *g* (Avanti J-20 XP – JA 25.50 rotor) for 20 minutes at 4ºC. The supernatant was filtered through a 0.45 µm filter (Millipore) and dialysed against ultra-pure water overnight at 4ºC. Dialysed supernatant was analysed by SDS-PAGE as subsequently indicated.

Concentration of protein extracts

Pollen protein and purified recombinant protein samples were filtered through a Centricon (Millipore) with a 10 kDa and 30 kDa cut-off respectively, in order to concentrate the total protein content in smaller volumes. Samples were centrifuged three times at 2500 *g* for 10 minutes (Eppendorf 5810 – swing-bucket rotor), resuspending the samples between centrifugations. Both concentrated protein samples and flow-through were stored at -20ºC for subsequent assays and for SDS-PAGE analysis.

Protein quantification

Total protein content from bacterial cultures was quantified with Qubit® Fluorometer (Thermo Fisher Scientific) according to manufacturer's protocol.

Total protein content from pollen samples and purified recombinant *An*CRT were quantified with Protein Assay kit (Bio-Rad), according to manufacturer's protocol for Standard Procedure for Microtiter Plates. Bovine Serum Albumin (BSA) was used as a protein standard at variable concentrations ranging from 25 µg/mL to 750 µg/mL. After the indicated time of incubation, absorbance values of standards and samples were read at 595 nm in a Spectra SLT spectrophotometer.

Zymography

To determine enzymatic activity of pollen extracts, total protein samples were electrophoretically separated in a 12.5% polyacrylamide gel copolymerized with 1 mg/mL gelatine. Protein extracts were incubated for 10 minutes at room temperature with gelatine's zymography Loading buffer [2x,125 mM Tris-HCl (pH 8.8), 4% (v/v) SDS, 20% (v/v) glycerol] in a 1:1 proportion. Samples were prepared under non-denaturing conditions to preserve their enzymatic activity. The proteins were separated electrophoretically in Electrophoresis buffer [25 mM Tris,192 mM Glycine, 10% (v/v) SDS] at constant voltage of 120 V for 100 minutes in a Mini Protean II system (Bio-Rad) covered with ice packs. Subsequently, to remove SDS and renature the retained proteins the gel was incubated twice in Renaturation buffer [0.25% (v/v) Triton X-100 in PBS] for 30 minutes with constant agitation at room temperature and overnight with fresh Renaturation buffer without Triton X-100 at 37ºC to increase sensitivity.

To detect gelatine's degradation by proteases existent in pollen protein extracts, polyacrylamide gels were stained with a Coomassie solution [0.2 % (w/v) Coomassie Brilliant Blue R-250, 1 V absolute ethanol, 1 V acetic acid, 5 V water] for 3 hours to overnight incubation at room temperature. The excess staining was removed by multiple washes with Destaining solution [1 V absolute ethanol, 1 V acetic acid, 5 V water].

Peptide proteolysis assay

To characterize proteolytic activity of pollen extracts, total pollen protein extracts (200 µL) were briefly incubated with 99 µM synthetic single- amino-acids/ peptides bound to an amine-containing fluorophore, the 7-amino-4-methylcoumarin (AMC). This experiment had three independent replicas, *i.e.* three independently prepared pollen extracts, with triplicates for each tested condition. The selected synthetic single- amino-acids/ peptides are represented on Table 4. After incubation with pollen extracts, the fluorescent peptides were hydrolysed resulting in the release of the AMC group. Consequently, the mixture's fluorescence increased due to the accumulation of the

released fluorescent molecule ($\lambda_{excitation}$ = 380 nm, $\lambda_{emission}$=460 nm). The fluorescence of the mixture was monitored for a 10- minute period divided in 20-second reads at 37ºC, using a SpectreMax-GeminiEM fluorimeter. The released AMC was graphically represented by relative fluorescence units (RFU) along the indicated 10-minute period. Subsequently, variation of RFU (ΔRFU) was calculated using two random points within the linear part of the reaction curve. To eliminate protein concentration variability of each pollen extract and subsequent statistical analysis, the ΔRFU values were normalized to ΔRFU per µg of protein.

Table 4 – Fluorescent AMC substrates used in enzymatic assays.

Substrate
L-LYS-AMC
L-ARG-AMC
L-MET-AMC
L-PHE-AMC
L-ALA-AMC
BENZOYL (BZ)-ARG
GLY-PRO-AMC
ALA-PRO-ALA-AMC
LEU-LEU-VAL-THE-AMC
BUTYLOXYCARBONYL (BOC)-PHE-SER-ARG-AMC
BOC-VAL-PRO-ARG-AMC
BOC-ALA-GLY-PRO-AMC

Peptide proteolysis assay after incubation with inhibitors

To classify proteases present in pollen extracts, peptide proteolysis assays were performed after incubation with class-specific protease inhibitors. Total pollen protein extracts (200 µL) were briefly incubated with 99 µM synthetic single- amino-acid bound to an amine-containing fluorophore, the 7-amino-4-methylcoumarin (AMC) – L-Phe-AMC – after incubation with class-specific protease inhibitors for 5 minutes at 37ºC (Table 5). Subsequently, fluorescence of the mixture was monitored for a 10- minute period divided in 20-second reads at 37ºC, using a SpectreMax-GeminiEM fluorimeter. This experiment also had three independent replicas, *i.e.* three independently prepared pollen extracts, with triplicates for each tested condition. Results were treated as previously described in "*Peptide proteolysis assay*".

Table 5 – Protease inhibitors used and correspondent effective concentration. It is also indicated the class of proteases that are inhibited and the reversibility of the inhibitory effects..

Inhibitor	Effective concentration (mM)	Targeted Protease Class	Reversibility of inhibition
Pefabloc	0.1	Serine	x
TLCK	0.1	Serine trypsin-like	x
TPCK	0.1	Serine chymotrypsin-like and some cysteine	x
Pepstatin a	0.001	Aspartic	✓
Bestatin	0.01	Aminopeptidases	✓
Leupeptin	0.01	Serine and cysteine	✓
EDTA	1	Metalloproteases	✓
$CaCl_2$	0.1	Metalloproteases	
$ZnCl_2$	0.1	Metalloproteases	
$MgCl_2$	0.1	Metalloproteases	
$MnCl_2$	0.1	Metalloproteases	

Cell culture

As experimental model, we selected a carcinogenic lung epithelial cell line obtained from the American Type Culture Collection – A549 (ATCC® CCL-185™). Cells were cultured in Eagle's Minimum Essential Medium (MEM – Sigma) supplemented with 0.22% (w/v) sodium bicarbonate, 10% (v/v) fetal bovine serum (FBS) heat-inactivated for 30 minutes at 56ºC and 5% PenStrep (Gibco). Cultures were maintained in 75 cm^2 flasks in a humidified atmosphere with 5% CO_2 at 37ºC. After reaching confluence, the cell culture was diluted 1:6 or 1:8 twice a week. In order to perform culture dilution, the cells were detached from the flask after incubation at 37ºC for 5-10 minutes with a Trypsin solution [0.25% (w/v) trypsin (Gibco), 1 mM EDTA in a saline solution with 130 mM NaCl, 3 mM KCl, 1 mM Na_2PO_4, 30 mM Hepes, 10 mM glucose; pH 7.3]. The experiments were performed between passages 18 and 34.

Stimuli application

After reaching confluence, cell cultures were washed with serum-free medium and the different stimuli were applied. Subsequently, cells were incubated for 6 and 24 hours or 24 hours only at 37ºC in a humidified atmosphere with 5% CO_2.

The stimuli consisted of concentrated protein extracts. To inhibit proteolytic activity of pollen extracts, concentrated protein samples were denatured for 20 minutes in boiling water and applied to cell cultures. Recombinant CRT was also denatured to alter its

conformational structure and annul potential interactions of the protein with cell receptors.

Pollen extracts were diluted in serum-free medium to reach a final concentration of 400 µg and 800 µg of total protein content per mL, except in indicated assays where only higher or lower protein concentration was tested. Recombinant protein was diluted in serum-free medium to reach a final concentration of 40 µg per mL. A mixture of pollen extract and purified recombinant protein was also diluted in serum-free medium to reach a final concentration of 400 µg per mL and 40 µg per mL, respectively. In Figure 4 it is represented the main test conditions.

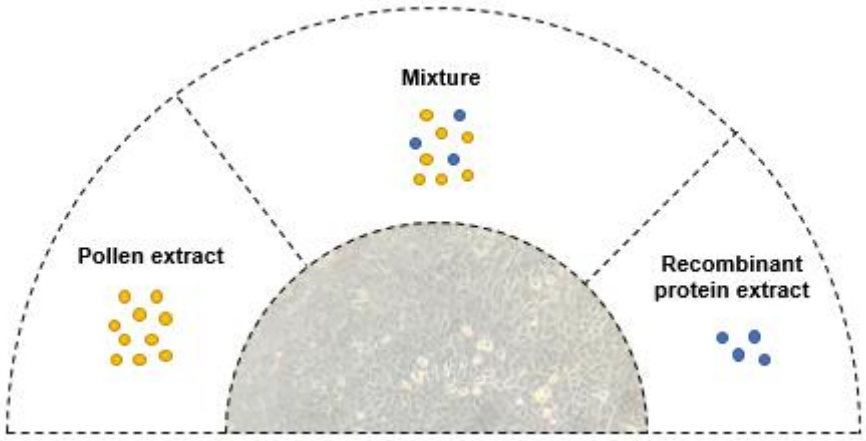

Figure 4 – Main conditions tested in cell cultures of A549 lineage. Cells were exposed to two distinct concentrations of pollen extracts diluted in serum-free media – 400 µg per mL and 800 µg per mL – and to the produced recombinant protein – 40 µg per mL. Cells were also exposed to a mixture of pollen and recombinant protein extracts – 400 µg per mL and 40 µg per mL, respectively. Extracts were heat-inactivated to eliminate any potential activity.

As control conditions, cell cultures were incubated with serum-free medium ($\mathbf{C^0}$), medium supplemented with FBS ($\mathbf{C^-}$) and serum-free medium diluted with 0.25% Trypsin solution (1:1) ($\mathbf{C^t}$).

Quantification of cellular detachment

Cellular detachment was quantified using methylene blue method (Hassim *et al*., 1998). Cells were cultured in 48-multiwell plates in a cellular density of $1x10^5$ cells/ cm^2. When confluence was reached, the culture was washed with MEM medium without FBS supplementation and incubated with the respective stimuli, as previously described. After the incubation period, culture media was removed or collected for further analysis and cells were washed twice with phosphate saline buffer (PBS – Sigma) and fixated for 20 minutes at room temperature with a paraformaldehyde solution (PFA - 4% (w/v)

paraformaldehyde, 4% sucrose dissolved in PBS). Subsequently to fixation, cultures were washed twice with 10 mM borate buffer (pH 8.4) and stained for 10 minutes at room temperature with 1% (w/v) methylene blue solution (in 10 mM borate buffer). Cells were washed with 10 mM borate buffer until excess dye was removed and allowed to air-dry overnight at room temperature or 3 hours at 37ºC. The formed precipitate was dissolved with 200 µL of 100% (v/v) ethanol – 100 mM Tris-HCl mixture (1:1) in constant agitation for 25 minutes at room temperature and transferred to a 96-multiwell plate. Absorbance values were read in Spectra SLT spectrophotometer with a 620-nm wavelength. Adherent cells (%) were relatively calculated by comparison with absorbance values of cells of the control condition, previously referred as C^0. Cellular detachment was determined in percentage using the following formula:

$$\textbf{Cellular detachment}\ (\%) = \textbf{100} - \textbf{Adherent cells}\ (\%)$$

This experiment had three independent replicas with triplicates for each condition tested.

Viability of detached cells

Viability of detached cells was evaluated by culture observation in an inverted light microscope 24, 48 and 72 hours after reculturing collected detached cells. Cells were cultured in 48-multiwell plates in a cellular density of $1x10^5$ cells per cm^2. When confluence was reached, the culture was washed with MEM medium without FBS supplementation and incubated with the respective stimuli, as previously described. After 24-hour incubation period, culture media was collected and centrifuged at 6000 g (Eppendorf 5714 R) for 5 minutes at 4ºC. The supernatant was collected and stored at -80ºC for further analysis and the cell pellet was washed with medium supplemented with FBS. Subsequently cell pellet was resuspended also in medium supplemented with FBS (300 µL) and plated in a 96-multiwell plate (100 µL/ well). To assess cell viability, the culture ability to re-adhere to the substrate and to proliferate was evaluated. This experiment had three independent replicas with triplicates for each condition tested.

Quantification of released cytokines

To proceed for released cytokines quantification cells were cultured in 48-multiwell plates in a cellular density of $1x10^5$ cells per cm^2. When confluence was reached, the culture was washed with MEM medium without FBS supplementation and incubated with the respective stimuli, as previously described. After 24-hour incubation period, culture

media was collected and centrifuged at 6000 g (Eppendorf 5417 R) for 5 minutes at 4ºC. The supernatant was collected and stored immediately at -80ºC until sample preparation for quantification. Released cytokines were quantified recurring to Cytometric Bead Array (CBA) assay using the FlowCytomix™ Multiple Analyte Detection Human Basic kit (discontinued – eBioscience® - Bender MedSystem GmbH) according to the manufacturer's instruction. This kit is composed by a bead mixture with different bead-sizes coated with capture antibodies that bind specifically to a set of cytokines – IL-6, IL-8, IFN-γ, IL-10, IL-5, TNF-α. After incubation of the bead mixture with an aliquot of collected supernatant containing the soluble cytokines, a biotin-conjugated secondary antibody was added to bind to the captured antibody. Subsequently, unbound antibodies were removed with several washes and a streptavidin-phycoerythrin substrate was added. Finally, the bead suspension was analysed in a FACSCalibur flow cytometer (BD Biosciences, San Jose, CA) to identify cytokines by bead size and correspondent fluorescence. Quantification of released cytokines was possible through the measurement of phycoerythrin fluorescence and comparison to standards of known concentrations. The obtained results were analysed with FlowCytomix™ Pro 2.4 Software (eBioscience® - Bender MedSystem GmbH) and expressed in picogram per millilitre (pg/mL). This experiment had three independent replicas with triplicates for each condition tested.

Cell extracts for immunodetection of proteins

To evaluate the integrity of proteins from intercellular junctional complexes, cell extracts were prepared after stimuli application in the specified conditions. Cells were cultured in 6-multiwell plates at in a cellular density of 8.5 $x10^4$ cells/ cm^2. When confluence was reached, the culture was washed with MEM medium without FBS supplementation and incubated with the respective stimuli, as previously described.

After incubation period, culture media was removed and cells were washed with ice-cold phosphate saline buffer (PBS – Sigma) supplemented with protease inhibitors – 1 µg/mL CLAP (Chymostatin, Leupeptin, Antipain and Pepstatin), 1 mM dithiothreitol (DTT) and 0.1 mM phenylmethanesulfonyl fluoride (PMSF). 300 µL of ice-cold PBS supplemented with protease inhibitors was added and adherent cells were scraped from the bottom of the well and transferred to Eppendorf tubes. Subsequently, the collected cells were centrifuged at 13000 rpm for 6 minutes and cell pellet was resuspended in boiled denaturing solution [2x, 100 mM Tris-Bicine or 100 mM Tris-HCl, 4% (v/v) sodium dodecyl sulphate (SDS), 6M Urea, 4% (w/v) β-mercaptoethanol, 0.001% (w/v)

Coomassie Brilliant Blue G-250]. Cells were incubated on ice for 20 minutes previously to cell lysis by sonication - 3 pulses of 5 seconds with 30 seconds rest between pulses. Samples were centrifuged at 13000 g for 6 minutes (Eppendorf 5417 R) at 4ºC and stored at -20ºC until needed. This experiment had three independent replicas with triplicates for each condition tested.

SDS-PAGE

Protein extracts were separated by sodium dodecyl sulphate polyacrylamide gel electrophoresis (SDS-PAGE) in 12.5% polyacrylamide gels under denaturing conditions in Electrophoresis buffer in a Mini Protean Tetra Cell system (Bio-Rad). Pollen and bacterial samples were denatured at 95ºC for 10 minutes. Cell extracts were denatured at 80ºC for 10 minutes. Pollen protein samples and cell extracts were denatured in 2x Denaturing solution [100 mM Tris-Bicine or 100 mM Tris-HCl, 4% (v/v) sodium dodecyl sulphate (SDS), 6M Urea, 4% (w/v) β-mercaptoethanol, 0.001% (w/v) Coomassie Brilliant Blue G-250]. Bacterial lysates were denatured in 1x Protein sample buffer [40 mM Tris, 1% (v/v) SDS, 5% (v/v) Glycerol, 0.0003% (v/v) Bromophenol blue, pH = 6.8]. To determine the molecular weight of protein bands an unstained protein standard (Precision Plus Protein ™ Standards - Bio-Rad) or a stained protein standard (PageRuler™ Plus Prestained Protein Ladder - ThermoScientific), both with known molecular masses ranging 10-250 kDa, respectively, were also applied in gels.

To detect proteins, polyacrylamide gels were stained with a Coomassie solution [0.2 % (w/v) Coomassie Brilliant Blue R-250, 1 V absolute ethanol, 1 V acetic acid, 5 V water] for 1 hour to overnight incubation at room temperature. The excess staining was removed by multiple washes with Destaining solution [1 V absolute ethanol, 1 V acetic acid, 5 V water].

Immunodetection of proteins

For immunodetection of proteins, the cell extracts prepared as previously described were denatured at 80 ºC for 10 minutes. Bacterial extracts were denatured at 95ºC for 5 minutes. Subsequently, samples were electrophoretically separated in a 12.5% SDS-PAGE gel as previously specified. After electrophoresis, proteins were transferred to a PVDF membrane after its activation in absolute ethanol for 30 minutes. The electrotransference was performed in Transfer buffer [25 mM Tris, 192 mM Glycine, 20% (v/v) absolute ethanol] supplemented with 1.5 mL of 10% (w/v) SDS per membrane, with

constant agitation in a Mini Protean II system (Bio-Rad) covered with ice-packs for 2 hours under a constant voltage of 100V.

Subsequently, the PVDF membranes were incubated in Blocking solution [5% (w/v) milk diluted in TBS-T (20 mM Tris-HCl; 137 mM NaCl; 0.1% Tween 20)] for 1 hour at 37ºC or overnight at 4ºC. After removing the excess of Blocking solution with TBS-T washes, membranes were incubated with primary antibody diluted in Blocking solution or in 0.1% Blocking solution with 0.2% Sodium Azide for 1 hour at room temperature or overnight at 4ºC. The membranes were then incubated with the respective secondary antibody conjugated with alkaline phosphatase. Primary and secondary antibodies varied accordingly to the detected protein, however their information and specific conditions are specified in Table 6. Immunodetection of β-actin was performed to assess the quality of loaded samples and to serve as reference protein between tested conditions.

Table 6 – Primary and secondary antibodies used in Immunoblotting techniques.

Antibody	Detected protein	Secondary antibody	Conjugated with	Revealed with	Detected with
Anti-Calreticulin	Calreticulin	Anti- rabbit IgG (1:10000 – invitrogen®)	Alkaline Phosphatase (AP)	Novex™ AP Chromogenic substrate (Thermo Fisher Scientific)	Chemidoc
Anti- E-cadherin	E-cadherin	Anti- mouse IgG (1:10000 – SIGMA)	Alkaline Phosphatase (AP)	ECF substrate (GE Healthcare)	STORM
Anti- Occludin	Occludin				
Anti- ZO- 1	Zonula occludens -1				
Anti- β- actin	β- actin				

Membranes were revealed using a Novex™ AP Chromogenic substrate (BCIP-NBT, Thermo Fisher Scientific) or ECF substrate (GE Healthcare) according to manufacturer's protocol, and photographed in a Chemidoc system (Bio-Rad) or in a STORM scanner respectively. After revelation, membranes were stored at 4ºC protected from light in order to proceed for membrane reprobing. Resulting bands were analysed and quantified using Image Lab (Bio-Rad) or Image Studio Lite (Li-cor). Relative quantity of each immunodetected protein was calculated after comparison to the reference protein β-actin of each sample.

Reprobing membranes

Membranes were prepared for reprobing after re-activation in absolute ethanol. Subsequently, membranes were equilibrated in TBS buffer (20 mM Tris-HCl; 137 mM NaCl). Bound antibodies were removed after washing membranes for 10-15 minutes with Stripping Buffer (0.2 M NaOH). After removing the excess of Stripping buffer with TBS-T washes, membranes were reprobed as specified in "*Immunodetection of proteins*" procedure after incubation with Blocking solution.

Datasets constructed for *in silico* analysis

Two datasets were used for *in silico* analysis: one containing CRT's coding sequences of *Arabidopsis thaliana*, *Brassica oleracea* var. *oleracea* and *Chlamydomonas reinhardtii* (dataset A – Table 7); and other containing CRT's coding sequences of *A. negundo*'s partial CRT and isoforms CRT1a and CRT1b from *A. thaliana* (dataset B). For dataset A construction nucleotide sequences of the different CRT isoforms of *A. thaliana* (*At*CRT1a, *At*CRT1b and *At*CRT3 – table 7) were obtained from GenBank databases via NCBI (http://www.ncbi.nlm.nih.gov). All sequences were used as query against the nucleotide collection database to obtain corresponding sequences of CRTs in *B. oleracea* var. *oleracea* by BLASTN analysis at NCBI. In order to obtain an out-group sequence previously used in other studies (Persson *et al*., 2003), it was performed a BLASTX analysis at NCBI using the same *A. thaliana* CRT sequences as query against the non-redundant protein sequences database limited to *C. reinhardtii* and a CRT nucleotide sequence of *C. reinhardtii* was retrieved from the analysis (Table 7). In regard of dataset B the same nucleotide sequence retrieved for dataset A were used. All sequences were translated into protein sequences using a translator tool from ExPASy portal (http://web.expasy.org/translate/) (Artimo *et al*., 2012).

Table 7 – Accession number, nomenclature given to the sequences retrieved from BLASTN and BLASTX analysis at NCBI for dataset A construction.

Accession no.	Calreticulin isoform	Source Organism
gi|186491349	*At*CRT1a	*Arabidopsis thaliana*
gi|145335312	*At*CRT1b	
gi|186478267	*At*CRT3	
gi|922566245	*Bo*CRT1a	*Brassica oleracea var. Oleracea*
gi|922544374	*Bo*CRT2 (1b)*	
gi|922552756	*Bo*CRT3	
gi| 159462861	*Cr*CRT	*Chlamydomonas reinhardtii*

*specified in this work as *Bo*CRT1b

Sequence alignments and Phylogenetic analysis

Multiple alignments of nucleotide sequences and respective protein-translated sequences from each dataset were performed using ClustalW (Thompson *et al*., 1994) and Muscle (Edgar, 2004) algorithms of the MEGA 7.0.26 software package (Tamura *et al*., 2013). The ClustalW alignment was carried out using the IUB DNA Weight matrix, with an open gap penalty of 15 and an extend gap penalty of 6.6. The Muscle alignment was carried out using a UPGMB clustering method with an open gap penalty of -400 and an extend gap penalty of 0. Although, only dataset A was used for phylogenetic analysis.

Two phylogenetic methods were used to infer the presented trees: neighbour-joining [NJ; (Saitou and Nei, 1987)] and maximum-likelihood [MLH; (Felsenstein, 1981)] methods under the default parameters – NJ with Tajima-Nei model as Substitution model for nucleotide sequences, Poisson model for protein sequences and Pairwise deletion in both analysis; MHL with Tamura-Nei model as Substitution model for nucleotide sequences, Jones-Taylor-Thornton model for protein sequences and partial deletion of missing data (site coverage cut-off : 95%) and Nearest-Neighbour- Interchange heuristic method for tree inference in both analysis –, both conducted in MEGA 7.0.26 software package (Tamura *et al*., 2013). The consensus trees presented were constructed and drawn with MEGA 7.0.26 tree display tools. The topology of the trees was evaluated by bootstrap analysis based on 1000 resamplings.

The alignments of dataset B were uploaded into Jalview software (Waterhouse *et al*., 2009) to analyse conservation values within the selected amino-acidic sequences.

In silico characterization of isolated *An*CRT sequence

The partial recombinant protein *An*CRT was characterized using several software and databases available online. Protein's theoretical isoelectric point and molecular weight were predicted recurring to ExPASy's "Compute pI/MW" tool (http://web.expasy.org/compute_pi/) (Artimo *et al*., 2012; Gasteiger *et al*., 2005). The respective hydropathicity was calculated by ProtParam web-tool (http://web.expasy.org/protparam/) (Artimo *et al*., 2012; Gasteiger *et al*., 2005). To evaluate recombinant protein predicted functionality we used several web-tools to assess distinct parameters. The isolated sequence was used as query in ScanProSite (http://prosite.expasy.org/scanprosite/) which retrieves functional domains of the submitted sequence (Artimo *et al*., 2012; de Castro *et al*., 2006). *An*CRT secondary and tertiary structures were predicted and analysed by Phyre^2 online software (http://www.sbg.bio.ic.ac.uk/~phyre2/html/page.cgi?id=index) (Kelley *et al*., 2015). At last, ligand binding sites were predicted with 3DLigand site web-tool (http://www.sbg.bio.ic.ac.uk/3dligandsite/) (Wass *et al*., 2010).

Prediction of post-translational modifications

Post-translational modifications, namely N- glycosylation and phosphorylation, were predicted recurring to a free online software. The glycosylation profile of the protein sequences previously translated – *An*CRT, *At*CRT1a and *At*CRT1b – was constructed using NetNGlyc 1.0 Server (http://www.cbs.dtu.dk/services/NetNGlyc/) – described elsewhere (Gupta *et al*., 2004). Phosphorylation profile of such sequences was determined using NetPhos 3.1 Server (http://www.cbs.dtu.dk/services/NetPhos/) (Blom *et al*., 1999). To assess the quality of prediction, *A. thaliana* sequences were submitted as query in PhosPhAt 4.0 web-tool (http://phosphat.uni-hohenheim.de) (Durek *et al*., 2010).

Statistical analysis

Results of this work were submitted into GraphPad Prism® 6 software to proceed for statistical treatment. Results are represented as mean ± standard error of the mean (SEM) of every independent experiment and correspondent replicas. Subsequently, results from each experiment were analysed by one- or two-way ANOVA followed by Dunnet's or Sidak's multiple comparisons test. Statistical differences were considered significant for p-values inferior to 0.05 ($p<0.05$).

Chapter III – Results

In previous works of our laboratory, complementary DNA (cDNA) coding for *Acer negundo*'s Calreticulin (*An*CRT) was isolated, cloned and recombinantly produced for preliminary immunoreactive assays. Although, BLASTN analysis of the obtained sequence revealed that it corresponded to an incomplete sequence.

The obtained sequence was aligned with both nucleotide and protein sequences of several calreticulin isoforms from *Arabidopsis thaliana* and *Brassica oleracea* var. *oleracea* in order to determine which isoform was close-related to the partial *AnCRT* isolated. As indicated in Figure 5, the distinct CRT isoforms grouped according to protein isoform and not according to the respective species.

Phylogenetic analysis revealed that the provided *An*CRT sequence was more close-related to isoforms CRT1a and CRT1b of *A. thaliana* and *B. oleracea* var. *oleracea* than to isoform CRT3 – which is supported by high bootstrap values (> 95%). However, it was not possible to verify which isoform was most similar to the isolated sequence giving that the evolutionary tree represents *An*CRT on an isolated branch. This could represent high variability of the sequence when compared to the node that included AtCRT1a/1b isoforms or insufficient information given by the provided sequence – since the AnCRT sequence had less nucleotides than the remaining sequences of the dataset.

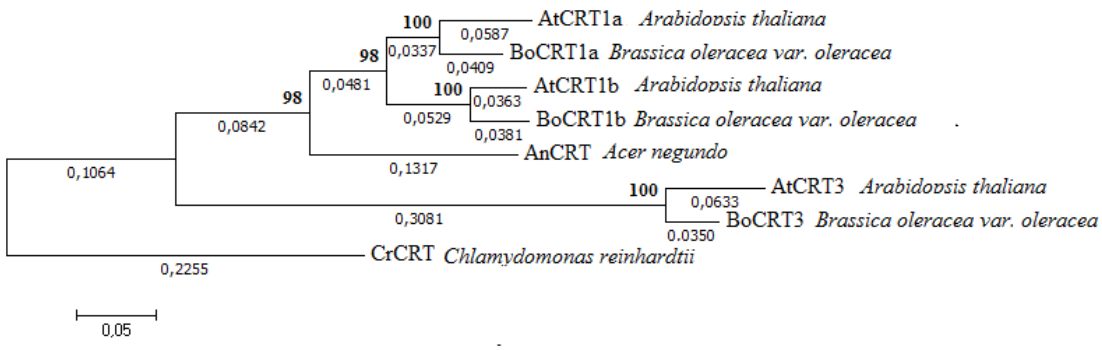

Figure 5 - Evolutionary relationships between *Arabidopsis thaliana*'s and *Brassica oleracea* var. *oleracea*'s CRT isoforms and provided CRT sequence of *Acer negundo*'s Calreticulin (Dataset B). The evolutionary history was inferred by using the Maximum Likelihood method based on the Tamura-Nei model (Tamura and Nei, 1993). The tree with the highest log likelihood (-6075,1678) is shown. The percentage of trees in which the associated taxa clustered together is shown next to the branches. Initial tree(s) for the heuristic search were obtained automatically by applying Neighbour-Join and BioNJ algorithms to a matrix of pairwise distances estimated using the Maximum Composite Likelihood (MCL) approach, and then selecting the topology with superior log likelihood value. The tree is drawn to scale, with branch lengths measured in the number of substitutions per site (next to the branches). The analysis involved 8 nucleotide sequences. Codon positions included were 1st+2nd+3rd+Noncoding. All positions with less than 95% site coverage were eliminated. That is, fewer than 5% alignment gaps, missing data, and ambiguous bases were allowed at any position. There was a total of 1119 positions in the final dataset. Evolutionary analyses were conducted in MEGA7 (Tamura *et al*., 2013).

Due to inconclusive results of the phylogenetic analysis performed, the obtained partial sequence was aligned with CRT1a/1b protein sequences from *A. thaliana*. As expected, the alignment revealed high conservation throughout the protein sequence

(Figure 6). The least conserved region of the alignment corresponds to a portion of the C-terminal domain. Additionally, there is a gap of 9 amino-acids in the *An*CRT sequence in the specified region. The initial region cannot be taken in consideration since it was lacking information on *An*CRT sequence.

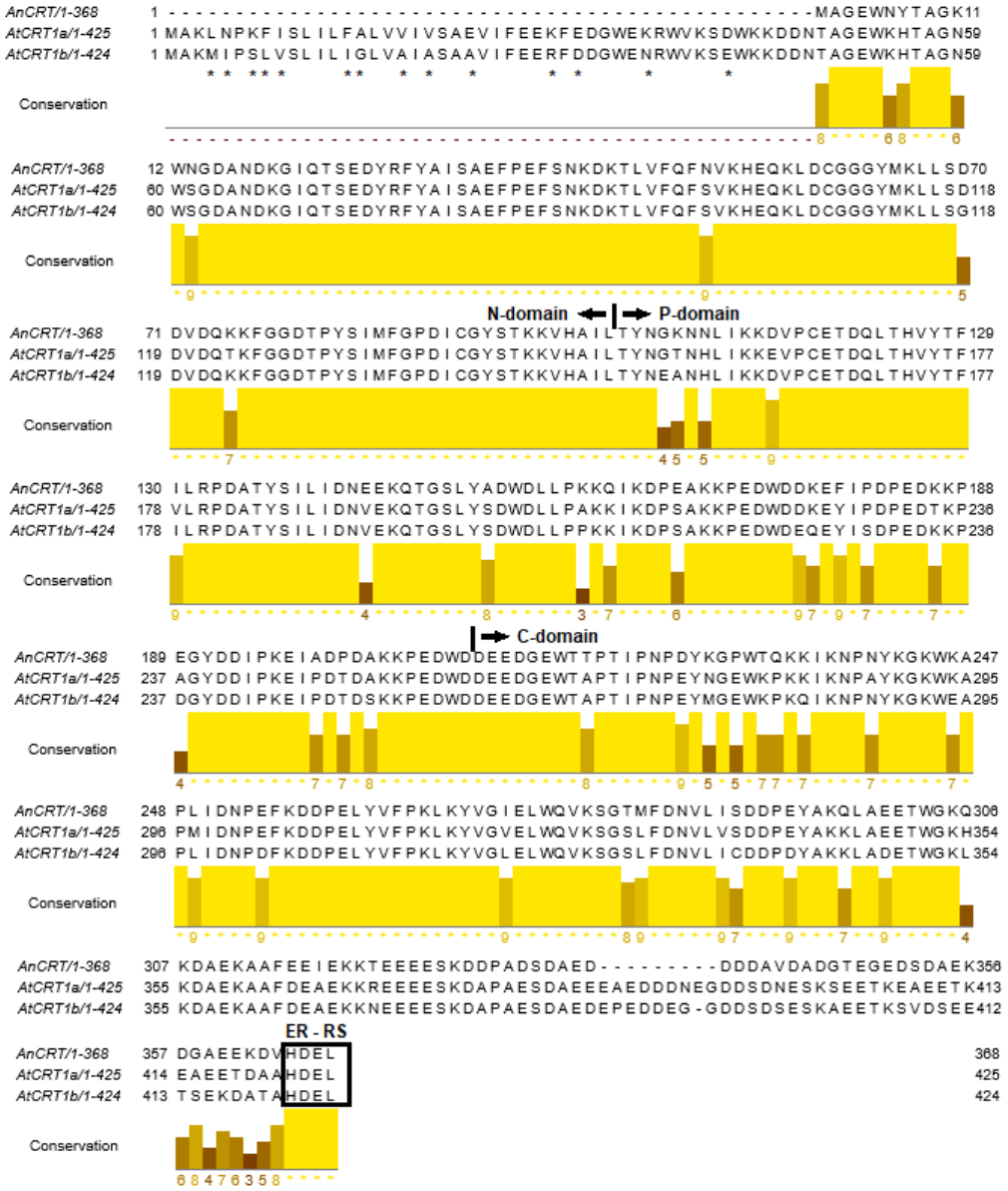

Figure 6 – Comparison of protein sequences of *Arabidopsis thaliana* isoforms and isolated partial CRT sequence of *Acer negundo*. Protein sequences of *A. thaliana* CRT1a and CRT1b were retrieved from GenBank (accession no. gi|186491349 and gi|145335312, respectively) and aligned with the obtained *An*CRT sequence. The aligned sequences were uploaded in Jalview software (Waterhouse *et al*., 2009) and conservation values are represented in a scale of 0 to 10 with corresponding colour-code. The putative domain limits (N-, P- and C-domain) and ER-retention signal (ER-RS) are also indicated. The asterisks indicate amino-acidic differences between *At*CRT1a and *At*CRT1b isoforms in the N-terminal portion of the protein. The figure was adapted from Christensen *et al*. (2008).

Generating complete cDNA molecules of *Acer negundo*'s Calreticulin

As previously presented, the partial cDNA lacks the 5' end that potentially corresponds to 48 amino-acids of the N-terminal domain. Given that one of the goals of this project was to obtain the complete coding sequence of *An*CRT it was implemented an optimized 5' – Rapid Amplification of cDNA Ends (RACE) technique – RNA Ligase Mediated RACE (RLM-RACE) (Suzuki *et al*., 1997). After reverse transcription of a selected pool of full transcripts, molecules harbouring the SMARTIIa adaptor were amplified recurring to an inner gene-specific primer (CRT_R2 or QCRT_R) and to a SMARTIIa complementary primer.

Gel electrophoresis of RLM-RACE amplification products revealed unspecific patterns and smears perchance due to molecule variability. However, template quality and gDNA contamination was assessed through control reactions – positive: α-actin gene amplification; negative: reactions with non-reverse transcribed RNA as template. Positive control reactions retrieved products with expected size (200 base-pairs - bps), despite having variable band intensity indicating variations in template concentration. Also, there was no gDNA contamination since negative control did not produce any band (Figure 7).

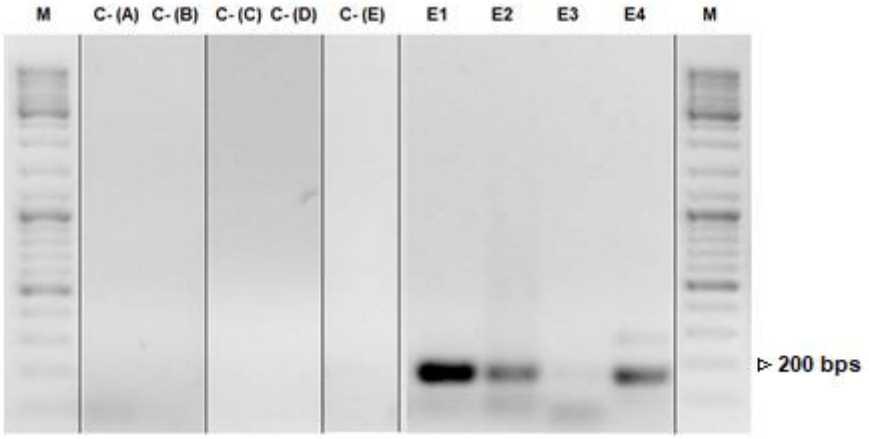

Figure 7 – Evaluation of template quality and assessment of gDNA contamination. Template quality was evaluated through amplification of α-actin gene and revealed amplification products with expected size (~200 bp – lanes E1-E4). The produced cDNA pool was not contaminated as confirmed by the absence of amplification products when used non-reverse transcribed RNA as template for PCR reactions [lanes C- (A-E)].

To increase the number of desired molecules, *i.e.* transcripts that suffered CAP replacement and possibly could encode the lacking sequence of *An*CRT, RLM-RACE products were reamplified in a SemiNested PCR using the inner gene-specific QCRT_R primer and the SMARTIIa complementary primer. Amplification products revealed a

specific band pattern in most reactions with bands ranging between 200 and 1500 bps in templates submitted to enzyme treatment prior to cDNA production (Figure 8 – top). Templates that were reverse transcribed directly after RNA extraction revealed a specific band pattern with lengths also comprised between 200 and 1500 bps, even though bands above 600 bps were not as visible as previously enzyme-treated cDNA amplification products. The noted differences between both templates indicated that the enzyme treatment performed prior to cDNA production increased the probability of isolating the missing portion of *An*CRT sequence. Only well-defined bands with a size superior to 900 bps were purified from gel since the reverse primer used annealed in a region comprised between bp number 544–563 of the known sequence. Moreover, according to the previously presented alignment it was still missing at least 144 bps until the 5'- end of the coding sequence.

Control reactions were also performed using inner gene-specific primers to assess template quality. All control reactions amplified products with expected size (~130 bps) except the ones that used RLM-RACE products originated from cDNA sample number 2 (Figure 8 – bottom).

After PCR product purification, the retrieved molecules were quantified in order to proceed for ligation reactions with pCR®-Blunt plasmid. Samples that did not provide positive A_{260}/A_{280} ratios due to possible ethanol contamination were quantified "in gel" by comparison with DNA GeneRuller. Although it should be noted that the ladder indicated concentration values may not correspond giving that the buffer used in gel electrophoresis was different from the indicated in DNA GeneRuller product information. After insert-vector ligation, the recombinant molecules were transformed in competent *E. coli* DH5α cells. DH5α *E. coli* cells were also transformed with linear pCR®-Blunt submitted to ligation reaction with and without T4 DNA Ligase to verify possible vector religation.

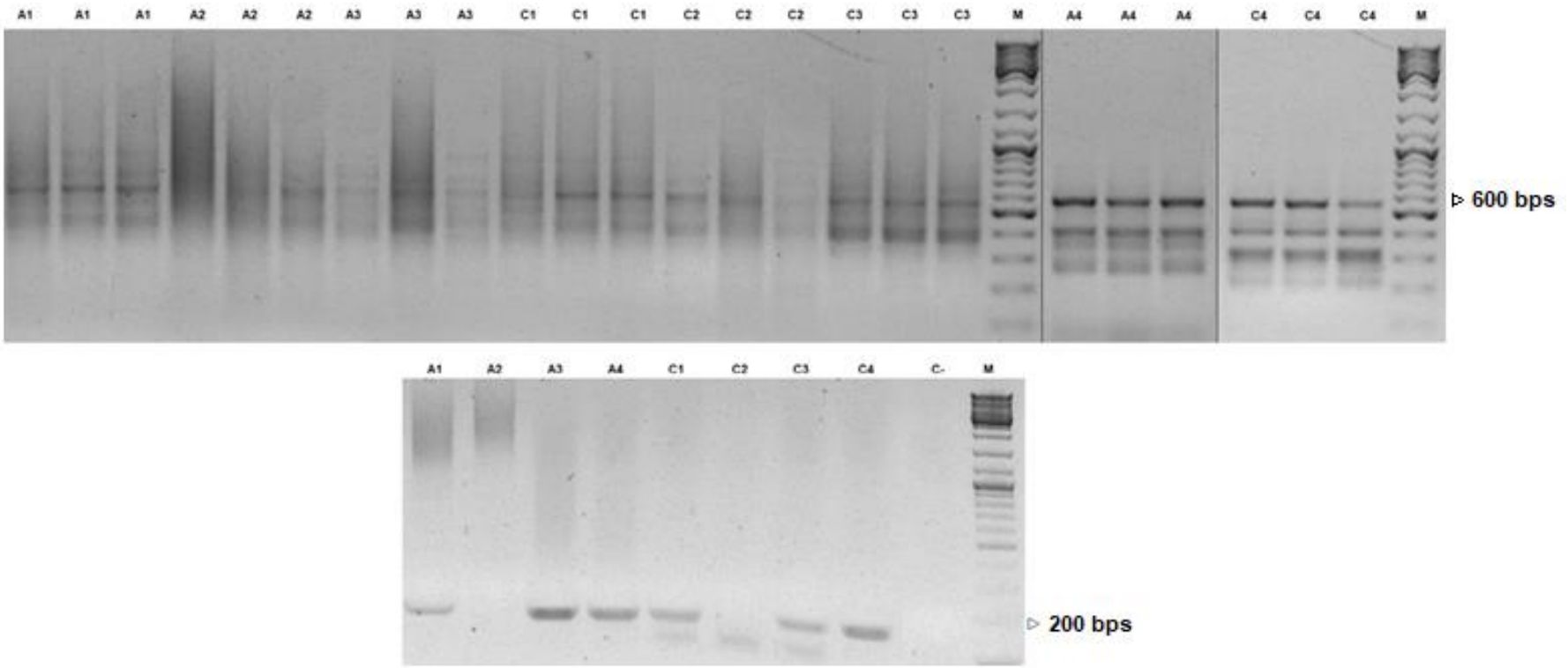

Figure 8 – SemiNested amplification products. SemiNested PCR reactions were performed to increase the desired molecules possibly harbouring the missing part of *Acer negundo*'s Calreticulin (*An*CRT) coding sequence. These reactions were performed in triplicates and with different templates – RLM-RACE products resulting from enzyme-treated RNA (A1-A3 and C1-C3) and products resulting from untreated RNA (A4 and C4).

Cells possibly harbouring the recombinant plasmid were selected recurring to selective media since the selected plasmid has a kanamycin resistant gene. A few colonies were selected to perform ColonyPCR using inner gene-specific primers (QCRT_F and QCRT_R). Electrophoretic analysis of ColonyPCR products revealed that some of the selected colonies used as template produced a band with the expected size of 130 bp (data not shown). Subsequently, the colonies that had positive results in ColonyPCR were selected for plasmid extraction in order to confirm insert presence and orientation by restriction reaction. The results of restriction reaction were inconclusive, since it was produced a single band of approximately 3500 bps, which correspond to the vector size (3519 bp, vector map in Supplemental Figure 1). However, the restriction reaction's positive control produced two fragments as expected since the plasmid used had three EcoRI restriction sites (data not shown).

Given the questionable results of the restriction reactions with the recombinant vector, it was performed a Ligation PCR as previously specified. Electrophoretic analysis of Ligation PCR products revealed two bands with ~3500 and ~200 bp, which corresponded to the size of the vector and to the distance between the universal primers used in the reaction (Figure 9). It was confirmed that the ligation reaction did not produce the desired recombinant molecule, *i.e.* insert-vector, and that potentially positive colonies grew selectively due to a vector-vector recombinant molecule formed.

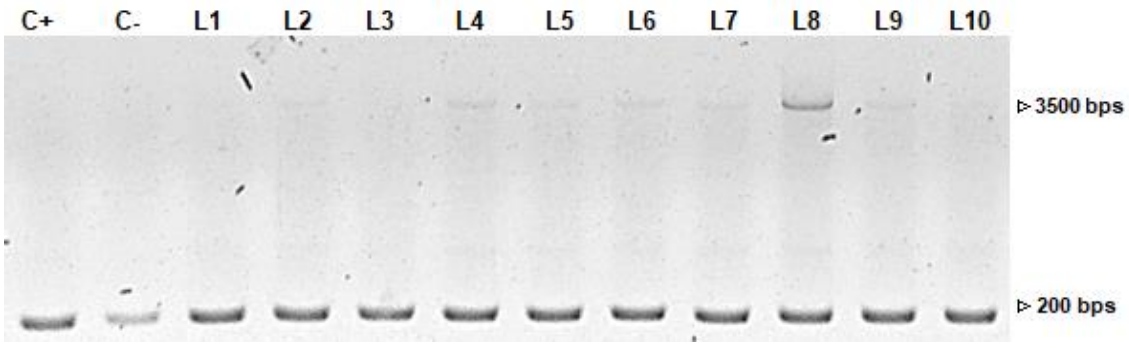

Figure 9 – Ligation PCR amplification products. Every amplification reaction produced a product with a size of approximately 200 bp, which corresponds to the distance between universal M13 primers used when there is not an insert flanking the region. Although only control reactions - with "religated" (C+) and linear (C-) pCR®-Blunt vector – produced single bands. When Ligation products (L1- L10) were used as templates, amplification products resulted in two bands – one additional band of approximately 3500 bp that corresponds to the size of the vector without insert.

Producing recombinant *Acer negundo*'s partial Calreticulin

Due to lack of time it was not possible to repeat the cDNA library construction to complete the partial form (Pf) of *An*CRT. Although, the incomplete recombinant protein was produced to accomplish the remaining goals of the project since there were previous indications of its immunoreactivity.

To proceed for protein production, BL21 (DE3) cells harbouring a pET-30a (+)::PfCRT were induced for protein expression and subdivided as previously indicated in *Materials and methods* chapter (pET-30a (+) vector map in Supplemental Figure 2). Three temperatures were tested – room temperature, 28ºC and 37ºC – to perceive which one was more indicated for this specific protein. Total soluble protein content of BL21 (DE3) *E. coli* cells with and without the recombinant plasmid exposed to the different temperatures after induction were evaluated through SDS-PAGE and Western Blot for immunodetection of recombinant protein (Figure 10). It was clear that at 37ºC occurred recombinant protein aggregation, retaining the protein in the insoluble fraction, since there is no signal of recombinant CRT in the soluble protein content of that culture – neither on SDS-PAGE nor on Western Blot. Although, in cultures submitted to room temperature and to 28ºC the expression of the recombinant protein was clear. By analysing the SDS-PAGE profile it was possible to verify that recombinant protein was produced with relatively high yields in both conditions taking into consideration that gels were loaded with 20 µg/mL of total protein content and that the heterologous protein produced a prominent band comparatively to other *E. coli* proteins. Although, for protein purification it was selected induction at 28ºC since room temperature had uncontrollable temperature variations.

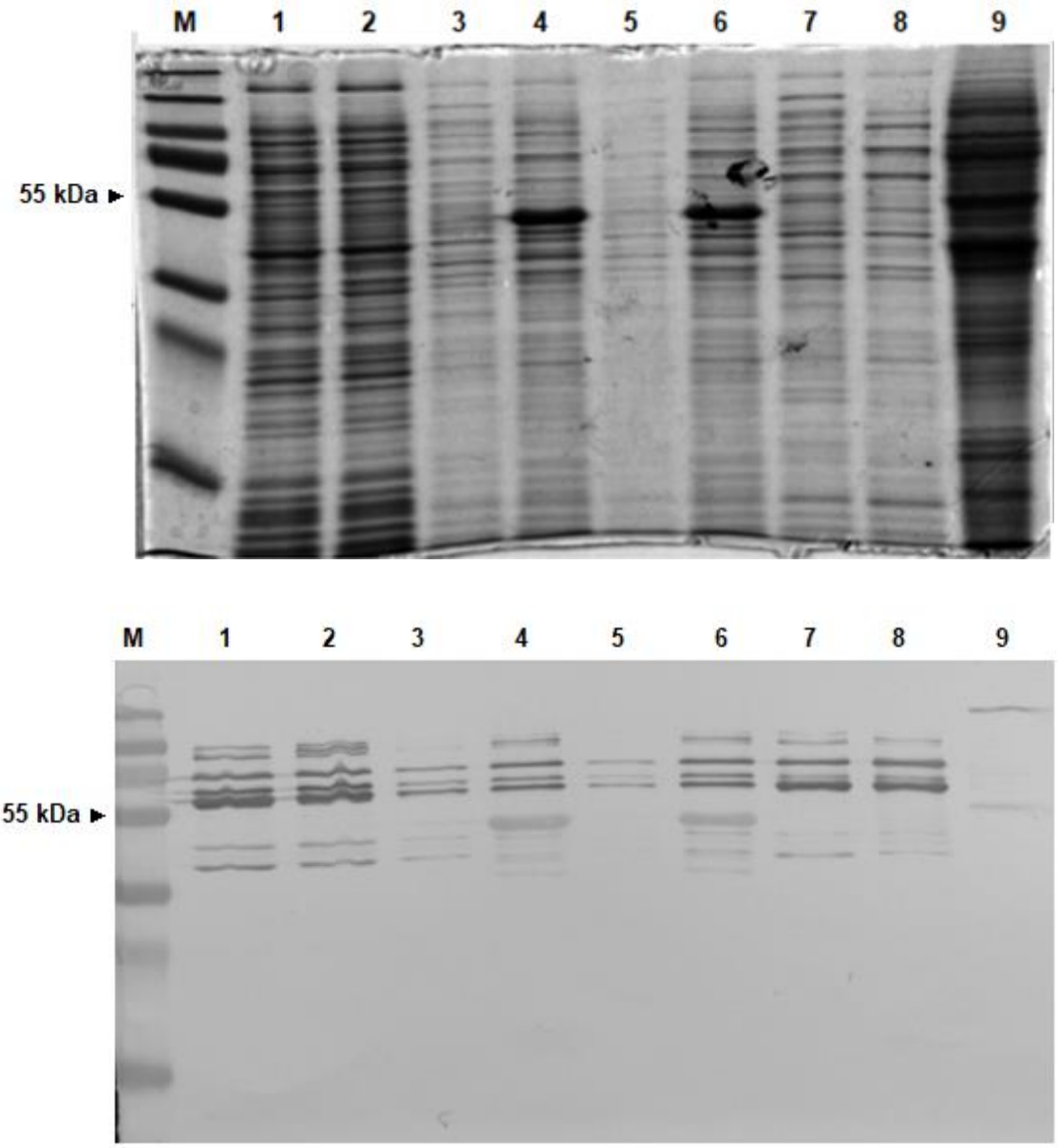

Figure 10 – (A) SDS-PAGE of total soluble proteins and (B) Immunodetection of recombinant Calreticulin in total soluble protein content of *E. coli* expression strain BL21 (DE3) without plasmid and with pET-30a (+)::PfCRT recombinant plasmid. It is represented the total protein content before induction with IPTG (300 µM) (lanes 1 and 2) and after induction post- overnight incubation at: room temperature (lanes 3 and 4); 28ºC (lanes 5 and 6); and 37ºC (lanes 7 and 8). As control sample, it was also separated the total soluble protein of *Acer negundo's* pollen extracts (lane 9). Total protein content of BL21 (DE3) harbouring the recombinant pET-30a (+) plasmid correspond to lanes 2, 4, 6 and 8. The same amount of protein was loaded (20 µg/µL). It is possible to distinguish an intense band in lanes 4 and 6 that represents the produced recombinant protein. Western Blot with anti-calreticulin rabbit IgG (1:10000) revealed the presence of the recombinant protein in total soluble protein content of induced *E. coli* BL21 (DE3) with approximately 50 kDa. The anti-calreticulin rabbit IgG also detected native Calreticulin in pollen protein extracts with approximately 55 kDa and 250 kDa.

Protein expression was scaled up for protein purification through IMAC. Subsequently to bacterial cell lysis, samples were centrifuged to collect supernatant containing soluble proteins. The supernatant was diluted with Binding Buffer to reduce binding of proteins with some nickel-affinity due to its histidine content. The lysate was loaded on the IMAC

column and washed with Wash Buffers with intermediate Imidazole concentration (Wash 1 with 20 or 100 mM Imidazole; Wash 2 with 60 or 200 mM Imidazole) to elute weakly bound contaminants without compromising the final yield of recombinant protein purification. Finally, recombinant protein was eluted from IMAC column with Elution Buffer containing higher Imidazole concentration (300 or 500 mM Imidazole).

It was necessary to adjust Imidazole concentration in Wash and Elution Buffers during purification procedure due to variation in protein expression yields of independently induced BL21(DE3) cultures. All collected fractions were analysed by SDS-PAGE, as previously referred. Consequently, fractions with no detectable contaminants were mixed and concentrated using a concentrator with a 30 kDa cut-off membrane. We detected two bands with ~50 kDa and ~100kDa in the concentrated extract, corresponding to rCRT and oligomerized rCRT respectively (Figure 11). The oligomerization of rCRT produced in prokaryotic systems was described in other works (Hong *et al*., 2010; Huang *et al*., 2013) and it is inevitable due to one of its main functions – *i.e*. binding of misfolded/ denatured proteins.

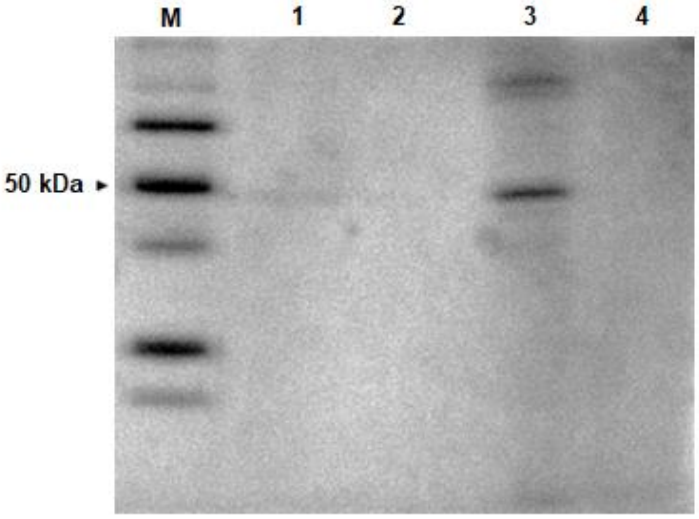

Figure 11 - Analysis by SDS-PAGE of processing steps of recombinant PfCRT produced by *E. coli* expression strain BL21 (DE3) harbouring pET30a::PfCRT recombinant plasmid. It is presented pre- and post- dialysis samples (lanes 1 and 2, respectively); post-concentration sample (lane 3) and its correspondent flow-through (lane 4). The same volume (25 µL) was loaded in each well without protein quantification. It is possible to distinguish an intense band with approximately 50 kDa in concentrated samples that possibly represents the produced recombinant protein. It is also noticeable the presence of a less intense band with approximately 100 kDa also in concentrated samples that possibly represents recombinant protein oligomerization. The pre- and post- dialysis samples did not reveal any bands, as well as flow-through fraction.

Characterizing recombinant *Acer negundo*'s partial Calreticulin

The recombinant CRT partial protein had a theoretical isoelectric point and molecular weight of 4.34 and 42055 Da, respectively. Relatively to its hydropathicity, the web-tool used suggested that the produced protein was hydrophilic with a grand average of hydropathicity (GRAVY) value corresponding to -1.121.

The partial protein sequence was submitted in another web-tool to analyse functional domains. The ScanProSite tool identified 5 hits from 4 distinct domain patterns: two calreticulin family signature between residues 53-68, and 85-93, that correspond to two signature motifs in plants CRT N-domain previously specified (KHEQKLDCGGGYVKLL and IMFGPDICG); two calreticulin family repeated motif signatures between position 163-175 and 198-210, that possibly correspond to the two proline-rich motifs A and B previously described, despite one of the signature motifs had a low confidence level; and the endoplasmic reticulum targeting sequence between residues 365-368, the HDEL tag.

Given the importance of protein structure to protein functions and interactions, the secondary and three-dimensional structure of the recombinant *An*CRT was predicted as previously described. The Phyre^2 web-server retrieved a three-dimensional structure modelled based on a similar (55% identity) known calreticulin (ID no. 3RG0 – Protein Data Bank - PDB) with 81% coverage of the submitted *An*CRT sequence. It is possible to distinguish a globular domain and an arm-like structure, characteristic of this protein family (Figure 12 – top). Moreover, this web-tool also indicated the protein's secondary structure. The predicted *An*CRT secondary structure (Figure 12 - bottom) was mainly composed by disordered structures (30%), followed by beta-sheets (24%) and alpha-helices (16%). Relatively to the confidence values of predicted structures it was noted that disordered structures had lower confidence values except on the C-terminal region where it reaches the highest values. The remaining secondary structures had high confidence levels in comparison to disordered structures.

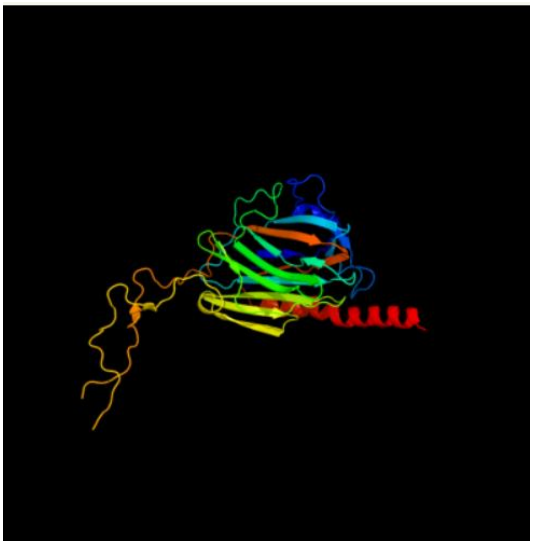

Figure 12 – Predicted tertiary (top) and secondary (bottom) structure of *Acer negundo*'s CRT predicted by Phyre[2] tool. Tertiary structure was modelled based on the most similar and with higher coverage homologue protein (id no. 3RG0, PDB) to the submitted partial *An*CRT coding sequence. The modelled structure revealed a globular structure with an arm-like protuberance as described for Calreticulin protein family. Relatively to secondary structure, the software predicted that the secondary structure of the protein is mostly composed by disordered regions (30% - represented by (?) on the bottom image); followed by β-sheets (24% - represented by blue arrows); and α- helices (16% - represented by green helices). Confidence values of the secondary structure are represented by colour-code: high values correspond to red and low values correspond to purple.

Phyre[2] web-server also allows a more in-depth analysis of the modelled protein based on the most similar entry through the Phyre[2] Investigator web-tool. It was possible to evaluate other parameters that enriched the analysis, *i.e.* pocket detection to assess protein active sites, relative conservation of predicted binding site and mutational sensitivity throughout the sequence. One large pocket was identified in the N-domain (Figure 13 – A) region which possible corresponds to the lectin binding site with high mutational sensitivity comparatively to the remaining domains (Figure 13 – B). The mutational sensitivity of the identified region was also supported by the relative conservation values – high conservation values on the predicted binding site (Figure 13 – C). As expected, the lowest conservation value was identified on the C-terminal region of the protein corresponding to the C-terminal domain.

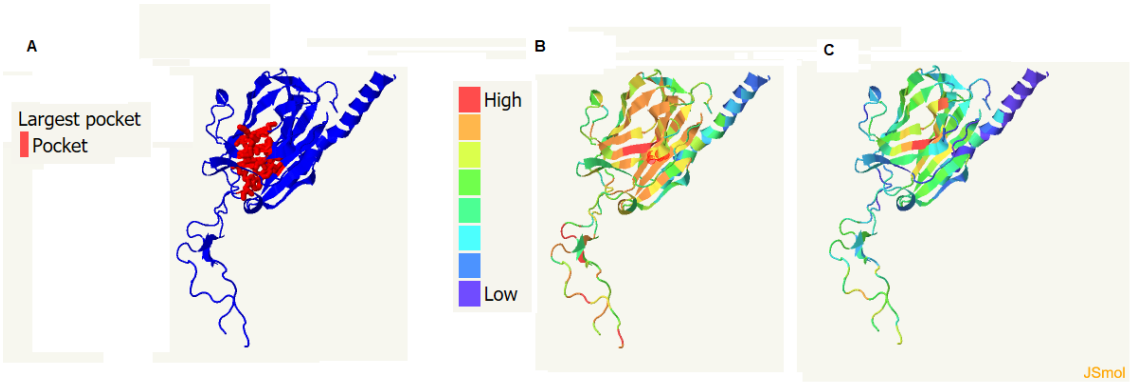

Figure 13 – Phyre[2] Investigator results of isolated partial *An*CRT sequence. The web-tool predicted possible active sites within the protein through detection of molecular pockets (A - red). It also indicates the mutational sensitivity of the protein (B), which is relatively high in the potential active site and lower in the C-terminal portion of the protein. Conservation values (C) are also in accordance with the mutational sensitivity predicted. The results obtained indicate higher conservation values in the predicted pocket region that decrease on its peripherical region, reaching the lowest values on the C-terminal region. Both mutational sensitivity and conservation values range through low - high values and are represented by colour-code. Red indicates higher values and blue indicates lower values.

Given the results on pocket detection which indicated a potentially active site, the partial *An*CRT sequence was submitted to another web-tool to predict possible binding sites and ligand clusters. 3D LigandSite predicts amino-acidic residues that form part of the binding site based on homologues identified by Phyre[2] software for protein modelling. We identified eleven ligand clusters with average mammoth scores ranging 8.7 – 24.4. The cluster with more predicted ligands, metallic and non-metallic, was associated to Asparagine (Asp)[115] residue. Although the cluster with higher average mammoth score was composed by a unique non-metallic ligand associated to Phenylalanine (Phe)[264] and Proline (Pro)[265] residues.

Besides protein's structure, post-translational modifications also modulate protein's function and IgE reactivity (Himly *et al*., 2003; Petersen *et al*., 1998). Therefore, the retrieved sequence was submitted as query in web-tools that predict most common post-translational modifications, *i.e.* phosphorylation and N-linked glycosylation. To validate the predicted post-translational modifications, it was also submitted as query protein sequences of *At*CRT isoforms most closely-related to *An*CRT protein – AtCRT1a and AtCRT1b. Predicted phosphosites from *A. thaliana*'s sequences were compared to PhosPhAt 4.0 results. Referenced phospho-sites of *A. thaliana* isoforms were also retrieved from PhosPhAt 4.0 web-tool.

Relatively to N- glycosylation, the *An*CRT sequence retrieved a unique glycosylation site with a relatively high score (>0.75 – Threshold = 0.5) – Asp_{6} residue. The *At*CRT1a sequence retrieved three potentially glycosylated sites, although only two were above threshold – Asp_{59} and Asp_{154} residue. As for the *At*CRT1b sequence the server also predicted a unique glycosylation site above the selected threshold – Asp_{59}. Regarding to phosphorylation, several sites were predicted by the server; however, only predicted sites with confidence scores >0.75 were considered since the selected threshold (0.5) reflected low confidence predictions. Analysis of the *An*CRT sequence indicated 18 phosphorylation sites – The_{28}, Tyr_{32}, Ser_{45}, The_{86}, Ser_{100}, The_{101}, The_{109}, Tyr_{196}, Tyr_{232}, The_{237}, Tyr_{267}, Tyr_{274}, Tyr_{299}, The_{326}, Ser_{331}, Ser_{338} The_{352} and Ser_{357}. As for *At*CRT1a and *At*CRT1b sequences the server predicted 22 and 27 phospho-sites, respectively. Although, in Table 8 only *A. thaliana* phospho-sites in common with PhosPhAt 4.0 results and referenced sites are indicated.

Table 8 – Predicted phosphorylation sites of *A. thaliana*'s CRT isoforms. The table indicates in **bold** predicted phospho-sites by NetPhos 3.1 server in common with the ones predicted by PhosPhAt 4.0 webtool. Underlined amino-acidic residues indicates an unpredicted phospho-site previously referenced in the literature.

***At*CRT1a**			***At*CRT1b**		
Amino-acidic residues	**Experimentally confirmed**	**First Referenced in**	**Amino-acidic residues**	**Experimentally confirmed**	**First Referenced in**
The$_{152}$	-	-	**Ser$_{61}$**	-	-
The$_{234}$	-	-	**Tyr$_{227}$**	-	-
Tyr$_{239}$	-	-	**Ser$_{229}$**	-	-
Tyr$_{310}$	-	-	**Tyr$_{239}$**	-	-
Tyr$_{317}$	-	-	**The$_{249}$**	-	-
Tyr$_{342}$	-	-	**Ser$_{251}$**	-	-
Ser$_{374}$	Yes	(Reiland *et al*., 2009)	Ser$_{117}$	Yes	Wu *et al*. (2013)
Ser$_{381}$	Yes	(Reiland *et al*., 2009)	**Tyr$_{275}$**	-	-
Ser$_{397}$	Yes	(Reiland *et al*., 2009)	**Tyr$_{289}$**	-	-
Ser$_{401}$	Yes	(Reiland *et al*., 2009)	**Tyr$_{310}$**	-	-
Ser$_{403}$	Yes	(Reiland *et al*., 2009)	**Tyr$_{317}$**	-	-
The$_{406}$	Yes	(Reiland *et al*., 2009)	Ser$_{374}$	Yes	(Reiland *et al*., 2009)
The$_{412}$	-	-	**Ser$_{381}$**	Yes	(Reiland *et al*., 2009)
The$_{418}$	Yes	Roitinger *et al*. (2015)	**Ser$_{396}$**	Yes	(Reiland *et al*., 2009)
			Ser$_{398}$	Yes	(Reiland *et al*., 2009)
			Ser$_{400}$	Yes	(Reiland *et al*., 2009)
			The$_{405}$	Yes	Nakagami *et al*. (2010)
			Ser$_{407}$	Yes	Wang *et al*. (2013)
			Ser$_{410}$	Yes	Wang *et al*. (2013)
			The$_{413}$	-	-
			Ser$_{414}$	-	-

Characterizing *A. negundo*'s pollen protein extract and its potential proteolytic activity

To respond to the raised question, it was necessary to characterize *A. negundo*'s pollen protein extract and to assess its potential proteolytic activity. Pollen grains were hydrated overnight at 4ºC with PBS (50 mg/mL) to promote the release of proteins, as it occurs in the respiratory airway. Subsequently, the pollen protein extracts were dialysed against pure water and concentrated using a concentrator with a molecular cut-off of 10 kDa. *A. negundo*'s pollen revealed to be slightly hydrophobic with an average of 0.27 mg/mL of total released proteins, which was as expected giving the fact that they are medium-sized pollen (PalDat.org - https://www.paldat.org/pub/Acer_negundo/301248). Protein content decreased about 28% post-dialysis (data not shown). This difference could be overestimated due to presence of components that affect the absorbance of the mixture extract - quantification reagent. In fact, it was noticed that post-dialysis the pollen extracts were lighter than the pre-dialysis samples. We decided to maintain the dialysis as a step of sample processing because PBS affected results in subsequent assays. The pollen extracts – post-dialysis and post-concentration – were separated by SDS-PAGE to obtain their protein profile in terms of molecular mass. The concentration resulting flow-through was also analysed by SDS-PAGE. Total protein content was constituted by proteins ranging between 20 and 150 kDa, although it was clear the predominance of high molecular weight proteins (<100 kDa – Figure 14 – left).

The increasing evidence regarding pollen's proteolytic activity contribution on the initiation of an allergic process raised the need to characterize the proteolytic activity of pollen extracts from distinct species. The presence of proteases in pollen extracts was determined by gelatine zymography. This technique allows to combine electrophoretic separation and identification of proteolytic activity, since pollen samples were loaded in a SDS-PAGE gel enriched with gelatine. Given the fact that gelatine derives from collagen, it functions as proteases substrate and detects a wide range of them. To preserve enzymatic activity, pollen extracts were prepared in non-denaturing conditions. After electrophoretical separation, SDS detergent was removed using Triton X-100 and stained with Coomassie Brilliant Blue. Following gel staining, it was possible to detect areas where gelatine was enzymatically digested. Due to substrate degradation, the digested area appears uncoloured (Figure 14 – right).

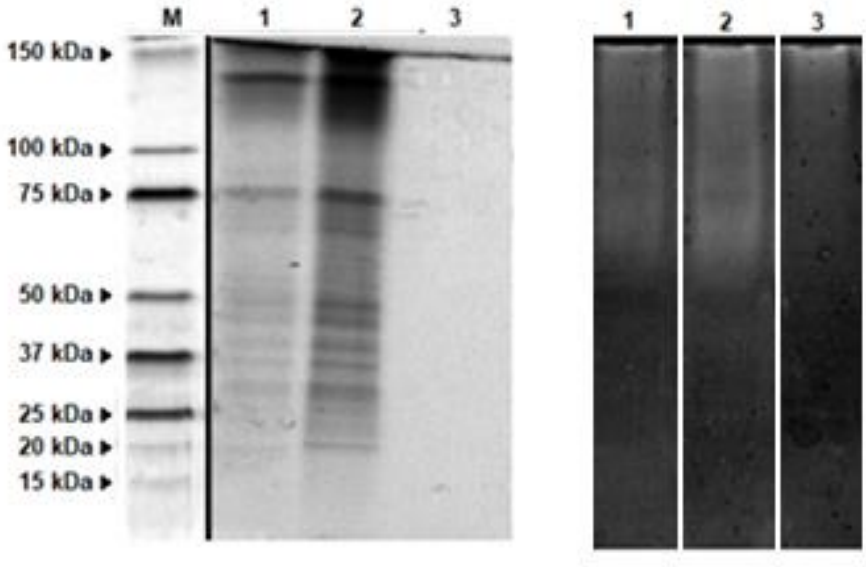

Figure 14 – *Acer negundo*'s pollen protein and proteolytic profile. It is presented the protein content of pollen samples post-dialysis (lane 1), post-concentration (lane 2) and its correspondent flow-through (lane 3) in an SDS- PAGE gel (left) and its correspondent proteolytic profile in a Zymography (right). The same volume of each sample was loaded, dependent of maximum well capacity (25 µL).

The zymogram revealed a diffuse proteolytic activity in dialysed extracts; however concentrated extracts revealed a better-defined band pattern suggesting proteolytic activity associated to high molecular proteins ranging 50 and 150 kDa. Lanes corresponding to flow-through also present slight gelatine degradation on top of the gel, possibly due to flow-through's cross-contamination or in-gel protease diffusion.

- Specific proteolytic activity

Dialysed extracts of pollen were incubated with synthetic single- amino-acids/ peptides bound to an amine- containing fluorophore, *i.e.* 7-amino-4-methylcoumarin (AMC), to determine substrate specificity of native proteases. Consequently, protease-hydrolysed substrates released the AMC group and cumulatively increased mixture's fluorescence. Fluorescence was monitored in 20 seconds intervals during 10 minutes at 37ºC. Results were expressed in variation of relative fluorescent units (ΔRFU) per µg of protein which correlates with the velocity of the proteolytic reaction.

Proteolytic activity against almost every tested substrate was verified as presented in Figure 15. It was noticeable highest ΔRFU/µg values with L-Phe-AMC (Phe) substrate; however, L-Leu-AMC (Leu) and L-Met-AMC (Met) also had high proteolytic rates (Figure 15 – left graph). It appears to also exist substrate specificity towards L-Lys-AMC (Lys), L-Arg-AMC (Arg), L-Ala-AMC (Ala), Benzoyl-Arg-AMC (BzArg), Gly-Pro-Arg-AMC

(GlyProArg), Butyloxycarbonyl (BOC)- Phe-Ser-Arg-AMC (BocPheSerArg), BOC-Val-Ser-Arg-AMC (BocValSerArg) and BOC-Ala-Gly-Pro-Arg-AMC (BocAlaGlyProArg) substrates (Figure 15 – right). However, the proteolytic activity occurred more slowly resulting in lower enzymatic rates. The obtained results possibly indicate that *A. negundo*'s pollen proteases have higher proteolytic activity towards some substrates (Phe, Leu, Met) than others, which might indicate higher prevalence of aminopeptidases in pollen extracts (Cortes *et al*., 2006).

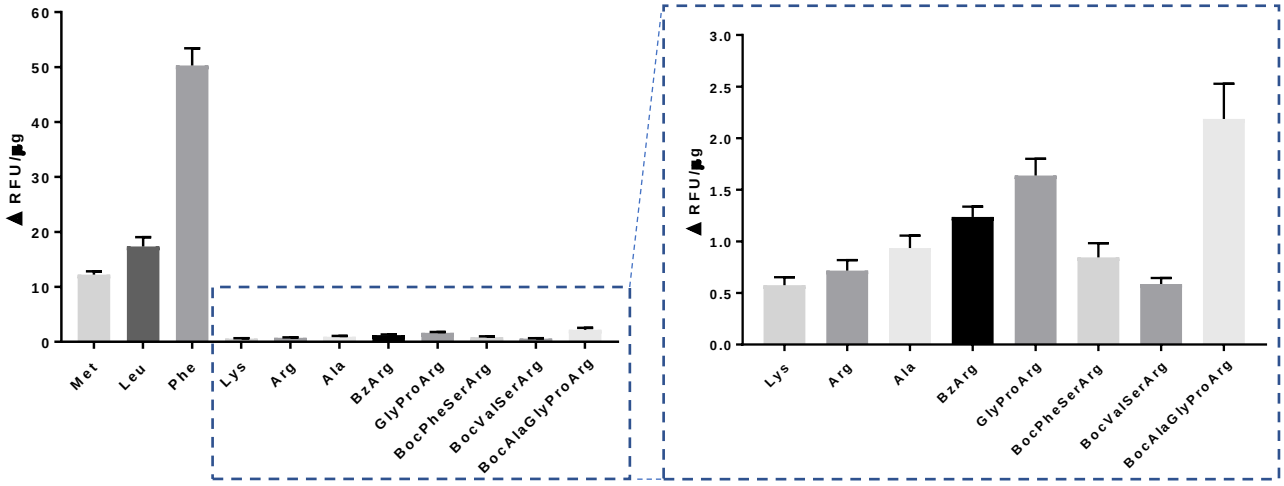

Figure 15 - Substrate specificity of proteases present in *A. negundo*' s pollen protein extract. It was tested several synthetic amino-acids and peptides bound to the 7-amino-4-methylcoumarin (AMC) fluorescent molecule. There was proteolytic activity against every substrate tested; however, it was verified higher proteolytic rates (>10 ΔRFU/µg) with L-Phe-AMC (Phe), L-Leu-AMC (Leu) and L-Met-AMC (Met) substrates. The remaining substrates were degraded more slowly, revealing inferior proteolytic rates (<10 ΔRFU/µg; right). The graphs indicate proteolytic rates per µg of protein present in *A. negundo*' s extracts. The used measure unit represents the velocity of enzymatic reaction which correlates with substrate specificity.

Presented results correspond to peptide proteolysis assay performed with initial pollen extracts, previously to protein concentration. The assay was repeated with concentrated extracts revealing a similar activity pattern, although higher proteolytic rates (ΔRFU/µg) with every tested substrate comparatively to non-concentrated extracts (data not shown). Since L-Phe-AMC had the highest proteolytic rate, this peptide was selected to perform peptide proteolysis assay after incubation with class-specific protease inhibitors.

Pollen extracts were incubated with inhibitors for 5 minutes at 37ºC. Subsequently, the selected substrate was added to the mixture and its fluorescence was measured as previously referred. Results were compared to control condition – L-Phe-AMC incubated with pollen extracts without addition of inhibitor (Figure 16).

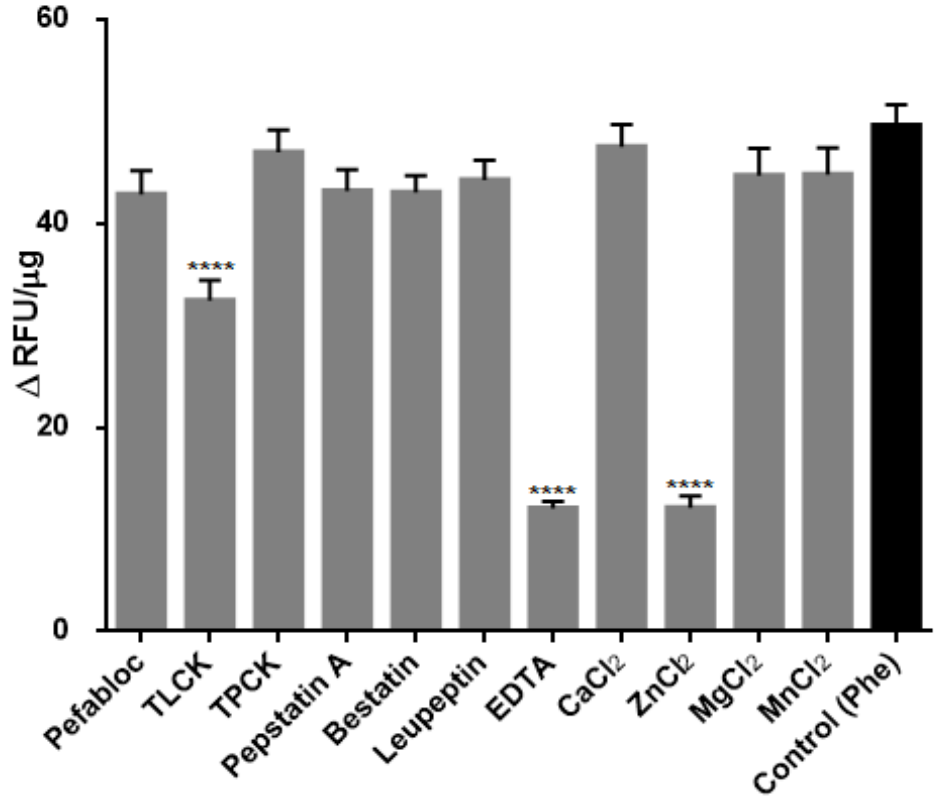

Figure 16 - Effects on proteolysis of Phenylalanine post incubation with class-specific proteases inhibitors. It was tested a wide range of inhibitors specific for certain classes of proteases. Only three of the tested inhibitors inhibited significantly proteolytic activity of *A. negundo*'s protein extracts – TLCK, EDTA and $ZnCl^2$. The graphs indicate proteolytic rates per µg of protein present in *A. negundo*' s extracts. Results were statistically analysed using Dunnett's multiple comparison test: **** P<0.0001 (n=3)

Every tested inhibitor had inhibitory effects, since it decreased the proteolytic rate of L-Phe-AMC comparatively to control condition. However, inhibitors that most affected proteolysis of L-Phe-AMC were TLCK, EDTA and $ZnCl_2$, revealing statistically significant differences to control condition (p value<0.0001).

Proteases are usually classified by their catalytic type into seven groups: aspartic, cysteine, serine, metalloproteases, threonine, glutamic and asparagine- peptidase (Oda, 2012). However, currently identified protease allergens belong mainly to the first five enzymatic classes enounced (McKenna *et al*., 2017). The results from enzymatic assays with and without inhibitors indicated that proteases present in *A. negundo*' s pollen grains have preferential zinc-dependent metalloproteinase and aminopeptidase activity, since EDTA – a metalloprotease and aminopeptidase inhibitor – reduced significantly the proteolytic activity of the extract towards L-Phe-AMC (Cortes *et al*., 2006). Moreover, metal ions were used at inhibitory concentrations to define protease-type within metalloprotease class. Only $ZnCl_2$ revealed highly significant inhibitory effects, similar to results obtained with EDTA.

A. negundo's pollen proteases also have significant serine trypsin-like activity, since one inhibitor with significant inhibitory effects was TLCK, which is an irreversible serine trypsin-like inhibitor (Cortes *et al*., 2006). However, the inhibitory effects were not as effective as the ones obtained with EDTA and $ZnCl_2$.

It should be noted that not all inhibitors used had irreversible inhibition effects. Reversible inhibitors could affect the proteolytic activity of the protein extract without reflecting significantly on the enzymatic rates of L-Phe-AMC proteolysis. This could explain the fact that it was not detected cysteine nor aspartic protease activity in proteolysis assay after incubation with class-specific inhibitors. Even though it was verified proteolytic activity towards Arg-AMC and Boc-Ala-Gly-Pro-Arg-AMC, which are substrates mainly hydrolysed by cysteine proteases according to their respective datasheets. It should be also taken in consideration that we evaluated an extract that is composed by a mixture of enzymatically active proteins with different affinities. Proteases of different classes might compete for the same substrate and inhibition of the activity of a specific class might potentiate the effects of others with affinity towards the same substrate. For example, the addition of a cysteine-blocking group, *i.e.* Bz, on the amino-terminal of Arg-AMC, which is also hydrolysed by serine proteases, increased peptide proteolysis. This increment was probably due to inhibition of cysteine activity, consequently eliminating eventual competition for the substrate between serine and cysteine proteases (Cortes *et al*., 2006).

Determining the cellular effects

The physical and mechanical properties of an organ are directly regulated by the extracellular matrix and its proteins, since matrix proteins regulate cell phenotypes and cell organisation in a tissue. Specifically in the lung, matrix protein's organisation is crucial and unique to facilitate gas exchange. However, integrity of a tissue can also be altered if intercellular junctions are affected somehow due to their importance in cell adhesion and communication processes (Georas and Rezaee, 2014; Grainge and Davies, 2013).

Given this, the effects of isolated and combined protein extracts on cell integrity were determined using A549 (ATCC® CCL-185™) cell line, which is a cell line resultant of carcinogenic human lung epithelial cells. After cell culture and reaching confluent state, A549 cells were exposed to: pollen extracts – with distinct final concentration values: high concentration (HC = 800 µg per mL of medium) and low concentration (LC = 400 µg per mL of medium); to purified recombinant protein (40 µg per mL of medium); to a mixture of both pollen extracts (LC) and purified recombinant CRT; and to denatured extracts of each condition. We decided to perform extract heat-denaturation to eliminate the verified effects since protease-specific inhibitors had injurious effects on cell cultures (data not shown). LC pollen extracts were selected in this condition to not compromise the detection of differences between isolated and combined extracts. Cells were exposed to each condition for 6 and/or 24 hours.

- Quantification of cellular detachment

To determine the effects of isolated and combined extracts on epithelial permeability of cell cultures, the cell attachment was determined recurring to Methylene Blue method, which allows a relative quantification of attached cells after removing detached ones. Cell detachment was quantified as previously indicated and results were expressed as percentage of detached cells comparatively to a control condition. Since cell cultures are not static and progress over a natural cycle of cell-proliferation/cell-death, cell detachment was expected to occur in cultures incubated only with MEM medium. However, this was corrected for every replica of each independent assay, by assuming their average absorbance value as correspondent to a full adherent culture.

Relatively to comparison of cellular detachment after exposure to HC *vs* LC pollen extracts for 6 and 24 hours, it was verified that cellular detachment correlated with protein concentration and incubation period. As verified in Figure 17, LC pollen extracts

exposure resulted in low rates of cellular detachment even in the maximum timepoint (24 hours). Contrarily, HC pollen extracts had higher cellular detachment after 6 hours and significant cellular detachment at the maximum timepoint. Denatured extracts had variable results, possibly due to the fact that denaturation conditions were not sufficient to irreversibly denature proteins present in the pollen extracts or due to formation of cell-distressing products after denaturation.

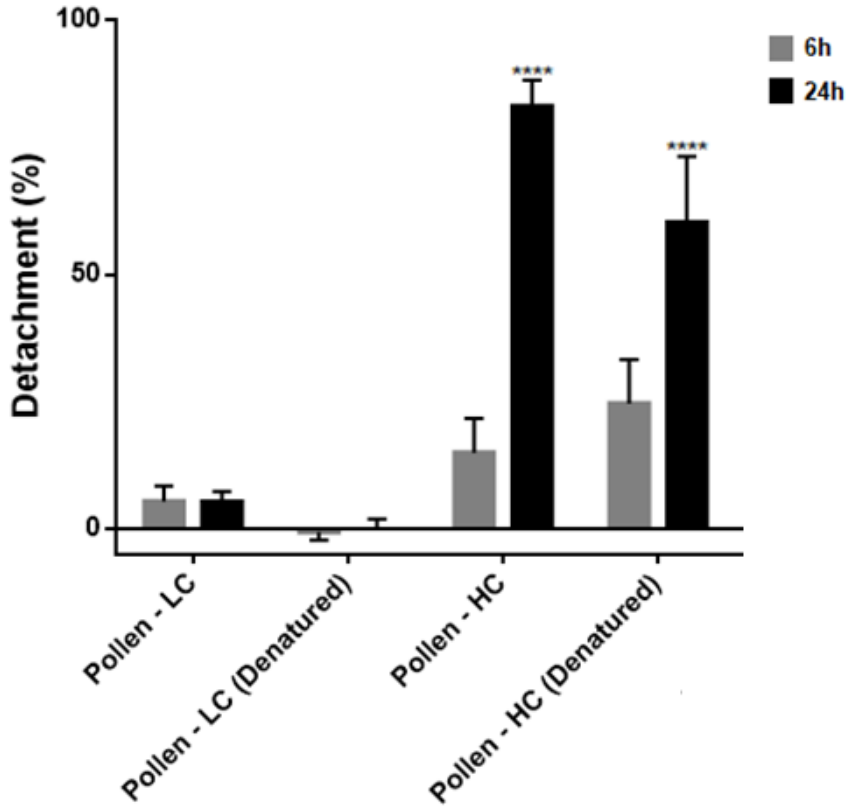

Figure 17 - Effects of *A. negundo*'s pollen extracts of on substrate adhesion of epithelial cells. Cells were exposed for 6 and 24 hours to distinct concentrations of pollen diffusates – LC and HC: 400 and 800 µg per mL of media, respectively. Cells were also incubated with heat-denatured extracts prepared in the same conditions as non-denatured extracts. Results are expressed in percentage of detachment relatively to a control condition of adherent cells and were statistically analysed using Dunnett's multiple comparison test: **** P<0.0001 (n=3).

Relatively to rCRT in isolated *vs* combined extracts exposure for 24 hours, it was verified higher cell detachment rates in LC pollen comparatively to the previous described results even after extract heat-denaturation. Cells exposed to purified rCRT had a lower detachment rate compared to cells exposed to LC pollen extracts which was almost null after extract denaturation. Although, it was verified that cells exposed to combined extracts had significantly higher detachment percentages comparatively to cultures exposed to isolated extracts (Figure 18).

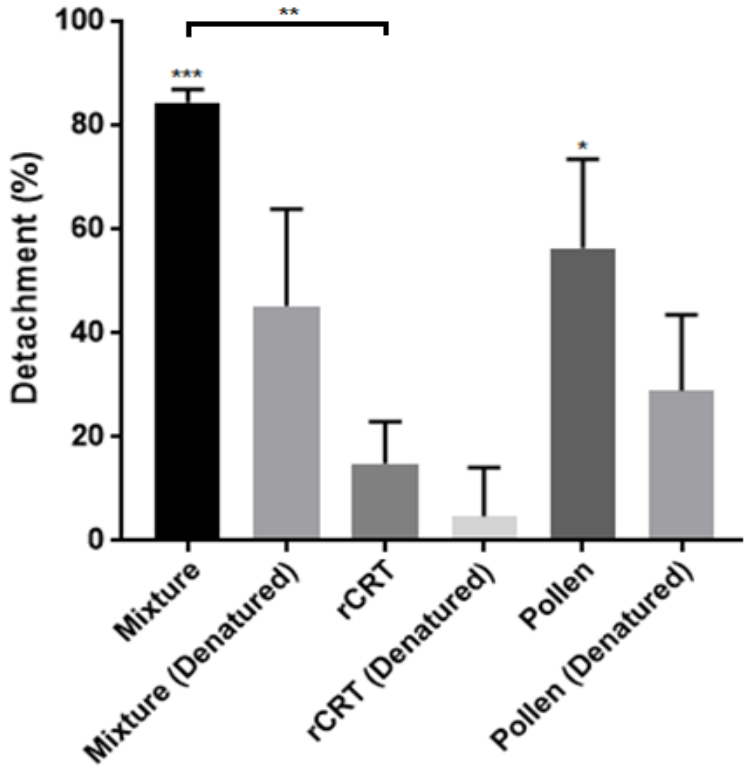

Figure 18 - Effects of isolated recombinant protein and *A. negundo*'s pollen extracts *versus* combined extracts on substrate adhesion of epithelial cells. Cells were exposed for 24 hours to: 1) LC pollen diffusates – 400 µg per mL of media; 2) purified recombinant Calreticulin (rCRT) – 40 µg per mL of media; and 3) mixture of both. Cells were also incubated with heat-denatured extracts prepared in the same conditions as non-denatured extracts. Cell detachment was relatively quantified by comparison with control condition. Results were statistically analysed using Dunnett's multiple comparison test for comparison of test and control conditions. Results were also analysed using Sidak's multiple comparison test for comparison between test conditions: *** p<0.001; ** p<0.01; * p<0.05 (n=3).

- Immunodetection of proteins involved in cell adhesion

To determine the effects in intercellular complexes after exposure to isolated and combined extracts proteins crucial for maintenance of intercellular junctions were immunodetected, *i.e.* E-cadherin, Zonula occludens-1 (ZO-1) and Occludin, subsequently to total protein extraction of A549 cell cultures. E-cadherin is a transmembrane protein of adherent junctions, while Zonula occludens-1 and Occludin are tight junctions' proteins. Occludin is also a transmembrane protein contrarily to ZO-1 which is located in cytosolic complexes (Ganesan *et al*., 2013; Schneeberger and Lynch, 2004). Immunodetected proteins were relatively quantified comparatively to the reference protein β-actin, also immunodetected in each condition, rather than to control conditions since it was expected sample loss due to eventual detachment of cells.

Analysis of E-cadherin's protein levels in cells exposed to HC pollen extracts during 6 and 24 hours was performed. It was possible to verify an increase in E-cadherin accumulation in cells exposed to HC pollen extracts, although after extract denaturation

protein's levels decreased comparatively to both control conditions tested – medium with and without FBS (Control (-) and Control, respectively). The used antibodies detected products with smaller size that possibly corresponded to E-cadherin's degradation. To relatively quantify the protein degradation, the most visible band was also quantified. We verified protein degradation in every tested condition, although denatured HC pollen extracts had lower percentage comparative to Control condition (Figure 19).

Analysis of E-cadherin's protein accumulation and degradation levels were also performed with other conditions (extracts of LC pollen, purified rCRT and combined extracts); however only samples from cells that were exposed for 24 hours were analysed since the conditions used in this analysis did not produce significant alterations after 6 hours incubations. Comparing HC pollen extracts to LC pollen extracts, it was verified that E-cadherin's protein levels after exposition to HC extracts for 24 hours increased comparatively to control conditions contrarily to what was detected in cells exposed to LC extracts for 24 hours (Figure 19 and 20). It was observed that LC pollen extracts decreased E-cadherin's protein levels comparatively to control conditions. LC pollen extracts denaturation did not reverse that effect, but it did affect protein's degradation levels by lowering them comparatively to non-denatured extracts. It was also observed that purified rCRT provoked an increase in E-cadherin's protein levels and did not affect significantly protein's degradation comparatively to control conditions. Moreover, denaturation of purified rCRT affected E-cadherin's accumulation reaching lower levels than its non-denatured homologue. The mixture had similar results to purified rCRT, *i.e.* increased E-cadherin's levels, although its denaturation increased significantly protein's accumulation but not its degradation (Figure 20).

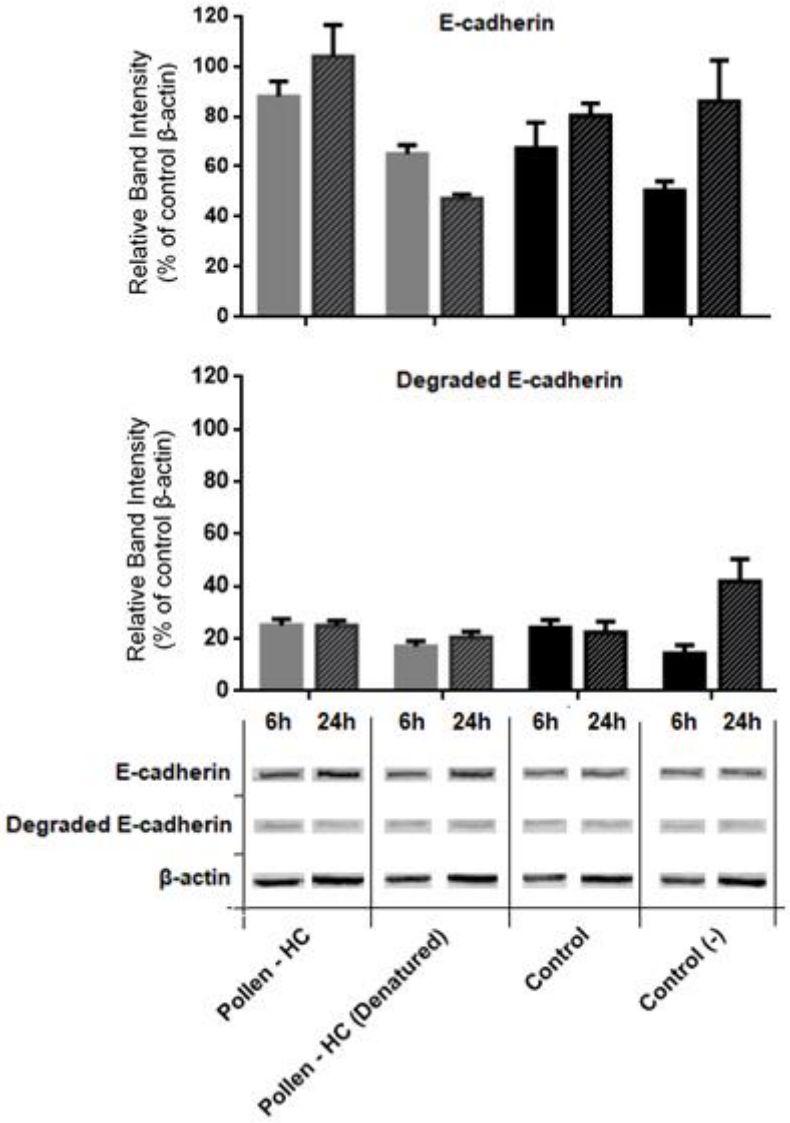

Figure 19 - Effects of *A. negundo*'s pollen extract on proteins of junctional complexes – E-cadherin. Cells were exposed for 6 and 24 hours to HC pollen diffusates – 800 µg per mL of media. Cells were also incubated with heat-denatured extracts prepared in the same conditions as non-denatured extracts. E-cadherin and degraded E-cadherin's band intensity was relatively quantified by comparison with control protein β-actin.

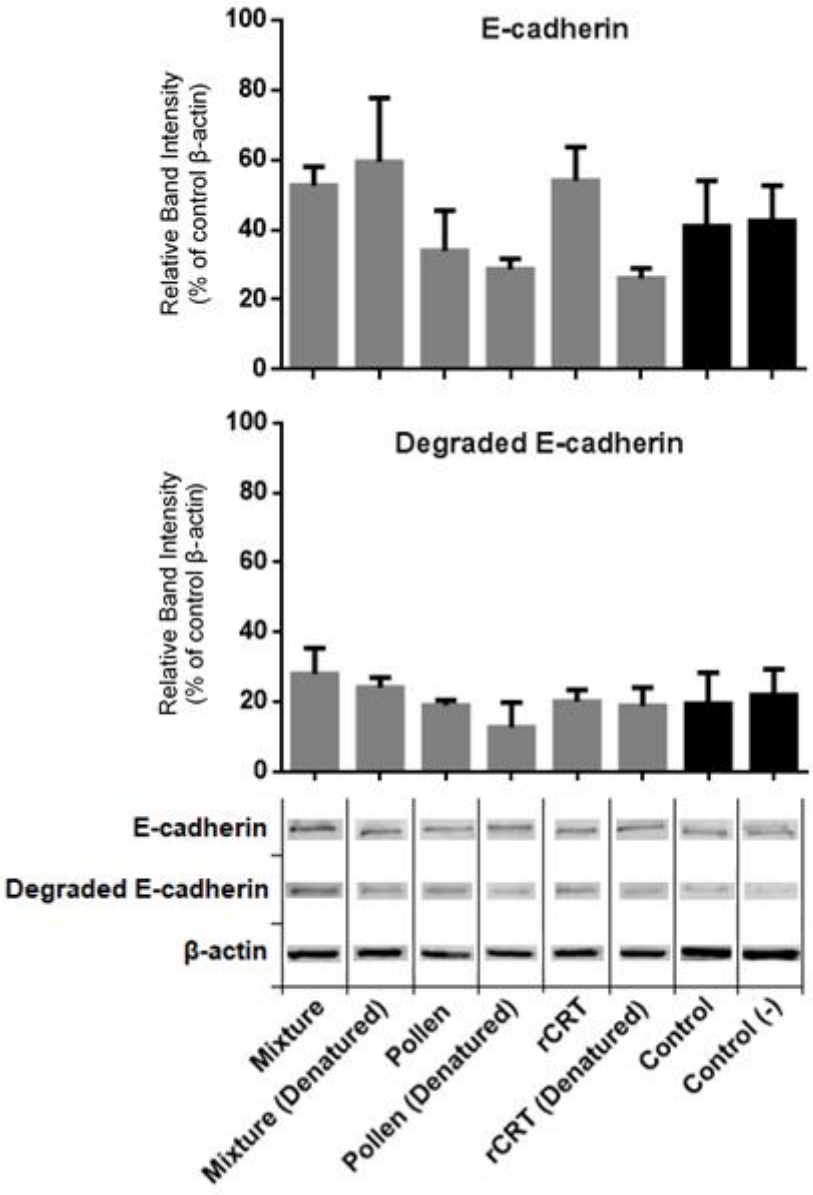

Figure 20 - Effects of purified recombinant protein and *A. negundo*'s pollen extracts *versus* mixture of both on proteins of junctional complexes – E-cadherin. Cells were exposed for 24 hours to: 1) LC pollen diffusates – 400 µg per mL of media; 2) purified recombinant Calreticulin (rCRT) – 40 µg per mL of media; and 3) mixture of both. Cells were also incubated with heat-denatured extracts prepared in the same conditions as non-denatured extracts. E-cadherin and degraded E-cadherin's band intensity was relatively quantified by comparison with control protein β-actin.

As E-cadherin, Occludin's protein levels of cells exposed to HC pollen extracts during 6 and 24 hours was also analysed (Figure 21). Occludin's dimers were also quantified since both forms co-occur and decreased dimerization was previously indicated as an effect of oxidative stress (Walter *et al*., 2009). It was not possible to assess Occludin's degradation, possibly due to cleavage of epitopes recognized by antibodies or small-sized degradation products. Cells exposed to HC extracts had a slight increase in protein

levels between 6 and 24 hours periods and a higher increase in protein's dimerization. Variations in protein accumulation in cells exposed to denatured HC pollen extracts was not significant, but protein's dimerization decreased after 24 hours incubation period.

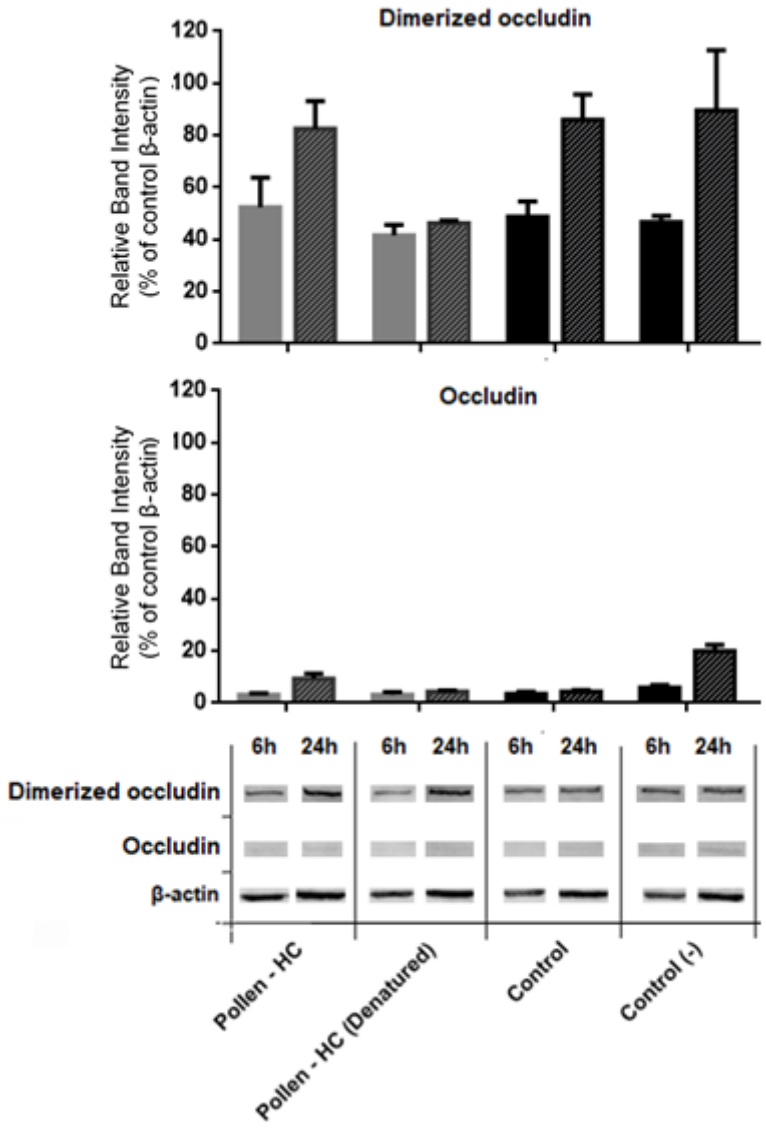

Figure 21 - Effects of *A. negundo*'s pollen extract on proteins of junctional complexes – Occludin. Cells were exposed for 6 and 24 hours to HC pollen diffusates – 800 µg per mL of media. Cells were also incubated with heat-denatured extracts prepared in the same conditions as non-denatured extracts. Occludin and dimerized Occludin's band intensity was relatively quantified by comparison with control protein β-actin.

Regarding cells exposed to LC extracts, we observed that Occludin's levels were higher comparatively to cells exposed to HC extracts – which could be an indicator of Occludin's degradation in the last condition. Denaturation of LC extracts did not affect accumulation of Occludin but it slightly decreased levels of protein dimers. In contrast, combined extracts and isolated purified rCRT did decrease protein levels comparatively

to control condition, as well as protein's dimerization levels – which could indicate Occludin's degradation in these conditions or decreased Occludin's expression as well. Denaturation of rCRT extract re-established protein's accumulation levels and increased protein levels of its dimerized form. As verified with denatured HC pollen extracts, also denatured LC extracts had lower levels of dimerized Occludin (Figure 22).

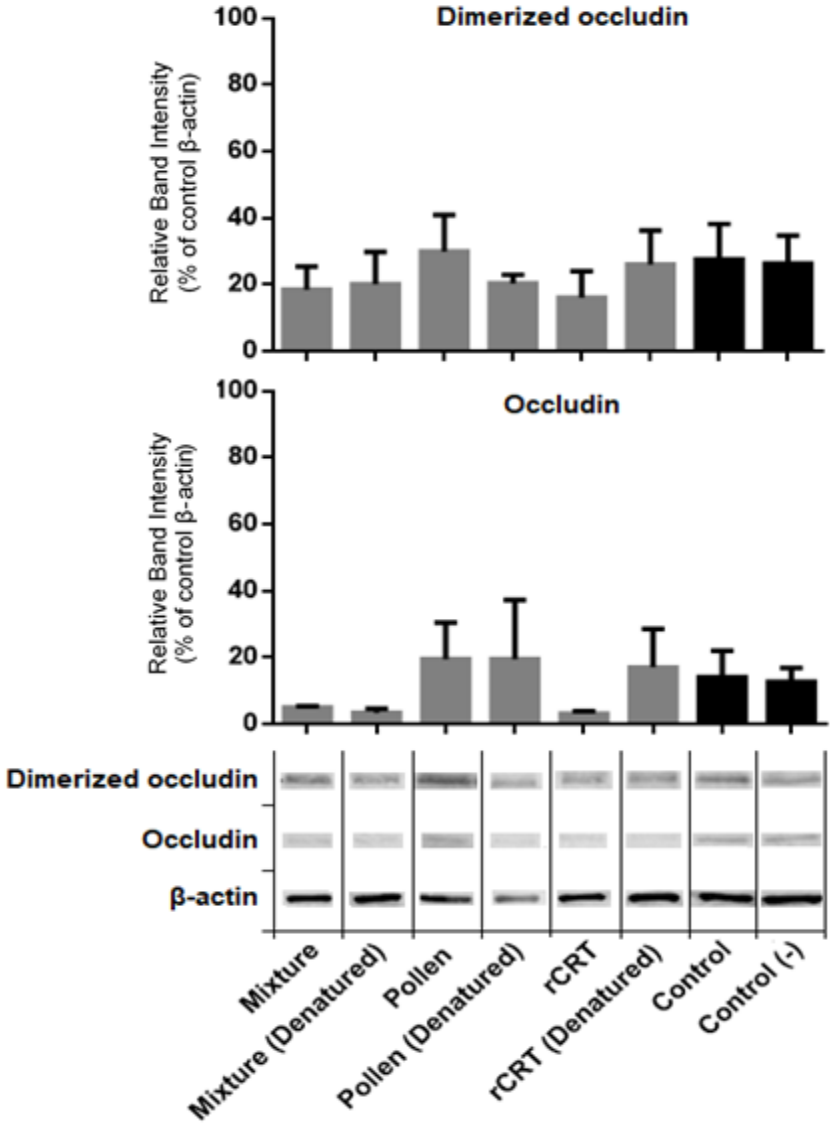

Figure 22 - Effects of purified recombinant protein and *A. negundo*'s pollen extracts *versus* mixture of both on proteins of junctional complexes – Occludin. Cells were exposed for 24 hours to: 1) LC pollen diffusates – 400 µg per mL of media; 2) purified recombinant Calreticulin (rCRT) – 40 µg per mL of media; and 3) mixture of both extracts. Cells were also incubated with heat-denatured extracts prepared in the same conditions as non-denatured extracts. Occludin and dimerized Occludin's band intensity was relatively quantified by comparison with control protein β-actin.

Relatively to Zonula occludens -1, it was verified that protein levels decreased between the two timepoints tested in HC pollen extract condition; although the same was observed in control conditions (Figure 23). It was not detected degradation products from this protein. Cells exposed to LC pollen extracts had higher protein levels of ZO-1 than cells exposed to HC extracts (Figure 23 and 24). Comparatively to their respective control condition, it was verified a decrease in protein's accumulation in cells exposed to LC extracts; however, extract denaturation resulted in protein levels higher than control conditions. Isolated purified rCRT did not affect cell's ZO-1 accumulation, contrarily to what was observed in samples of cells exposed to combined extracts. Although, cells exposed to denatured mixture extracts had a slight increase in protein levels as verified in cells exposed to denatured LC pollen extracts (Figure 24).

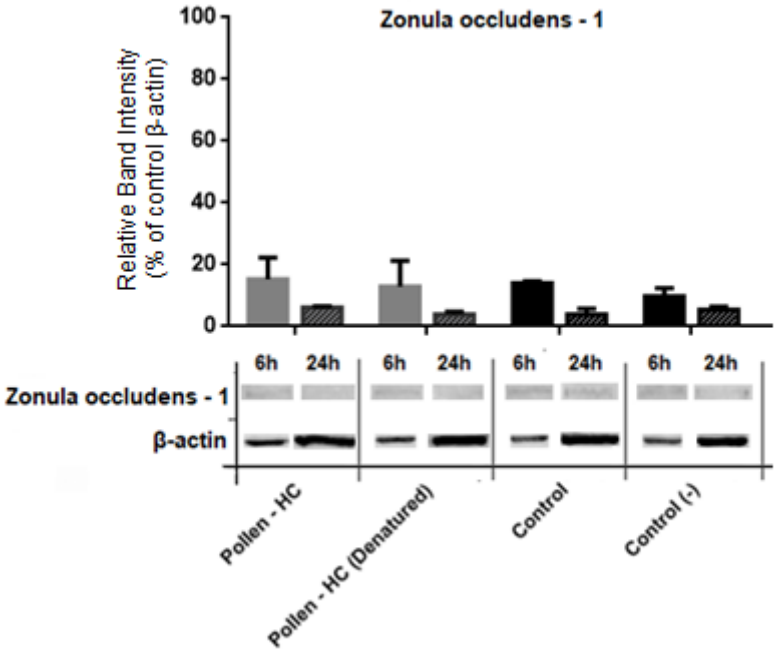

Figure 23 - Effects of *A. negundo*'s pollen extract on proteins of junctional complexes – Zonula occludens-1 (ZO-1). Cells were exposed for 6 and 24 hours to HC pollen diffusates – 800 µg per mL of media. Cells were also incubated with heat-denatured extracts prepared in the same conditions as non-denatured extracts. ZO-1's band intensity was relatively quantified by comparison with control protein β-actin**.**

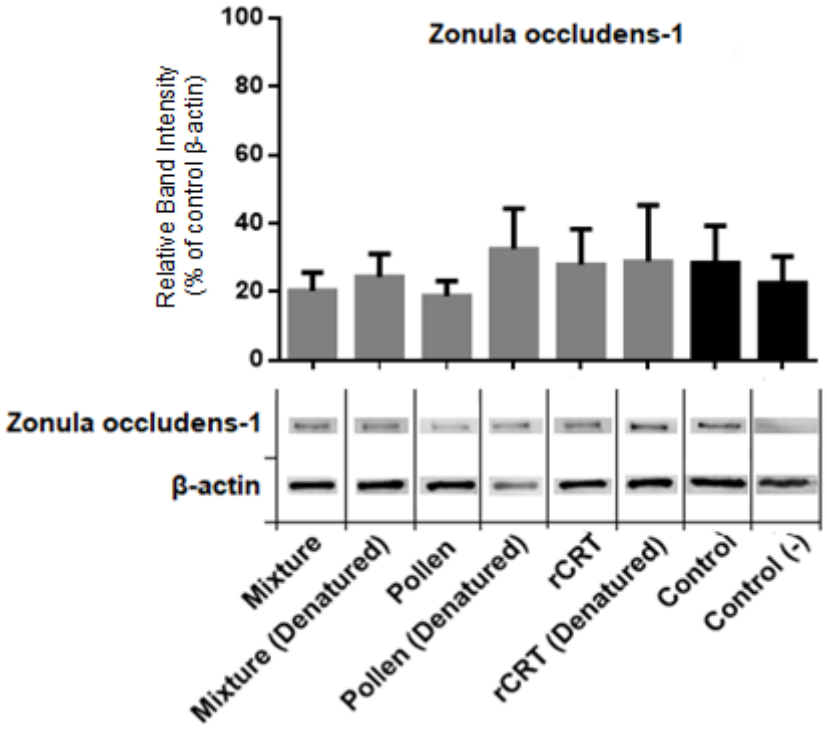

Figure 24 - Effects of purified recombinant protein and *A. negundo*'s pollen extracts *versus* mixture of both on proteins of junctional complexes – Zonula occludens-1 (ZO-1). Cells were exposed for 24 hours to: 1) LC pollen diffusates – 400 µg per mL of media; 2) purified recombinant Calreticulin (rCRT) – 40 µg per mL of media; and 3) mixture of both extracts. Cells were also incubated with heat-denatured extracts prepared in the same conditions as non-denatured extracts. ZO-1's band intensity was relatively quantified by comparison with control protein β-actin.

- Quantification of released cytokines

Since several studies indicated cytokine release by alveolar epithelial cells after exposure to allergens extracts, the released cytokines were quantified recurring to CBA assay as previously specified. Despite detection of a set of cytokines only two were considered since they were detected in all samples of each condition tested with relatively low variability – IL-6 and IL-8. Relatively to IL-6, it was possible to verify that cells exposed to HC pollen extracts released considerable amounts of this cytokine. Although, highest concentration of detected IL-6 was obtained from cells exposed to HC denatured extracts possibly due to cell's oxidative stress provoked by resulting products of HC extracts denaturation. Analysing the results obtained from cells exposed to LC pollen extracts, purified rCRT and combination of both extracts, it was verified that IL-6 release increased in mixed extracts comparatively to LC pollen extract, despite the significantly lower concentration comparatively to results obtained from cells exposed to denatured HC extracts. Purified rCRT did not induce significant cytokine release to be detected (Figure 25).

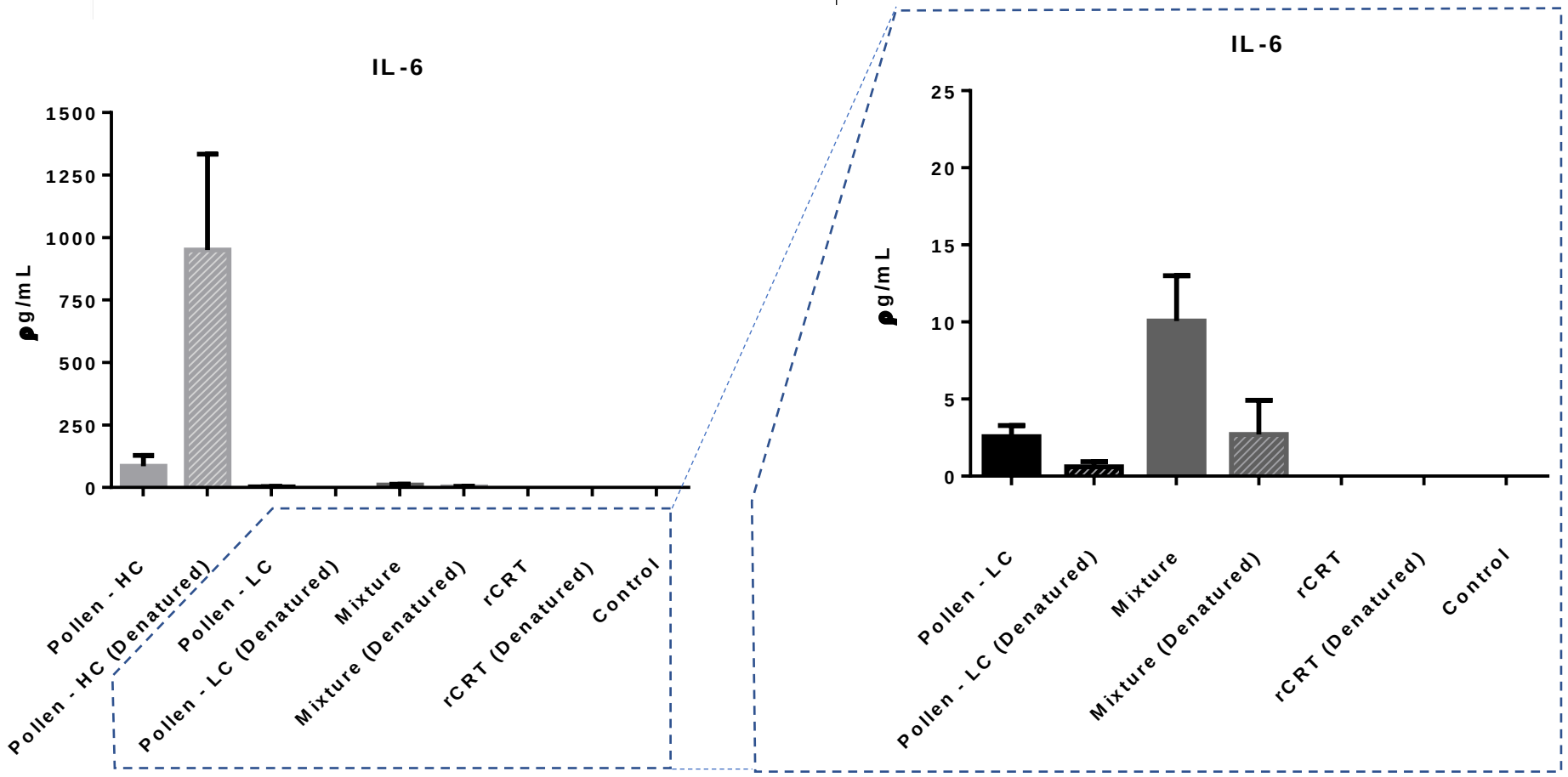

Figure 25 - Effects of purified recombinant protein and *A. negundo*'s pollen extracts *versus* mixture of both on IL-6 release by epithelial cells. Cells were exposed for 24 hours to: 1) pollen diffusates – LC and HC: 400 and 800 µg per mL of media, respectively; 2) recombinant Calreticulin (rCRT) – 40 µg per mL of media; and 3) mixture of LC pollen extracts and purified rCRT. Cells were also incubated with heat-denatured extracts prepared in the same conditions as non-denatured extracts.

Conversely, it was verified that cells released significantly higher amounts of IL-8 comparatively to IL-6 in every condition tested. Released IL-8 reached highest values in samples of cells exposed to HC pollen extracts. Similar to what was verified in IL-6 quantification, cells exposed to denatured HC extracts also released significant more IL-8 than cells exposed to non-denatured extract (p-value < 0.01). Denaturation of LC pollen extracts also resulted in increased release of IL-8, although it was not possible to verify difference's significance due to variability of obtained results. Regarding this cytokine, it was verified that purified rCRT induced its release and denaturation of the extract did not alter that effect. Moreover, combined extracts increased IL-8 release comparatively to both isolated extracts even after extract denaturation (Figure 26).

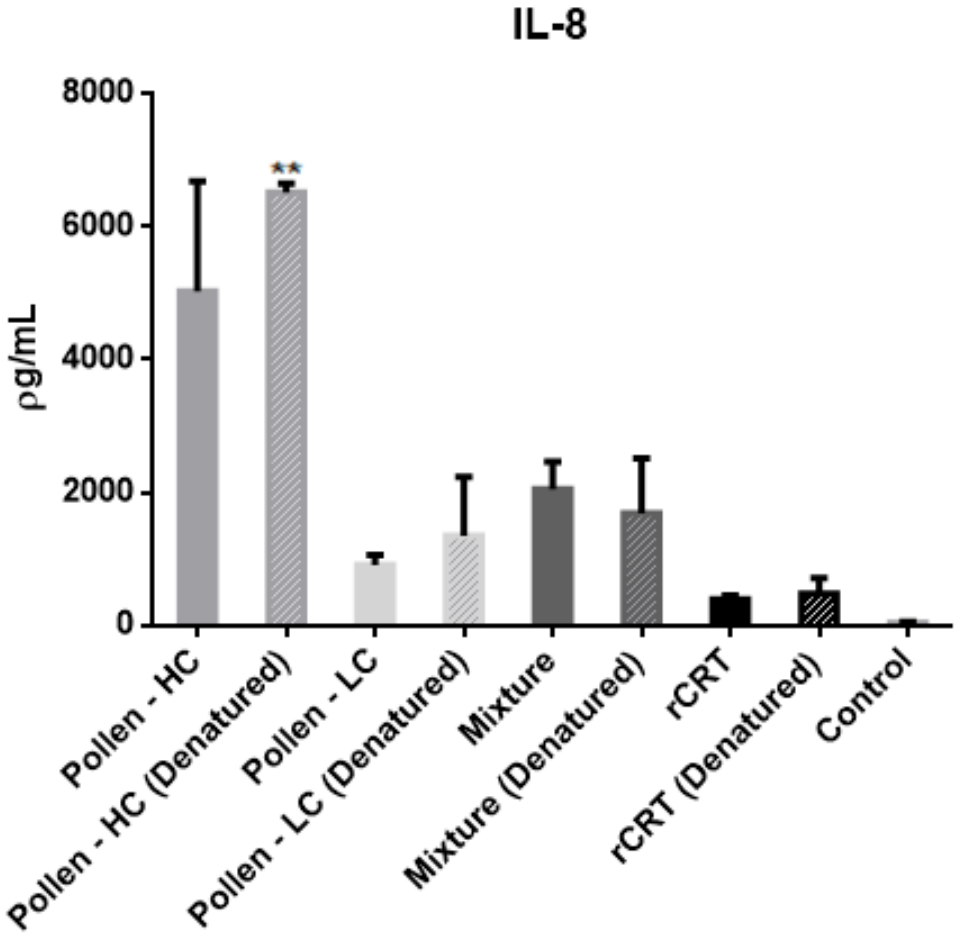

Figure 26 - Effects of purified recombinant protein and *A. negundo*'s pollen extracts *versus* mixture of both on IL-8 release by epithelial cells. Cells were exposed for 24 hours to: 1) pollen diffusates – LC and HC: 400 and 800 µg per mL of media, respectively; 2) recombinant Calreticulin (rCRT) – 40 µg per mL of media; and 3) mixture of LC pollen extracts and purified rCRT. Cells were also incubated with heat-denatured extracts prepared in the same conditions as non-denatured extracts. Results were statistically analysed using Dunnett's multiple comparison test for comparison of test and control conditions: ** p<0.01; (n=3).

Chapter IV – Discussion

The airway is constantly being exposed to damaging agents that trigger cellular responses to eliminate them. The protection mechanisms induced by these cells are important to rapidly return the respiratory system to its homeostatic state. However, sometimes the immune system has an exacerbated response to exogenous substances. This could be due to genetic predisposition, environmental conditions or other factors (*e.g.* age) that influence an individual to develop such reaction – the allergic reaction (Ober and Yao, 2011; Wang, 2005). Due to the complexity of the immune system and its functions, the culminant effects of an exacerbated immune response could be accomplished by several ways. Although, the allergic process is still commonly associated to specific IgE-mediated responses.

The allergic process first occurs after a sensitization process to an allergen. However, for this process to occur it is necessary that the allergen overcomes the epithelial barrier to be processed by antigen-presenting cells (APCs) present in subeptihelial layers. The exact mechanisms behind allergen transposition of epithelial barriers are yet to be fully understood, thus explaining the interest of many research studies. Pollen grains are one of the main sources of air allergens and it has been suggested that their proteolytic activity is responsible for their major contribution as allergenic elicitors, either by direct activity in intercellular junctional complexes or by cell receptors' activation – *e.g.* Protease-activated receptor – 2 (PAR-2) (Vinhas *et al*., 2011). A previous study by Runswick *et al*. (2007) indicated that proteolytic activity of pollen extracts did not correlate specifically with pollen's allergenic potential. Although, it enhanced allergen distribution across epithelial barrier through disruption of tight junctions.

Inhaled pollen grains can release high levels of soluble molecules in the respiratory tract (up to 50 mg/mL) depending on individual's exposure intensity, geographic location and climacteric conditions (Vinhas *et al*., 2011). The released molecules include proteins with or without enzymatic activities, lipoproteins, polysaccharides, lipids and phenolic compounds. Given that, it seemed plausible to infer that any molecule capable of altering epithelial barrier integrity and/or permeability could influence allergen-crossing of epithelial layer. As previously referred, CRT was one of the previously identified immunoreactive proteins of *A. negundo*'s pollen protein extracts. Due to the functional and structural similarity between plants and mammalian CRT several questions aroused regarding the potential immunogenic effects of this protein besides the ones associated with IgE-mediated immune responses.

The main goal of this project was to investigate the immunogenic potential of *An*CRT. We wanted to explore the ability of this protein to elicit an inflammatory response through

inducing expression of proinflammatory molecules; and/or interacting with cell receptors as extracellular mammalian CRT, consequently compromising cell-adhesion processes. We also questioned if the presumable allergenicity of *An*CRT derived from specific interactions with membrane receptors of lung's epithelial cells activating alternative non-IgE mediated immunogenic responses; or if it was a consequence of the inflammatory reaction initiated from the pollen – epithelium contact that consequently initiates an allergic response and produce *An*CRT-specific IgE antibodies that modulate immune responses as well. To respond to the main questions, it was necessary to achieve secondary milestones.

A. negundo's Calreticulin – recombinant protein production and *in silico* characterization

We aimed to complete the partial *An*CRT previously obtained since we were not certain if the lacking region affected the potential immunogenicity of the protein. Due to lack of time it was not possible to complete *An*CRT CDS, although this part of the work will be further discussed. We decided to perform the designed experiences with partial *An*CRT, since it was previously produced and used for preliminary immunoreactive assays. Besides, previous works were capable to prove immunostimulatory activities of a murine CRT also using partial recombinant proteins (Hong *et al*., 2010; Huang *et al*., 2013). Preliminary immunoreactive assays with partial *An*CRT were performed with sera of sensitized patients revealing *An*CRT's IgE-reactivity. The partial protein was extensively characterized using *in silico* web-tools to identify which CRT isoform was isolated, since it lacks information on plants CRTs comparatively to their mammalian homologues.

To retrieve the missing region of the previously isolated partial *An*CRT, we decided to implement an optimized 5' RACE technique, *i.e.* RNA Ligase Mediated – RACE (RLM-RACE) previously described (Kazuo and Sumio, 1994; Matsumoto *et al*., 2014; Suzuki *et al*., 1997). This technique involved CIAP treatment of extracted RNA that eliminated potential reverse transcription – inhibiting molecules (*e.g.* ribosomal RNA, fragmented mRNA, tRNA and contaminating genomic DNA) without affecting the full-length capped mRNAs. Subsequently, the pool of molecules was treated with RppH which removed the cap structure from full-length mRNA by hydrolysing the triphosphate bond that links a 5'-7-methylguanosine to mRNA, leaving a 5'- monophosphate end capable of accepting a free 3' – hydroxyl end. A synthetic single-stranded DNA (ssDNA) adapter was ligated to the accepting RNA molecules within the treated RNA population, *i.e.* full-length mRNA

molecules with free 5'- monophosphates, recurring to a T4 RNA ligase and reverse transcribed. After reverse transcription, the cDNA 5' ends were amplified recurring to a gene-specific primer and to a ssDNA adapter – complementary oligonucleotide. Analysis of amplified products were not as informative as expected since no well-defined bands were visible. This result was probably due to molecule variability given that RNA molecules were not eliminated from the reaction. To increase the amount of desired molecules that resulted from RLM-RACE reaction, we performed SemiNested PCR using a gene-specific primer and the ssDNA adapter – complementary primer (Scotto-Lavino *et al*., 2007). The analysis of the resulting amplification products indicated that the applied RLM-RACE technique did in fact increased the probability of isolating the missing portion of *An*CRT CDS, since previously enzyme-treated cDNA revealed more bands >600 bp comparatively to untreated cDNA.

Posteriorly, we performed PCR product purification to proceed to pCR®-Blunt ligation and bacterial transformation to select recombinant plasmids possibly harbouring the region of interest. Potentially positive clones were selected for plasmid extraction and restriction reactions were performed to assess insert's presence and orientation; however, results of restriction reactions were inconclusive leading us to use Ligation PCR as described by Chandra and Wikel (2005). This technique revealed to be highly informative and long term cost-effective since it indicated that ligation proceedings resulted in vector:vector molecules rather than the desired vector:insert recombinant molecule. Despite being the most versatile and easiest cloning method, blunt-end cloning is much less efficient than other existent methods (Honoré, 1996). Besides the reduced colonies, the probability of finding a desired recombinant molecule (*i.e.* insert:vector plasmid with insert in the right orientation) is substantially low, since this technique is based on transient ligation of free 5' phosphate and 3' hydroxyl groups by T4 DNA ligase (Honoré, 1996). It is possible to treat both vector and insert to increase probability of a successful blunt-end ligation, although a ligation method dependent on complementary overhangs – *e.g.* TOPO®-TA or "Sticky ends" Restriction Enzyme cloning – is suggested for further works (Holton and Graham, 1991; Honoré, 1996).

Given that we decided to perform subsequent experiments with the previously obtained partial *An*CRT it was necessary to further characterize this protein and assess its behaviour during protein's expression and purification methods. Several web-tools were used to characterize *in silico* the isolated partial protein. Prediction of structure and functional domains retrieved a typical conformation of a protein belonging to Calreticulin family, as expected given the known structure conservation of plants' CRTs (Bakiu,

2014). Moreover, protein's conservation values and mutational sensitivity throughout the sequence were in accordance with other works since previous studies highlighted the high conservation of N- and P- domains responsible for chaperone functions of CRT opposing the variability of the C-terminal domain – which is possibly responsible for variations in Ca^{2+} binding potential of existent CRT isoforms (Christensen *et al*., 2010; Persson *et al*., 2003; Thelin *et al*., 2011). Regarding post-translational modifications, we verified that predicted N-glycosites were in accordance with previous indications of Christensen *et al*. (2010) study – three putative N-glycosites in *At*CRT1a isoform and one in *At*CRT1b. Despite existing a referenced highly conserved consensus site for N-glycosylation in 32nd amino-acid (N-domain), it was not predicted by used web-tools in any of the used sequences (Opas *et al*., 1996). Taken in consideration molecular conservation of glycosites, our results possibly indicate higher similarity between *An*CRT and *At*CRT1b (Strasser, 2016). Only one glycosite was predicted in both sequences with high scores in corroboration with *At*CRT1b N-glycosite referenced in the literature (Christensen *et al*., 2010). As for putative phosphorylation sites, the obtained results were compared to the ones retrieved using complete sequences of CRT isoforms of *A. thaliana*. We verified high variability of predicted sites depending on the web-tool used. Although, it was notable that most phosphosites predicted with high scores were located within the C-domain of the protein as previously stated by other studies which indicated higher prevalence of consensus phosphosites in C-terminus (Baldan *et al*., 1996; Mariani *et al*., 2003).

Regarding production and purification of recombinant partial *An*CRT we verified that cultures at 28ºC resulted in protein retrieval at high yields. At 37ºC no recombinant protein was detected in cultures' soluble fractions probably due to protein precipitation (Structural Genomics *et al*., 2008). For purification it was necessary to adjust imidazole concentration in Wash and Elution buffers due to variability in protein yields of induced *E. coli* cultures since different clones of BL21(DE3) cells harbouring pET-30a (+)::PfCRT recombinant plasmid were used. We decided to induce different clones of the same transformed strain to ensure that results obtained were consistent and independent of the use of a recombinant protein produced by the same culture. During purification step, soluble fractions of cultures that yielded higher amounts of recombinant protein needed to suffer an adjustment on Imidazole concentration of Wash and Elution buffer since the pre-defined buffer led to high loss of recombinant *An*CRT during wash steps. This occurred probably due to large amounts of bacterial lysates loaded onto affinity columns which were slightly above resin's biding capacity; although loss of recombinant protein

during purification steps is inevitable even if resin's binding capacity is not reached (Structural Genomics *et al*., 2008). Moreover, the pET-30a vector adds a C-terminal His-tag to the produced protein which might have variable accessibility depending on protein's conformation structure (Bornhorst and Falke, 2000). As previously referred, the predicted structure retrieved a typical CRT protein with an exposed C-terminal portion where the K/HDEL ER retention motif is located, therefore the added His-tag is probably exposed as well. Although, given the oligomerization potential of rCRT, the structure of the oligomeric form could alter the accessibility of the His-tag thus decreasing the affinity towards nickel ions present in the IMAC column and facilitating protein elution at lower Imidazole concentrations.

We observed the formation of recombinant *An*CRT oligomers, which was expected since recombinant CRT oligomerization was previously described by Li *et al*. (2015) and Huang *et al*. (2013). This might occur due to CRT's affinity towards misfolded or not fully processed proteins present in the collected protein extracts, since when protein samples are collected there are still recombinant proteins being produced by the bacterial culture. Moreover, levels of oligomerized proteins increased over-time if protein samples were not stored correctly at -20ºC thus suggesting that oligomerization is incremented by protein degradation. Regardless, purification of recombinant protein yielded high amounts of soluble recombinant partial *An*CRT to proceed for subsequent experiments.

The effects of *A. negundo*'s pollen proteolytic activity

Another goal of this project was to further characterize protein content of *A. negundo*'s pollen, specifically its proteolytic activities given that proteolytic potential of pollen extracts has an important role in initiating inflammatory responses and facilitating the access of allergens to immune cells in subeptihelial layers. *A. negundo*'s proteolytic activity was assessed by zymography method and further characterized using peptide proteolysis assays with and without class-specific proteases' inhibitors. The effects of pollen extracts on respiratory epithelium integrity were also verified to assess if they correlated with pollen extracts concentration variations.

In vitro hydration of pollen grains was performed to mimic *in vivo* hydration that occurs in the airways. However, it should be noted that is not possible to replicate exactly *in vivo* conditions since there is not sufficient information regarding the amount of protein that reaches the lower part of the respiratory tract (Runswick *et al*., 2007). Soluble proteins' concentration levels did not exceed 0.5 mg/mL, which raised the need to concentrate pollen extracts in order to proceed for certain experiments.

Proteolytic activity of pollen extracts was detected by zymography as previously referred. Gelatine was used as proteases' substrate, which is a collagen derivate previously used for collagenase detection specifically. Although, given gelatine's heterologous structure it can be used as substrate for several proteases besides collagenases. It was verified difuse proteolytic activity despite the relatively low release of proteins from *A. negundo*'s pollen extracts comparatively to other tree species. The observed proteolytic activity corresponded mainly to high molecular weight proteases ranging 50 - 100 kDa, as observed by Vinhas *et al*. (2011) in pollen extracts of *Olea europaea*, *Dactylis glomerate*, *Cupressus sempervirens* and *Pinus sylvestris*.

As previously referred, currently identified protease allergens belong mainly to aspartic, cysteine, serine, metalloproteases and threonine enzymatic classes (McKenna *et al*., 2017). Given that, pollen proteolytic activity was further characterized to classify the present proteases and to determine potential substrate specificity. The highest proteolytic rate observed was towards Phe-AMC, although Met-AMC and Leu-AMC synthetic peptides also revealed high values. Proteolysis of others synthetic peptides was also observed at lower rates possibly due to the presence of a small amount of specific enzymes with affinity to such peptides, *i.e.* Arg-AMC and Boc-Ala-Gly-Pro-Arg-AMC which are cysteine specific. Results from peptide proteolysis assays post incubation with class-specific inhibitors revealed higher prevalence of metalloproteases and other zinc-dependent aminopeptidases. Serine trypsin-like activity and possibly cysteine activity was also observed, although the last should be confirmed using other inhibitors specific only for cysteine class (*e.g.* E-64 inhibitor). Moreover, additional enzymatic assays should be performed to thoroughly determine protease specificity (Bisswanger, 2014).

The classification of proteases present in a pollen extract is of extreme importance since it differs accordingly to plant organisms. The variability of protease content could affect the way pollen proteolytic activity affects alveolar epithelial integrity. It could have direct effect on tight junctions by cleaving transmembrane domains of intercellular junctional proteins (Runswick *et al*., 2007; Vinhas *et al*., 2011); or induce tight junction disruption through cleavage and activation of PAR receptors by serine proteases as observed by Suzuki *et al*. (2005). Besides, there is also indication of activation of alternative pathways by exogenous proteases that result in T_{H2}-mediated responses characteristic of allergic reactions which consequently damage the alveolar epithelial tissue as well (Kheradmand *et al*., 2002).

Epithelial barrier disruption has been suggested as crucial for development of respiratory diseases such as allergic conditions, asthma or dyspnea. A disrupted alveolar epithelium results in activation of innate mechanisms and cellular components, and in increased allergen paracellular movement recognized by adaptive immune components (Ganesan *et al*., 2013; Georas and Rezaee, 2014; Kauffman *et al*., 2000; Pichavant *et al*., 2005; Runswick *et al*., 2007; Vinhas *et al*., 2011). Consequently, lung homeostasis is compromised and a chronic and more severe condition could be achieved if regulatory mechanisms are undermined. Regarding the diverse ways that proteolytic activity of pollen proteins could affect pulmonary epithelium integrity, the cellular effects of *A. negundo*'s pollen extracts were observed. We used a cell culture of A549 alveolar epithelial lineage, as previously indicated in *Material and methods* section. Despite the selected cell lineage not being able to form fully functional tight junctions *in vitro*, it is the most frequently used alveolar epithelial model specifically in substance's metabolism and cytotoxicity studies (Foster *et al*., 1998; Mao *et al*., 2015; Ren and Suresh, 2014).

Barrier disruption was evaluated through detachment assays since other type of assays, *i.e.* transepithelial permeability, could be influenced by the characteristics of the selected cell culture (Winton *et al*., 1998). It should be noted that pollen proteases probably do not reach sufficient concentrations to elicit detachment of alveolar epithelial cells *in vivo*, but *in vitro* cell detachment is a strong indicator that barrier integrity could be affected (Runswick *et al*., 2007). The effects of *A. negundo* on cellular detachment correlated with protein concentration and incubation periods, reaching almost full detachment of cell culture after 24-hour incubation with HC pollen extracts. Heat-denaturation of pollen extracts reduced detachment levels at 24 hours despite not eliminating such effect. As previously indicated, proteolytic activities of *A. negundo*'s pollen are mainly attributed to metalloproteases and other zinc-dependent aminopeptidases with some serine trypsin-like and possibly cysteine activity. Several studies have already identified the damaging effects of serine and cysteine activity on epithelial integrity (Kheradmand *et al*., 2002; Runswick *et al*., 2007; Sun *et al*., 2001; Wan *et al*., 1999), although our results suggest that exogenous metalloproteases also play a part in epithelial barrier damage.

Besides cellular detachment, the effects of epithelium exposure to pollen extracts on intercellular junctional proteins were assessed due to their role in cell adhesion processes. The integrity of a specific tissue is guaranteed by cell adhesion, which by definition, is the ability of a single cell to attach to other or to the extracellular matrix (ECM). Since cell adhesion is essential to cell communication and regulation processes,

a modification in this ability subsequent to a stressing stimulus reflects that tissue integrity was somehow compromised. Contrarily to Vinhas *et al*. (2011) study, we observed a decrease on cytoplasmic ZO-1 levels after 24-hour exposure to pollen extracts, despite undetected degradation products. We also observed an increase on both Occludin's and E-cadherin's protein levels post- 24 hours of applied stimulus, except when LC pollen extracts were heat-denatured. Dimerized Occludin's accumulation levels increased as observed in monomeric forms, except in conditions that increased oxidative stress in cell cultures – *i.e.* cells cultures exposed to heat-denatured extracts. In a previous work, Walter *et al*. (2009) proved the vulnerability of Occludin's oligomerization to redox-variations, which decreased in oxidative stress conditions.

The increased protein levels observed could be a result of protein internalization in response to pollen's proteolytic activity. Internalization of TJ and AJ proteins may occur via caveolae-mediated endocytosis or via clathrin-coated vesicles in response to pro-inflammatory mediators – *e.g.* chemokine (C-C motif) ligand 2 (CCL2), vascular endothelial growth factor (VEGF), IFN-Ɣ. –, or to variations in cytosolic-free Ca^{2+} levels (Bruewer *et al*., 2005; Hommelgaard *et al*., 2005; Ivanov *et al*., 2004; Stamatovic *et al*., 2009). Moreover, degradation levels of E-cadherin did not alter comparatively to control conditions which possibly indicates that the observed degradation corresponded to protein's turnover. The obtained results indicate that the observed cellular detachment was probably indirectly caused by proteolysis of surfaced cell receptors – *e.g.* activation of PARs –, rather than direct hydrolysis of transmembrane domains of intercellular proteins (Shpacovitch *et al*., 2008). Our results regarding immunodetected intercellular complex proteins go against what is described in the literature. Although, it should be noted that previous works analysed either the activity of different plant species with different proteolytic profiles due to variations in classes of proteases present in total protein extracts (Runswick *et al*., 2007; Vinhas *et al*., 2011); or the effects of isolated proteases, recombinantly produced or not, with possibly higher affinity towards transmembrane domains of intercellular proteins than cell-surfaced receptors (Cortes *et al*., 2006; Wan *et al*., 1999). Moreover, Sun *et al*. (2001) verified PAR-2 activation by interactions with isolated mite proteases Der p3 and Der p9, although in this work it was only verified the effects of PAR-2 activation on cytokine expression.

The involvement of PARs in physiological responses to exogenous peptidases has been extensively described in literature (Kauffman *et al*., 2000; Oida *et al*., 2017; Pichavant *et al*., 2005; Shpacovitch *et al*., 2008). These receptors are 7-transmembrane

proteins coupled to G proteins apically expressed on epithelial cells' surface. Currently four PARs have been described – PAR-1, PAR-2, PAR-3 and PAR-4 – and each one modulates several physiological processes, *e.g.* expression of cytokines and chemical mediators, vasodilation, cellular proliferation, smooth muscle contraction or relaxation, *etc*. These receptors are self-activated by tethered ligands, which correspond to their new N-terminal domain post serine proteolysis of a specific site. Although, there is indication of PARs activation independent of proteolytic cleavage using residue peptides that correspond to tethered ligands (Asokananthan *et al*., 2002). PARs activation results in hydrolysis of inositol phospholipid and increased cytosolic-free Ca^{2+}, thus activating cell's signalling cascades leading to expression and release of pro-inflammatory cytokines; and indirect disruption of epithelial barrier through transactivation of epidermal growth factor receptor (Gandhi and Vliagoftis, 2015; Heijink *et al*., 2010). Given that cytokine expression also reflects PAR activation, it was performed quantification of released pro-inflammatory cytokines after exposing cells to pollen extracts using Cytometric Bead Array (CBA) assays.

We observed that cells released higher amounts of IL-8 comparatively to IL-6. The release of both cytokines was concentration-dependent, since there was a substantial increase on released IL-6 and IL-8 from cells exposed to HC pollen extracts comparatively to the ones exposed to LC extracts. However, we observed higher amounts of released cytokines – specially IL-6 – in samples collected from cells exposed to heat-denatured extracts. It is possible that this could be an effect of cells' exposure to pollen's denaturation products which increased oxidative stress in cell cultures, as previously reflected by decreased dimerization levels of Occludin. Although, heat-denatured extracts should be characterized regarding its proteolytic activities through the peptide proteolysis assays in the same conditions previously specified to confirm if heat-denaturation completely eliminated proteolytic activities of pollen extracts. Our results are in accordance with previous studies that proved that exogenous proteases from air allergens (house dust mites, fungus and pollens) activated functional responses of innate and adaptive immune cells through induction of pro-inflammatory cytokines expression and release (including IL-6 and IL-8), either by disruption of epithelial integrity or by activation of cell-surfaced receptors (Asokananthan *et al*., 2002; Atkinson and Strachan, 2004; Calderon *et al*., 2015; Runswick *et al*., 2007; Shpacovitch *et al*., 2008; Vinhas *et al*., 2011). Besides cytokine release, interactions between air allergens proteases and cells' receptors also incite epithelial barrier disruption through loosening of tight junctions, IgE production amplification and eosinophils degranulation furtherly contributing to

increased inflammation (Reed and Kita, 2004). Additionally to proteins' immunodetection, quantitative reverse transcription PCR (qRT-PCR) with TJ proteins (ZO-1 and Occludin) and AJ proteins (E-cadherin) genes as templates could provide more information relatively to cellular responses, *i.e.* alterations in gene expression, to the exogenous stimulus applied. Moreover, given that activated PARs increase cytosolic-free Ca^{2+}, applying Single-Cell Calcium Imaging would also provide further proof of what was suggested by the results obtained in our work.

The immunogenic effects of *An*CRT

It is well known that respiratory diseases are increasing worldwide. Notwithstanding the high incidence, current therapeutics are mostly symptomatic and with limitable action in uncontrolled conditions that might evolve to chronic states, such as severe asthma and chronic obstructive pulmonary disease. Moreover, besides allergen-specific immunotherapy not being available to all individuals with diagnosed uncontrolled conditions this treatment is not effective in all patients. Allergens are generally associated as IgE-reactive molecules that induce a typical hypersensitive response in predisposed individuals; although, Schulten *et al*. (2013) indicated undescribed proteins that induced T_{H2}-mediated responses without being recognized by IgE. In previous works of the same group, it was highlighted that not all individuals allergic to *Timothy grass* proteins reacted to IgE-reactive allergens (Oseroff *et al*., 2010). This could be an explanation why some patients do not respond as expected to allergen-specific immunotherapy, thus the need to understand how potentially allergenic proteins interact with immune system components to improve existent therapies or develop new ones.

Previous studies highlighted the potent immunostimulatory activities of a recombinant murine CRT in macrophage, monocyte and B cells inducing cellular responses via TLR-4/CD14 pathway – *e.g.* NO_2 release, cytokine secretion and antibody production (Hong *et al*., 2010; Huang *et al*., 2013). Li *et al*. (2015) proved that the same murine rCRT activated bone marrow derived dendritic cells to secrete cytokines via the same TLR-4/CD14 pathway and induced DC maturation through PI3K/Akt signalling pathway. Moreover, Duo *et al*. (2014) also evidenced macrophage activation by oligomeric rCRT through Scavenger receptor A (SRA). Besides immune cells, TLR-4 receptors are also expressed in epithelial cells since these receptors have an important role in innate immunity. Given the extensive proof of heterologous interactions of rCRT with cell-receptors from immune cell components, our work aimed to assess if *An*CRT was capable of inducing cellular responses that could lead to alterations on epithelial barrier

permeability or induce inflammatory reactions. The immunogenic effects of the *An*CRT were evaluated by incubating A549 alveolar epithelial cells with purified recombinant *An*CRT in isolated extracts and in combination with LC pollen extracts.

Barrier disruption was evaluated once more through detachment assays. We observed some cell detachment in cultures exposed to isolated purified rCRT; although the observed effect was potentiated by the presence of total protein content from LC pollen extracts since detachment rates increased almost 60%. Our results suggest that rCRT affects cellular adhesion, although not in the same proportion as pollen extracts. Possibly, these effects could be a result of rCRT interactions with cell receptors that led to cell detachment. We propose that *An*CRT interacts with TLR-4 receptors expressed in cells' surface leading to activation of signalling pathways, as evidenced by previous works with other cell types, that induced slight cell detachment. Moreover, the expression of TLR-4 increases during barrier disruption (Wang *et al*., 2017), which could explain the verified increase in cellular responses, *i.e.* cell detachment, to combined extracts. The proteolytic activity of LC pollen extracts induced cell detachment – which mimic barrier disruption *in vitro* as previously discussed -, possibly increasing the expression of TLR-4 receptors and consequently, increasing rCRT-TLR-4 interactions that resulted in higher detachment rates. Besides, during epithelial injury, thrombospondin 1 (TSP-1) expression increases and becomes soluble after serine proteases cleavage (Orr *et al*., 2003). Soluble TSP-1 binds to the co-receptor CRT/LRP1 provoking focal disassembly and increasing even more barrier disruption (Gardai *et al*., 2003; Villagomez *et al*., 2009), which possibly also explains the verified increase on detachment rate of combined extracts.

Additionally to cell detachment assays, alterations in intercellular junctional proteins were also analysed to further evaluate *An*CRT effects on barrier disruption. We observed that both rCRT isolated and combined extracts increased E-cadherin's protein levels contrarily to the decrease verified in cells exposed to LC pollen extracts. Regarding monomeric and dimeric Occludin's protein levels we observed that both purified rCRT and combined extracts provoked a decrease in accumulated protein in both forms. In this case we did not verify that Occludin's dimerization was affected by oxidative stress provoked by denaturation of extracts, except when cells were exposed to isolated heat-denatured LC pollen extracts. In fact, it seems that rCRT provided some kind of oxidative stress protection to cells exposed to denatured mixture extract, since it was observed a slight increase on Dimerized Occludin's protein levels. As for ZO-1 protein, we observed no significant differences in protein accumulation after incubation with isolated purified

rCRT. The lower protein levels in cells exposed to combined extracts are more likely to be a consequence of LC pollen extracts activity, since LC pollen extracts resulted in the same decrease on protein levels, which was eliminated when both LC pollen and combined extracts were denatured. Once again, our results indicate that observed effects were possibly due to rCRT ability to interact with cell-surfaced receptors. These interactions have been widely described throughout the literature and we propose a potential explanation for the results obtained during the analysis of intercellular complex proteins integrity.

Ma and Hottiger (2016) reviewed the interferences between Wnt/β-catenin and nuclear factor kappa-light-chain-enhancer of activated B cells (NF-κB) signalling pathways, in which E-cadherin plays an important role. When epithelial barrier integrity is compromised, epithelial cells respond by increasing E-cadherin's expression and internalization for recruitment of β-catenin to AJ to regulate overexpression of TLRs (Ma and Hottiger, 2016). The translocation of β-catenin from the nucleus to AJ results in NF-κB activation, which induce target-gene expression – *e.g.* expression of cytokines, chemokines and growth factors –, and activation of cell-surfaced receptors – *e.g.* IL-1 receptor (IL-1R) and TLRs. Besides IL-6 and IL-8 expression after NF-κB activation, IL-1β is also expressed. In their work, Al-Sadi and Ma (2007) proved that this cytokine increased NF-κB activation while decreasing Occludin's expression levels without affecting ZO-1 expression, as observed in our work regarding cells exposed to purified rCRT and combined extracts. Our results strongly suggest *An*CRT involvement in TLR activation that resulted in the observed effects, since AJ and TJ protein levels differed in cells exposed to LC pollen extracts comparatively to extracts including the recombinant protein.

On that line of thought, we proceeded for quantification of other pro-inflammatory cytokines as previously referred. Our results revealed no IL-6 release from cells exposed to isolated purified rCRT, despite the release of IL-8. However, the presence of rCRT in combined extracts increased both cytokines release provoked by LC pollen extracts activities. Cells exposed to isolated purified rCRT probably released IL-6 since both cytokines are expressed upon activation of the same pathways (NF-κB, IRF and MAPK) (Kawasaki and Kawai, 2014; Kimura *et al*., 2013). However, considering all tested conditions, the maximum of released IL-6 did not surpass 1000 ρg/mL contrarily to the much higher IL-8 maximum levels (>6000 ρg/mL). Probably IL-6 was not released in sufficient levels to be detected and quantified by CBA assays. Quantification of released IL-1β would further support what the obtained results suggest. Moreover, phenotypic

characterization of A549 regarding TLR-4 receptors by intracellular immunostaining techniques, previously described by Chougule *et al*. (2012), and flow cytometry would confirm TLR-4-expression variations in cells exposed to combined extracts.

Chapter V – Conclusions and Perspectives

In concordance with current literature, our work verified that the proteolytic activity of *A. negundo*'s pollen extracts – mainly composed by metalloproteases and other zinc-dependent aminopeptidases, serine trypsin-like and probably cysteine proteases – contributes to destabilization of alveolar epithelial tissue. Conversely, our results strongly suggest that the observed effects of *A. negundo*'s pollen proteolytic activity was probably indirectly caused by proteolysis and activation of PARs rather than direct hydrolysis of transmembrane domains of intercellular proteins. Consequently, barrier disruption occurs increasing epithelial permeability to allergen crossing. Allergens are recognized by APCs which trigger adaptive immune responses, resulting in inflammation amplification. Although, additional enzymatic assays with synthetic substrates should be performed to thoroughly determine protease specificity (Bisswanger, 2014). Besides, PAR activation should be confirmed through the incubation of synthetic peptides correspondent to PARs N-terminal residues with pollen extracts, as described by Sun *et al*. (2001); or through Single-Cell Calcium Imaging to quantify cytosolic-free Ca^{2+} variations, as described by Asokananthan *et al*. (2002).

Although, our main focus was regarding Calreticulin of *A. negundo*'s pollen and its potential immunogenic effects besides the ones associated to IgE-mediated responses. We verified that isolated recombinant *An*CRT induced cellular responses probably through activation of TLR-4, since we observed slight effects on alveolar cell cultures' integrity subsequently to purified rCRT exposition. Moreover, we also observed that adding rCRT to pollen extracts resulted in increased cellular detachment and cytokine release and alterations in TJ and AJ proteins' accumulation. These results also suggest TLR-4 involvement – besides activated PAR by pollen proteolytic activity – in response to combined extracts exposure.

Specifically addressing the raised questions in the beginning of this work, the isolated partial *An*CRT protein is capable of inducing pro-inflammatory cytokines' expression and impairment of epithelial barrier integrity, possibly through interactions with cell receptors thus compromising cell adhesion processes and inflammatory responses, including T_{H2}-mediated immune responses characteristic of allergic states (Figure 27). We conclude that *An*CRT has immunogenic potential besides IgE immunoreactivity, since its presence in a context of epithelial damage exponentiates the observed effects. However, isolated *An*CRT does not provoke alarming effects on epithelial cells, which does not eliminate the hypothesis of provoking effects when framed in the airway where there are several cell types present that might induce inflammatory responses.

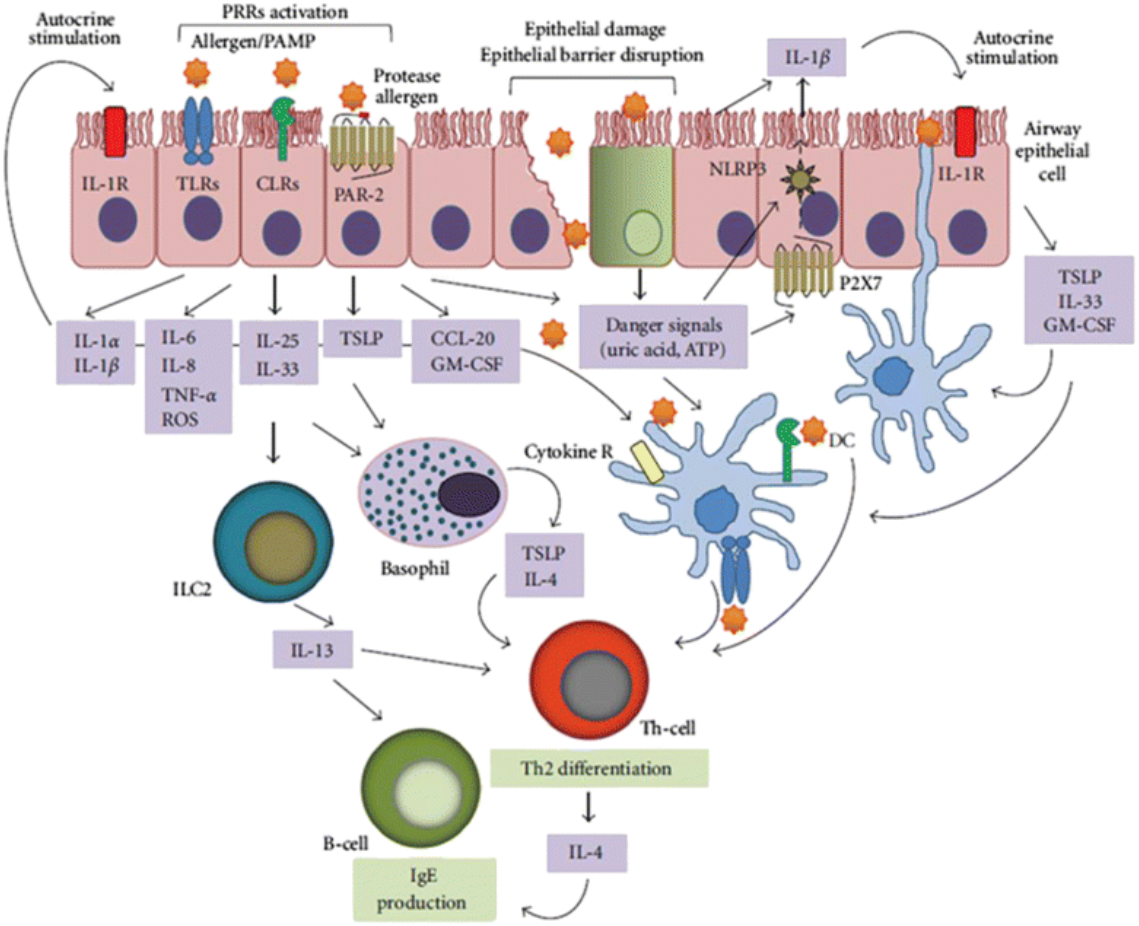

Figure 27 – Simplified model of innate immune activation by allergens exposure that activate adaptive immune responses mediated by T_{H2} cells. The induction of T_{H2}-mediated responses involves several innate immune pathways. Allergens with proteolytic activity affect receptors sensitive to proteolysis (*e.g.* PARs) and directly disrupt intercellular junctional complexes, consequently inducing the release of DAMPs and compromising epithelial barrier integrity. Moreover, other allergens with no proteolytic activity associated can lead to activation of others PRRs (*e.g.* TLRs) which can also induce the release of DAMPs and activate signalling pathways that result in pro-inflammatory cytokines expression, such as IL-1β, IL-6 or IL-8. Released cytokines and chemokines recruit and activate other immune cells that induce T_{H2} differentiation and polarized responses, which includes inducing IgE secretion by B cells to allergens that crossed the injured epithelial barrier typical of allergic reactions. Image retrieved from: Sanchez-Borges *et al*. (2017)

In subsequent works TLR-4 expression variations in cells exposed to combined extracts should be confirmed by intracellular immunostaining techniques, previously described by Chougule *et al*. (2012), and flow cytometry. Given the obtained results in immunodetection of intercellular complexes proteins, qRT-PCR using ZO-1, Occludin and E-cadherin's genes as templates could provide additional information of alterations in gene expression in response to the exogenous stimuli applied. Moreover, rCRT-TLR-4 interaction should be experimentally confirmed using a TLR blocking system, *i.e.* TLR antibodies that block binding to TLRs, and assess NF-κB activation in both situations as described by Uehori *et al*. (2003).

Our work intended to highlight the complexity of immune responses, particularly those involved in allergic reactions. The importance of identifying potentially immunogenic

proteins in total protein extracts of allergy-elicitors and characterizing their effects has been extensively referred in the literature and in our work (Asam *et al*., 2015; Gandhi and Vliagoftis, 2015; Gutowska-Owsiak and Ogg, 2017; Schulten *et al*., 2013). In some cases, it leads to identification of new allergens with undetected interactions that exacerbate the allergic reaction by non IgE-mediated mechanisms. Consequently, new therapeutics might arise from the discovery of alternative routes that initiate or intensify allergic states with possible better outcomes for unresponsive patients to existent treatment.

References

- Al-Sadi, R.M., and Ma, T.Y. (2007). IL-1β Causes an Increase in Intestinal Epithelial Tight Junction Permeability. The Journal of Immunology *178*, 4641.
- Aranda, P.S., LaJoie, D.M., and Jorcyk, C.L. (2012). Bleach Gel: A Simple Agarose Gel for Analyzing RNA Quality. Electrophoresis *33*, 366-369.
- Artimo, P., Jonnalagedda, M., Arnold, K., Baratin, D., Csardi, G., de Castro, E., Duvaud, S., Flegel, V., Fortier, A., Gasteiger, E.*, et al.* (2012). ExPASy: SIB bioinformatics resource portal. Nucleic Acids Research *40*, W597-W603.
- Asam, C., Hofer, H., Wolf, M., Aglas, L., and Wallner, M. (2015). Tree pollen allergens—an update from a molecular perspective. Allergy *70*, 1201-1211.
- Asokananthan, N., Graham, P.T., Fink, J., Knight, D.A., Bakker, A.J., McWilliam, A.S., Thompson, P.J., and Stewart, G.A. (2002). Activation of Protease-Activated Receptor (PAR)-1, PAR-2, and PAR-4 Stimulates IL-6, IL-8, and Prostaglandin E2; Release from Human Respiratory Epithelial Cells. The Journal of Immunology *168*, 3577.
- Atkinson, R.W., and Strachan, D.P. (2004). Role of outdoor aeroallergens in asthma exacerbations: epidemiological evidence. Thorax *59*, 277-278.
- Ayers, M.M., and Jeffery, P.K. (1988). Proliferation and differentiation in mammalian airway epithelium. European Respiratory Journal *1*, 58-80.
- Bacharier, L.B., and Geha, R.S. (2000). Molecular mechanisms of IgE regulation. Journal of Allergy and Clinical Immunology *105*, S547-S558.
- Bakiu, R. (2014). Calreticulin molecular evolution: a strong purifying and episodic diversifying selection result. Biologia *69*, 270-280.
- Baldan, B., Navazio, L., Friso, A., Mariani, P., and Meggio, F. (1996). Plant calreticulin is specifically and efficiently phosphorylated by protein kinase CK2. Biochemical Biophysical Research Communication *221*, 498-502.
- Basu, S., Binder, R.J., Ramalingam, T., and Srivastava, P.K. (2001). CD91 Is a Common Receptor for Heat Shock Proteins gp96, hsp90, hsp70, and Calreticulin. Immunity *14*, 303-313.
- Bedard, K., Szabo, E., Michalak, M., and Opas, M. (2005). Cellular Functions of Endoplasmic Reticulum Chaperones Calreticulin, Calnexin, and ERp57. In International Review of Cytology (Academic Press), pp. 91-121.
- Bhattacharya, J., and Matthay, M.A. (2013). Regulation and repair of the alveolar-capillary barrier in acute lung injury. Annual Review of Physiology *75*, 593-615.
- Bisswanger, H. (2014). Enzyme assays. Perspectives in Science *1*, 41-55.
- Blom, N., Gammeltoft, S., and Brunak, S. (1999). Sequence and structure-based prediction of eukaryotic protein phosphorylation sites. Edited by F. E. Cohen. Journal of Molecular Biology *294*, 1351-1362.

- Bornhorst, J.A., and Falke, J.J. (2000). Purification of Proteins Using Polyhistidine Affinity Tags. Methods in Enzymology *326*, 245-254.

- Brody, A.R., Hill, L.H., Adkins Jr, B., and O'Connor, R.W. (1981). Chrysotile Asbestos Inhalation in Rats: Deposition Pattern and Reaction of Alveolar Epithelium and Pulmonary Macrophages 1, 2. American Review of Respiratory Disease *123*, 670-679.

- Broide, D.H. (2001). Molecular and cellular mechanisms of allergic disease. Journal of allergy and clinical immunology *108*, S65-S71.

- Bruewer, M., Utech, M., Ivanov, A.I., Hopkins, A.M., Parkos, C.A., and Nusrat, A. (2005). Interferon-γ induces internalization of epithelial tight junction proteins via a macropinocytosis-like process. The FASEB Journal *19*, 923-933.

- Calderon, M.A., Linneberg, A., Kleine-Tebbe, J., De Blay, F., Hernandez Fernandez de Rojas, D., Virchow, J.C., and Demoly, P. (2015). Respiratory allergy caused by house dust mites: What do we really know? Journal of Allergy and Clinical Immunology *136*, 38-48.

- Canning, B.J., Chang, A.B., Bolser, D.C., Smith, J.A., Mazzone, S.B., McGarvey, L., and Panel, C.E.C. (2014). Anatomy and neurophysiology of cough: CHEST Guideline and Expert Panel report. Chest *146*, 1633-1648.

- Carr, T.F., Zeki, A.A., and Kraft, M. (2017). Eosinophilic and Non-Eosinophilic Asthma. American Journal of Respiratory and Critical Care Medicine. Published online: doi.org/10.1164/rccm.201611-2232PP

- Casalino-Matsuda, S.M., Monzon, M.E., and Forteza, R.M. (2006). Epidermal growth factor receptor activation by epidermal growth factor mediates oxidant-induced goblet cell metaplasia in human airway epithelium. American Journal of Respiratory Cell and Molecular Biology *34*, 581-591.

- Chandra, P.K., and Wikel, S.K. (2005). Analyzing ligation mixtures using a PCR based method. Biological Procedures Online *7*, 93-100.

- Chapman, J.A. (1986). Aeroallergens of southeastern Missouri, USA. Grana *25*, 235-246.

- Chaput, N., De Botton, S., Obeid, M., Apetoh, L., Ghiringhelli, F., Panaretakis, T., Flament, C., Zitvogel, L., and Kroemer, G. (2007). Molecular determinants of immunogenic cell death: surface exposure of calreticulin makes the difference. Journal of Molecular Medicine (Berlin) *85*, 1069-1076.

- Chen, M., Xu, J., Devis, D., Shi, J., Ren, K., Searle, I., and Zhang, D. (2016). Origin and Functional Prediction of Pollen Allergens in Plants. Plant Physiology *172*, 341-357.

- Chiang, W.F., Hwang, T.Z., Hour, T.C., Wang, L.H., Chiu, C.C., Chen, H.R., Wu, Y.J., Wang, C.C., Wang, L.F., Chien, C.Y.*, et al.* (2013). Calreticulin, an endoplasmic reticulum-resident protein, is highly expressed and essential for cell proliferation and migration in oral squamous cell carcinoma. Oral Oncology *49*, 534-541.

- Chougule, P., Herlenius, G., Hernandez, N.M., Patil, P.B., Xu, B., and Sumitran-Holgersson, S. (2012). Isolation and characterization of human primary enterocytes from small intestine using a novel method. Scandinavian Journal of Gastroenterology *47*, 1334-1343.

- Christensen, A., Svensson, K., Persson, S., Jung, J., Michalak, M., Widell, S., and Sommarin, M. (2008). Functional characterization of *Arabidopsis* calreticulin1a: a key alleviator of endoplasmic reticulum stress. Plant Cell Physiology *49*, 912-924.

- Christensen, A., Svensson, K., Thelin, L., Zhang, W., Tintor, N., Prins, D., Funke, N., Michalak, M., Schulze-Lefert, P., Saijo, Y.*, et al.* (2010). Higher plant calreticulins have acquired specialized functions in *Arabidopsis*. PLoS One *5*, e11342.

- Coppolino, M.G., and Dedhar, S. (1998). Calreticulin. International Journal of Biochemistry & Cell Biology *30*, 553-558.

- Coppolino, M.G., and Dedhar, S. (1999). Ligand-specific, transient interaction between integrins and calreticulin during cell adhesion to extracellular matrix proteins is dependent upon phosphorylation dephosphorylation events. Biochemical Journal *340*, 41-50.

- Coppolino, M.G., Woodside, M.J., Demaurex, N., Grinstein, S., St-Arnaud, R., and Dedhar, S. (1997). Calreticulin is essential for integrin-mediated calcium signalling and cell adhesion. Nature *386*, 843-847.

- Cortes, L., Carvalho, A.L., Todo-Bom, A., Faro, C., Pires, E., and Verissimo, P. (2006). Purification of a novel aminopeptidase from the pollen of *Parietaria judaica* that alters epithelial integrity and degrades neuropeptides. Journal of Allergy and Clinical Immunology *118*, 878-884.

- Crapo, J.D., Barry, B.E., Gehr, P., Bachofen, M., and Weibel, E.R. (1982). Cell Number and Cell Characteristics of the Normal Human Lung 1–3. American Review of Respiratory Disease *126*, 332-337.

- de Castro, E., Sigrist, C.J., Gattiker, A., Bulliard, V., Langendijk-Genevaux, P.S., Gasteiger, E., Bairoch, A., and Hulo, N. (2006). ScanProsite: detection of PROSITE signature matches and ProRule-associated functional and structural residues in proteins. Nucleic Acids Research *34*, W362-W365.

- De Water, R., Willems, L.N., Van Muijen, G.N., Franken, C., Fransen, J.A., Dijkman, J.H., and Kramps, J.A. (1986). Ultrastructural localization of bronchial antileukoprotease in central and peripheral human airways by a gold-labeling technique using monoclonal antibodies. American Review of Respiratory Disease *133*, 882-890.

- Duo, C.C., Gong, F.Y., He, X.Y., Li, Y.M., Wang, J., Zhang, J.P., and Gao, X.M. (2014). Soluble Calreticulin Induces Tumor Necrosis Factor-α (TNF-α) and Interleukin (IL)-6 Production by Macrophages through Mitogen-Activated Protein Kinase (MAPK) and NFκB Signaling Pathways. International Journal of Molecular Sciences *15*, 2916.

- Durek, P., Schmidt, R., Heazlewood, J.L., Jones, A., MacLean, D., Nagel, A., Kersten, B., and Schulze, W.X. (2010). PhosPhAt: the *Arabidopsis thaliana* phosphorylation site database. An update. Nucleic Acids Research *38*, D828-D834.

- Edgar, R.C. (2004). MUSCLE: multiple sequence alignment with high accuracy and high throughput. Nucleic Acids Research *32*, 1792-1797.

- Eggleton, P., Ward, F.J., Johnson, S., Khamashta, M.A., Hughes, G.R.V., Hajela, V.A., Michalak, M., Corbett, E.F., Staines, N.A., and Reid, K.B.M. (2000). Fine specificity of autoantibodies to calreticulin: epitope mapping and characterization. Clinical & Experimental Immunology *120*, 384-391.

- Enerback, L. (1986). Mast cell heterogeneity: the evolution of the concept of a specific mucosal mast cell. In Mast Cell Differentiation and Heterogeneity, Befus, D., and Bienenstock, J., eds. (Raven Press), pp. 1-26.

- Evans, M.J., Cabral, L.J., Stephens, R.J., and Freeman, G. (1973). Renewal of alveolar epithelium in the rat following exposure to NO_2. The American Journal of Pathology *70*, 175.

- Fadel, M.P., Dziak, E., Lo, C.-M., Ferrier, J., Mesaeli, N., Michalak, M., and Opas, M. (1999). Calreticulin Affects Focal Contact-dependent but Not Close Contact-dependent Cell-substratum Adhesion. Journal of Biological Chemistry *274*, 15085-15094.

- Fadel, M.P., Szewczenko-Pawlikowski, M., Leclerc, P., Dziak, E., Symonds, J.M., Blaschuk, O., Michalak, M., and Opas, M. (2001). Calreticulin Affects β-Catenin-associated Pathways. Journal of Biological Chemistry *276*, 27083-27089.

- Felsenstein, J. (1981). Evolutionary trees from DNA sequences: a maximum likelihood approach. Journal of Molecular Evolution *17*, 368-376.

- Foster, K.A., Oster, C.G., Mayer, M.M., Avery, M.L., and Audus, K.L. (1998). Characterization of the A549 Cell Line as a Type II Pulmonary Epithelial Cell Model for Drug Metabolism. Experimental Cell Research *243*, 359-366.

- Gandhi, V.D., and Vliagoftis, H. (2015). Airway Epithelium Interactions with Aeroallergens: Role of Secreted Cytokines and Chemokines in Innate Immunity. Frontiers in Immunology *6*, 147.

- Ganesan, S., Comstock, A.T., and Sajjan, U.S. (2013). Barrier function of airway tract epithelium. Tissue Barriers *1*, e24997.

- Gardai, S.J., McPhillips, K.A., Frasch, S.C., Janssen, W.J., Starefeldt, A., Murphy-Ullrich, J.E., Bratton, D.L., Oldenborg, P.-A., Michalak, M., and Henson, P.M. (2005). Cell-Surface Calreticulin Initiates Clearance of Viable or Apoptotic Cells through trans-Activation of LRP on the Phagocyte. Cell *123*, 321-334.

- Gardai, S.J., Xiao, Y.Q., Dickinson, M., Nick, J.A., Voelker, D.R., Greene, K.E., and Henson, P.M. (2003). By binding SIRP alpha or calreticulin/CD91, lung collectins act as dual function surveillance molecules to suppress or enhance inflammation. Cell *115*, 13-23.

- Gasteiger, E., Hoogland, C., Gattiker, A., Duvaud, S., Wilkins, M.R., Appel, R.D., and Bairoch, A. (2005). Protein identification and analysis tools on the ExPASy server. In: The Proteomics Protocols Handbook, Walker, J. M., ed. (Humana Press: Springer), pp. 571-607.

- Georas, S.N., and Rezaee, F. (2014). Epithelial barrier function: at the front line of asthma immunology and allergic airway inflammation. Journal of Allergy and Clinical Immunology *134*, 509-520.

- Gil, J., and Weibel, E.R. (1971). Extracellular lining of bronchioles after perfusion-fixation of rat lungs for electron microscopy. Anatomical Record *169*, 185-199.

- Goicoechea, S., Pallero, M.A., Eggleton, P., Michalak, M., and Murphy-Ullrich, J.E. (2002). The Anti-adhesive Activity of Thrombospondin Is Mediated by the N-terminal Domain of Cell Surface Calreticulin. Journal of Biological Chemistry *277*, 37219-37228.

- Gold, L.I., Eggleton, P., Sweetwyne, M.T., Van Duyn, L.B., Greives, M.R., Naylor, S.M., Michalak, M., and Murphy-Ullrich, J.E. (2010). Calreticulin: non-endoplasmic reticulum functions in physiology and disease. The FASEB Journal *24*, 665-683.

- Grainge, C.L., and Davies, D.E. (2013). Epithelial injury and repair in airways diseases. Chest *144*, 1906-1912.

- Gupta, R., Jung, E., and Brunak, S. (2004). NetNGlyc 1.0 Server: Prediction of N-glycosylation sites in human proteins.

- Gutowska-Owsiak, D., and Ogg, G.S. (2017). Therapeutic vaccines for allergic disease. npj Vaccines *2*, 12.

- Hartsock, A., and Nelson, W.J. (2008). Adherens and tight junctions: structure, function and connections to the actin cytoskeleton. Biochimica et Biophysica Acta (BBA)-Biomembranes *1778*, 660-669.

- Hassim, Z., Maronese, S.E., and Kumar, R.K. (1998). Injury to murine airway epithelial cells by pollen enzymes. Thorax *53*, 368-371.

- Heijink, I.H., van Oosterhout, A., and Kapus, A. (2010). Epidermal growth factor receptor signalling contributes to house dust mite-induced epithelial barrier dysfunction. European Respiratory Journal *36*, 1016-1026.

- Himly, M., Jahn-Schmid, B., Dedic, A., Kelemen, P., Wopfner, N., Altmann, F., van Ree, R., Briza, P., Richter, K., and Ebner, C. (2003). Art v 1, the major allergen of mugwort pollen, is a modular glycoprotein with a defensin-like and a hydroxyproline-rich domain. The FASEB Journal *17*, 106-108.

- Hollbacher, B., Schmitt, A.O., Hofer, H., Ferreira, F., and Lackner, P. (2017). Identification of Proteases and Protease Inhibitors in Allergenic and Non-Allergenic Pollen. International Journal of Molecular Sciences *18*, 1199.

- Holton, T.A., and Graham, M.W. (1991). A simple and efficient method for direct cloning of PCR products using ddT-tailed vectors. Nucleic Acids Research *19*, 1156-1156.

- Hommelgaard, A.M., Roepstorff, K., Vilhardt, F., Torgersen, M.L., Sandvig, K., and van Deurs, B. (2005). Caveolae: stable membrane domains with a potential for internalization. Traffic *6*, 720-724.

- Hong, C., Qiu, X., Li, Y., Huang, Q., Zhong, Z., Zhang, Y., Liu, X., Sun, L., Lv, P., and Gao, X.M. (2010). Functional analysis of recombinant calreticulin fragment 39–272: implications for immunobiological activities of calreticulin in health and disease. The Journal of Immunology *185*, 4561-4569.

- Honoré, B. (1996). DNA Cloning 2. A Practical Approach. Expression Systems. FEBS Letters *393*, 321-321.

- Huang, S.H., Zhao, L.X., Hong, C., Duo, C.C., Guo, B.N., Zhang, L.J., Gong, Z., Xiong, S.D., Gong, F.Y., and Gao, X.M. (2013). Self-oligomerization is essential for enhanced immunological activities of soluble recombinant calreticulin. PLoS one *8*, e64951.

- Ivanov, A.I., Nusrat, A., and Parkos, C.A. (2004). Endocytosis of epithelial apical junctional proteins by a clathrin-mediated pathway into a unique storage compartment. Molecular Biology of the Cell *15*, 176-188.

- Jeffery, P.K. (1983). Morphologic features of airway surface epithelial cells and glands. American Review of Respiratory Disease *128*, S14-S20.

- Jeffery, P.K., and Reid, L.M. (1981). The effect of tobacco smoke, with or without phenylmethyloxadiazole (PMO), on rat bronchial epithelium: a light and electron microscopic study. The Journal of Pathology *133*, 341-359.

- Jones, C.J. (2012). Epithelia: Advances in cell physiology and cell culture (Springer Science & Business Media), 358.

- Kaltreider, H.B. (1982). Alveolar macrophages. Enhancers or suppressors of pulmonary immune reactivity? Chest *82*, 261-262.

- Kasper, G., Brown, A., Eberl, M., Vallar, L., Kieffer, N., Berry, C., Girdwood, K., Eggleton, P., Quinnell, R., and Pritchard, D.I. (2001). A calreticulin-like molecule from the human hookworm *Necator americanus* interacts with C1q and the cytoplasmic signalling domains of some integrins. Parasite Immunology *23*, 141-152.

- Kato, A., and Schleimer, R.P. (2007). Beyond inflammation: airway epithelial cells are at the interface of innate and adaptive immunity. Current Opinion in Immunology *19*, 711-720.

- Kauffman, H.F., Tomee, J.F.C., van de Riet, M.A., Timmerman, A.J.B., and Borger, P. (2000). Protease-dependent activation of epithelial cells by fungal allergens leads to morphologic changes and cytokine production. Journal of Allergy and Clinical Immunology *105*, 1185-1193.

- Kawasaki, T., and Kawai, T. (2014). Toll-Like Receptor Signaling Pathways. Frontiers in Immunology *5*, 461.
- Kazuo, M., and Sumio, S. (1994). Oligo-capping: a simple method to replace the cap structure of eukaryotic mRNAs with oligoribonucleotides. Gene *138*, 171-174.
- Kelley, L.A., Mezulis, S., Yates, C.M., Wass, M.N., and Sternberg, M.J. (2015). The Phyre^2 web portal for protein modeling, prediction and analysis. Nature Protocols *10*, 845-858.
- Kheradmand, F., Kiss, A., Xu, J., Lee, S.H., Kolattukudy, P.E., and Corry, D.B. (2002). A protease-activated pathway underlying Th cell type 2 activation and allergic lung disease. The Journal of Immunology *169*, 5904-5911.
- Kimura, H., Yoshizumi, M., Ishii, H., Oishi, K., and Ryo, A. (2013). Cytokine production and signaling pathways in respiratory virus infection. Frontiers in Microbiology *4*, 276.
- Korbie, D.J., and Mattick, J.S. (2008). Touchdown PCR for increased specificity and sensitivity in PCR amplification. Nature Protocols *3*, 1452-1456.
- Koval, M. (2013a). Claudin heterogeneity and control of lung tight junctions. Annual Review of Physiology *75*, 551-567.
- Koval, M. (2013b). Differential pathways of claudin oligomerization and integration into tight junctions. Tissue Barriers *1*, e24518.
- LaFemina, M.J., Sutherland, K.M., Bentley, T., Gonzales, L.W., Allen, L., Chapin, C.J., Rokkam, D., Sweerus, K.A., Dobbs, L.G., Ballard, P.L.*, et al.* (2014). Claudin-18 deficiency results in alveolar barrier dysfunction and impaired alveologenesis in mice. American Journal of Respiratory Cell and Molecular Biology *51*, 550-558.
- Li, Y., Zeng, X., He, L., and Yuan, H. (2015). Dendritic cell activation and maturation induced by recombinant calreticulin fragment 39-272. International Journal of Clinical and Experimental Medicine *8*, 7288.
- Ling, S., Cline, E.N., Haug, T.S., Fox, D.A., and Holoshitz, J. (2013). Citrullinated calreticulin potentiates rheumatoid arthritis shared epitope signaling. Arthritis & Rheumatism *65*, 618-626.
- Ma, B., and Hottiger, M.O. (2016). Crosstalk between Wnt/β-Catenin and NF-κB Signaling Pathway during Inflammation. Frontiers in Immunology *7*, 378.
- Mao, P., Wu, S., Li, J., Fu, W., He, W., Liu, X., Slutsky, A.S., Zhang, H., and Li, Y. (2015). Human alveolar epithelial type II cells in primary culture. Physiological Reports *3*, e12288.
- Marcet, B., Libert, F., Boeynaems, J.M., and Communi, D. (2007). Extracellular nucleotides induce COX-2 up-regulation and prostaglandin E2 production in human A549 alveolar type II epithelial cells. European Journal of Pharmacology *566*, 167-171.

- Mariani, P., Navazio, L., and Zuppini, A. (2003). Calreticulin and the endoplasmic reticulum in plant cell biology. Calreticulin, 94-104.

- Martins, I., Kepp, O., Galluzzi, L., Senovilla, L., Schlemmer, F., Adjemian, S., Menger, L., Michaud, M., Zitvogel, L., and Kroemer, G. (2010). Surface-exposed calreticulin in the interaction between dying cells and phagocytes. Annals of the New York Academy of Sciences *1209*, 77-82.

- Matsumoto, K., Suzuki, A., Wakaguri, H., Sugano, S., and Suzuki, Y. (2014). Construction of mate pair full-length cDNAs libraries and characterization of transcriptional start sites and termination sites. Nucleic Acids Research *42*, e125-e125.

- Mayer, A.K., Bartz, H., Fey, F., Schmidt, L.M., and Dalpke, A.H. (2008). Airway epithelial cells modify immune responses by inducing an anti-inflammatory microenvironment. European Journal of Immunology *38*, 1689-1699.

- McKenna, O.E., Posselt, G., Briza, P., Lackner, P., Schmitt, A.O., Gadermaier, G., Wessler, S., and Ferreira, F. (2017). Multi-Approach Analysis for the Identification of Proteases within Birch Pollen. International Journal of Molecular Sciences *18*, 1433.

- Michalak, M., Groenendyk, J., Szabo, E., Gold, L.I., and Opas, M. (2009). Calreticulin, a multi-process calcium-buffering chaperone of the endoplasmic reticulum. Biochemical Journal *417*, 651-666.

- Nakagami, H., Sugiyama, N., Mochida, K., Daudi, A., Yoshida, Y., Toyoda, T., Tomita, M., Ishihama, Y., and Shirasu, K. (2010). Large-Scale Comparative Phosphoproteomics Identifies Conserved Phosphorylation Sites in Plants. Plant Physiology *153*, 1161.

- Obeid, M., Tesniere, A., Ghiringhelli, F., Fimia, G.M., Apetoh, L., Perfettini, J.L., Castedo, M., Mignot, G., Panaretakis, T., Casares, N.*, et al.* (2007). Calreticulin exposure dictates the immunogenicity of cancer cell death. Nature Medicine *13*, 54-61.

- Ober, C., and Yao, T.C. (2011). The Genetics of Asthma and Allergic Disease: A 21(st) Century Perspective. Immunological Reviews *242*, 10-30.

- Oda, K. (2012). New families of carboxyl peptidases: serine-carboxyl peptidases and glutamic peptidases. The Journal of Biochemistry *151*, 13-25.

- Oida, K., Einhorn, L., Herrmann, I., Panakova, L., Resch, Y., Vrtala, S., Hofstetter, G., Tanaka, A., Matsuda, H., and Jensen-Jarolim, E. (2017). Innate function of house dust mite allergens: robust enzymatic degradation of extracellular matrix at elevated pH. World Allergy Organization Journal *10*, 23.

- Opas, M., Tharin, S., Milner, R.E., and Michalak, M. (1996). Identification and localization of calreticulin in plant cells. Protoplasma *191*, 164-171.

- Orr, A.W., Pedraza, C.E., Pallero, M.A., Elzie, C.A., Goicoechea, S., Strickland, D.K., and Murphy-Ullrich, J.E. (2003). Low density lipoprotein receptor–related

protein is a calreticulin coreceptor that signals focal adhesion disassembly. The Journal of Cell Biology *161*, 1179-1189.

- Oseroff, C., Sidney, J., Kotturi, M.F., Kolla, R., Alam, R., Broide, D.H., Wasserman, S.I., Weiskopf, D., McKinney, D.M., Chung, J.L.*, et al.* (2010). Molecular Determinants of T Cell Epitope Recognition to the Common Timothy Grass Allergen. The Journal of Immunology *185*, 943.

- Papp, S., Fadel, M.P., and Opas, M. (2007). Dissecting focal adhesions in cells differentially expressing calreticulin: a microscopy study. Biology of the Cell *99*, 389-402.

- Pehlivan, S., Özler, H., and Bayrak, F. (2003). Pollen morphology and total protein analysis in some species of Salicaceae and Aceraceae families in Turkey. Mellifera *3*.

- Persson, S., Rosenquist, M., Svensson, K., Galvao, R., Boss, W.F., and Sommarin, M. (2003). Phylogenetic analyses and expression studies reveal two distinct groups of calreticulin isoforms in higher plants. Plant Physiology *133*, 1385-1396.

- Petersen, A., Schramm, G., Schlaak, M., and Becker, W.M. (1998). Post-translational modifications influence IgE reactivity to the major allergen Phl p 1 of timothy grass pollen. Clinical and Experimental Allergy *28*, 315-321.

- Pichavant, M., Charbonnier, A.S., Taront, S., Brichet, A., Wallaert, B., Pestel, J., Tonnel, A.B., and Gosset, P. (2005). Asthmatic bronchial epithelium activated by the proteolytic allergen Der p 1 increases selective dendritic cell recruitment. Journal of Allergy and Clinical Immunology *115*, 771-778.

- Pichavant, M., Taront, S., Jeannin, P., Breuilh, L., Charbonnier, A.S., Spriet, C., Fourneau, C., Corvaia, N., Heliot, L., Brichet, A.*, et al.* (2006). Impact of bronchial epithelium on dendritic cell migration and function: modulation by the bacterial motif KpOmpA. The Journal of Immunology *177*, 5912-5919.

- Pinto, A.M., and Todo-Bom, A. (2009). A intervenção da célula epitelial na asma. Revista Portuguesa de Pneumologia (English Edition) *15*, 461-472.

- Pohl, C., Hermanns, M.I., Uboldi, C., Bock, M., Fuchs, S., Dei-Anang, J., Mayer, E., Kehe, K., Kummer, W., and Kirkpatrick, C.J. (2009). Barrier functions and paracellular integrity in human cell culture models of the proximal respiratory unit. European Journal of Pharmaceutics and Biopharmaceutics *72*, 339-349.

- Raghavan, M., Wijeyesakere, S.J., Peters, L.R., and Del Cid, N. (2013). Calreticulin in the immune system: ins and outs. Trends in Immunology *34*, 13-21.

- Rao, R. (2009). Occludin Phosphorylation in Regulation of Epithelial Tight Junctions. Annals of the New York Academy of Sciences *1165*, 62-68.

- Ray, A., and Kolls, J.K. (2017). Neutrophilic Inflammation in Asthma and Association with Disease Severity. Trends in Immunology *17*, S1471-4906.

- Reed, C.E., and Kita, H. (2004). The role of protease activation of inflammation in allergic respiratory diseases. Journal of Allergy and Clinical Immunology *114*, 997-1008.

- Reibman, J., Hsu, Y., Chen, L.C., Bleck, B., and Gordon, T. (2003). Airway epithelial cells release MIP-3α/CCL20 in response to cytokines and ambient particulate matter. American Journal of Respiratory Cell and Molecular Biology *28*, 648-654.

- Reiland, S., Messerli, G., Baerenfaller, K., Gerrits, B., Endler, A., Grossmann, J., Gruissem, W., and Baginsky, S. (2009). Large-Scale *Arabidopsis* Phosphoproteome Profiling Reveals Novel Chloroplast Kinase Substrates and Phosphorylation Networks. Plant Physiology *150*, 889.

- Ren, H., and Suresh, V. (2014). A cell culture model for alveolar epithelial transport. PeerJ PrePrints.

- Ribeiro, H., Duque, L., Sousa, R., and Abreu, I. (2013). Ozone effects on soluble protein content of *Acer negundo*, *Quercus robur* and *Platanus* spp. pollen. Aerobiologia *29*, 443-447.

- Ribeiro, H., Duque, L., Sousa, R., Cruz, A., Gomes, C., da Silva, J.E., and Abreu, I. (2014). Changes in the IgE-reacting protein profiles of Acer *negundo*, *Platanus x acerifolia* and *Quercus robur* pollen in response to ozone treatment. International Journal of Environmental Health Research *24*, 515-527.

- Ribeiro, H., Oliveira, M., Ribeiro, N., Cruz, A., Ferreira, A., Machado, H., Reis, A., and Abreu, I. (2009). Pollen allergenic potential nature of some trees species: A multidisciplinary approach using aerobiological, immunochemical and hospital admissions data. Environmental research *109*, 328-333.

- Robinson, C., Zhang, J., and Stewart, G.A. (2008). Interactions between Allergens and the Airway Epithelium. The Pulmonary Epithelium in Health and Disease, 301-328.

- Roitinger, E., Hofer, M., Kocher, T., Pichler, P., Novatchkova, M., Yang, J., Schlogelhofer, P., and Mechtler, K. (2015). Quantitative phosphoproteomics of the ataxia telangiectasia-mutated (ATM) and ataxia telangiectasia-mutated and rad3-related (ATR) dependent DNA damage response in Arabidopsis thaliana. Molecular & Cellular Proteomics *14*, 556-571.

- Runswick, S., Mitchell, T., Davies, P., Robinson, C., and Garrod, D.R. (2007). Pollen proteolytic enzymes degrade tight junctions. Respirology *12*, 834-842.

- Saetta, M., Turato, G., Baraldo, S., Zanin, A., Braccioni, F., Mapp, C.E., Maestrelli, P., Cavallesco, G., Papi, A., and Fabbri, L.M. (2000). Goblet cell hyperplasia and epithelial inflammation in peripheral airways of smokers with both symptoms of chronic bronchitis and chronic airflow limitation. American Journal of Respiratory and Critical Care Medicine *161*, 1016-1021.

- Saitou, N., and Nei, M. (1987). The neighbor-joining method: a new method for reconstructing phylogenetic trees. Molecular Biology and Evolution *4*, 406-425.

- Sanchez-Borges, M., Fernandez-Caldas, E., Thomas, W.R., Chapman, M.D., Lee, B.W., Caraballo, L., Acevedo, N., Chew, F.T., Ansotegui, I.J., Behrooz, L., *et al.* (2017). International consensus (ICON) on: clinical consequences of mite hypersensitivity, a global problem. World Allergy Organization Journal *10*, 14.

- Schleh, C., and Hohlfeld, J.M. (2009). Aeroallergen-Lung Interactions. Particle-Lung Interactions *241*, 266.

- Schneeberger, E.E., and Lynch, R.D. (2004). The tight junction: a multifunctional complex. American Journal of Physiology-Cell Physiology *286*, C1213-C1228.

- Schulten, V., Greenbaum, J.A., Hauser, M., McKinney, D.M., Sidney, J., Kolla, R., Lindestam Arlehamn, C.S., Oseroff, C., Alam, R., Broide, D.H.*, et al.* (2013). Previously undescribed grass pollen antigens are the major inducers of T helper 2 cytokine-producing T cells in allergic individuals. Proceedings of the National Academy of Sciences of the United States of America *110*, 3459-3464.

- Schwab, M. (2008). Encyclopedia of cancer. Springer Science & Business Media.

- Scotto-Lavino, E., Du, G., and Frohman, M.A. (2007). 5' end cDNA amplification using classic RACE. Nature Protocols *1*, 2555-2562.

- Shi, F., Shang, L., Pan, B.-Q., Wang, X.-M., Jiang, Y.-Y., Hao, J.-J., Zhang, Y., Cai, Y., Xu, X., Zhan, Q.-M.*, et al.* (2014). Calreticulin Promotes Migration and Invasion of Esophageal Cancer Cells by Upregulating Neuropilin-1 Expression via STAT5A. Clinical Cancer Research *20*, 6153.

- Shin, K., Fogg, V.C., and Margolis, B. (2006). Tight Junctions and Cell Polarity. Annual Review of Cell and Developmental Biology *22*, 207-235.

- Shpacovitch, V., Feld, M., Hollenberg, M.D., Luger, T.A., and Steinhoff, M. (2008). Role of protease-activated receptors in inflammatory responses, innate and adaptive immunity. Journal of Leukocyte Biology *83*, 1309-1322.

- Silva, M., Ribeiro, H., Abreu, I., Cruz, A., and Esteves da Silva, J.C. (2015). Effects of CO_2 on *Acer negundo* pollen fertility, protein content, allergenic properties, and carbohydrates. Environmental Science and Pollution Research International *22*, 6904-6911.

- Sousa, R., Duque, L., Duarte, A.J., Gomes, C.R., Ribeiro, H., Cruz, A., Esteves da Silva, J.C., and Abreu, I. (2012). In vitro exposure of *Acer negundo* pollen to atmospheric levels of SO_2 and NO_2: effects on allergenicity and germination. Environmental Science & Technology *46*, 2406-2412.

- Stamatovic, S.M., Keep, R.F., Wang, M.M., Jankovic, I., and Andjelkovic, A.V. (2009). Caveolae-mediated Internalization of Occludin and Claudin-5 during CCL2-induced Tight Junction Remodeling in Brain Endothelial Cells. Journal of Biological Chemistry *284*, 19053-19066.

- Stone, K.D., Prussin, C., and Metcalfe, D.D. (2010). IgE, mast cells, basophils, and eosinophils. Journal of Allergy and Clinical Immunology *125*, S73-S80.

- Strasser, R. (2016). Plant protein glycosylation. Glycobiology *26*, 926-939.

- Structural Genomics, C., Architecture et Fonction des Macromolécules, B., Berkeley Structural Genomics, C., China Structural Genomics, C., Integrated Center for, S., Function, I., Israel Structural Proteomics, C., Joint Center for Structural, G., Midwest Center for Structural, G., New York Structural Genomi, X.R.C.f.S.G.*, et al.* (2008). Protein production and purification. Nature Methods *5*, 135-146.

- Sun, G., Stacey, M.A., Schmidt, M., Mori, L., and Mattoli, S. (2001). Interaction of mite allergens Der p3 and Der p9 with Protease-Activated Receptor-2 expressed by lung epithelial cells. The Journal of Immunology *167*, 1014-1021.

- Suzuki, T., Moraes, T.J., Vachon, E., Ginzberg, H.H., Huang, T.T., Matthay, M.A., Hollenberg, M.D., Marshall, J., McCulloch, C.A., Abreu, M.T.*, et al.* (2005). Proteinase-activated receptor-1 mediates elastase-induced apoptosis of human lung epithelial cells. American Journal of Respiratory Cell and Molecular Biology *33*, 231-247.

- Suzuki, Y., Yoshitomo-Nakagawa, K., Maruyama, K., Suyama, A., and Sugano, S. (1997). Construction and characterization of a full length-enriched and a 5′-end-enriched cDNA library. Gene *200*, 149-156.

- Tai, H.Y., Tam, M.F., Chou, H., Peng, H.J., Su, S.N., Perng, D.W., and Shen, H.D. (2006). Pen ch 13 allergen induces secretion of mediators and degradation of occludin protein of human lung epithelial cells. Allergy *61*, 382-388.

- Tamura, K., and Nei, M. (1993). Estimation of the number of nucleotide substitutions in the control region of mitochondrial DNA in humans and chimpanzees. Molecular Biology and Evolution *10*, 512-526.

- Tamura, K., Stecher, G., Peterson, D., Filipski, A., and Kumar, S. (2013). MEGA6: molecular evolutionary genetics analysis version 6.0. Molecular Biology and Evolution *30*, 2725-2729.

- Thelin, L., Mutwil, M., Sommarin, M., and Persson, S. (2011). Diverging functions among calreticulin isoforms in higher plants. Plant Signaling & Behavior *6*, 905-910.

- Thompson, J.D., Higgins, D.G., and Gibson, T.J. (1994). CLUSTAL W: improving the sensitivity of progressive multiple sequence alignment through sequence weighting, position-specific gap penalties and weight matrix choice. Nucleic Acids Research *22*, 4673-4680.

- Tomee, J.F.C., van Weissenbruch, R., de Monchy, J.G.R., and Kauffman, H.F. (1998). Interactions between inhalant allergen extracts and airway epithelial cells: effect on cytokine production and cell detachment. Journal of Allergy and Clinical Immunology *102*, 75-85.

- Trautmann, A., Kruger, K., Akdis, M., Muller-Wening, D., Akkaya, A., Brocker, E.B., Blaser, K., and Akdis, C.A. (2005). Apoptosis and loss of adhesion of bronchial epithelial cells in asthma. International Archieves of Allergy and Immunology *138*, 142-150.

- Uehori, J., Matsumoto, M., Tsuji, S., Akazawa, T., Takeuchi, O., Akira, S., Kawata, T., Azuma, I., Toyoshima, K., and Seya, T. (2003). Simultaneous Blocking of Human Toll-Like Receptors 2 and 4 Suppresses Myeloid Dendritic Cell Activation Induced by *Mycobacterium bovis* Bacillus Calmette-Guérin Peptidoglycan. Infection and Immunity *71*, 4238-4249.

- Villagomez, M., Szabo, E., Podcheko, A., Feng, T., Papp, S., and Opas, M. (2009). Calreticulin and focal-contact-dependent adhesion. Biochemistry and Cell Biology *87*, 545-556.

- Vinhas, R., Cortes, L., Cardoso, I., Mendes, V.M., Manadas, B., Todo-Bom, A., Pires, E., and Verissimo, P. (2011). Pollen proteases compromise the airway epithelial barrier through degradation of transmembrane adhesion proteins and lung bioactive peptides. Allergy *66*, 1088-1098.

- Walter, J.K., Castro, V., Voss, M., Gast, K., Rueckert, C., Piontek, J., and Blasig, I.E. (2009). Redox-sensitivity of the dimerization of occludin. Cellular and Molecular Life Sciences *66*, 3655.

- Wan, H., Winton, H.L., Soeller, C., Tovey, E.R., Gruenert, D.C., Thompson, P.J., Stewart, G.A., Taylor, G.W., Garrod, D.R., Cannell, M.B.*, et al.* (1999). Der p 1 facilitates transepithelial allergen delivery by disruption of tight junctions. The Journal of Clinical Investigation *104*, 123-133.

- Wang, D.Y. (2005). Risk factors of allergic rhinitis: genetic or environmental? Therapeutics and Clinical Risk Management *1*, 115-123.

- Wang, P., Xue, L., Batelli, G., Lee, S., Hou, Y.J., Van Oosten, M.J., Zhang, H., Tao, W.A., and Zhu, J.K. (2013). Quantitative phosphoproteomics identifies SnRK2 protein kinase substrates and reveals the effectors of abscisic acid action. Proceedings of the National Academy of Sciences of the United States of America *110*, 11205-11210.

- Wang, X., Gao, X.H., Zhang, X., Zhou, L., Mi, Q.S., Hong, Y., Song, B., McGovern, N., Lim, S., Tang, M.B.Y.*, et al.* (2017). Cells in the Skin. In Practical Immunodermatology, Gao X.H., and Chen. H.D., eds. (Dordrecht: Springer Netherlands), pp. 63-113.

- Wass, M.N., Kelley, L.A., and Sternberg, M.J. (2010). 3DLigandSite: predicting ligand-binding sites using similar structures. Nucleic Acids Research *38*, W469-W473.

- Waterhouse, A.M., Procter, J.B., Martin, D.M., Clamp, M., and Barton, G.J. (2009). Jalview Version 2—a multiple sequence alignment editor and analysis workbench. Bioinformatics *25*, 1189-1191.

- Weitnauer, M., Mijosek, V., and Dalpke, A.H. (2016). Control of local immunity by airway epithelial cells. Mucosal Immunology *9*, 287-298.

- Wendt, M.K., Smith, J.A., and Schiemann, W.P. (2010). Transforming growth factor-β-induced epithelial-mesenchymal transition facilitates epidermal growth factor-dependent breast cancer progression. Oncogene *29*, 6485-6498.

- Wharton, J., Polak, J.M., Bloom, S.R., Ghatei, M.A., Solcia, E., Brown, M.R., and Pearse, A.G. (1978). Bombesin-like immunoreactivity in the lung. Nature *273*, 769-770.

- Whitsett, J.A., and Alenghat, T. (2015). Respiratory epithelial cells orchestrate pulmonary innate immunity. Nature Immunology *16*, 27-35.

- Wiersma, V.R., Michalak, M., Abdullah, T.M., Bremer, E., and Eggleton, P. (2015). Mechanisms of Translocation of ER Chaperones to the Cell Surface and Immunomodulatory Roles in Cancer and Autoimmunity. Frontiers in Oncology *5*, 7.

- Wine, J.J. (1999). The genesis of cystic fibrosis lung disease. The Journal of Clinical Investigation *103*, 309-312.

- Winton, H.L., Wan, H., Cannell, M.B., Gruenert, D.C., Thompson, P.J., Garrod, D.R., Stewart, G.A., and Robinson, C. (1998). Cell lines of pulmonary and non-pulmonary origin as tools to study the effects of house dust mite proteinases on the regulation of epithelial permeability. Clinical and Experimental Allergy *28*, 1273-1285.

- Wu, X.N., Sanchez Rodriguez, C., Pertl-Obermeyer, H., Obermeyer, G., and Schulze, W.X. (2013). Sucrose-induced receptor kinase SIRK1 regulates a plasma membrane aquaporin in *Arabidopsis*. Molecular & Cellular Proteomics *12*, 2856-2873.

Supplemental material

Supplemental material 1

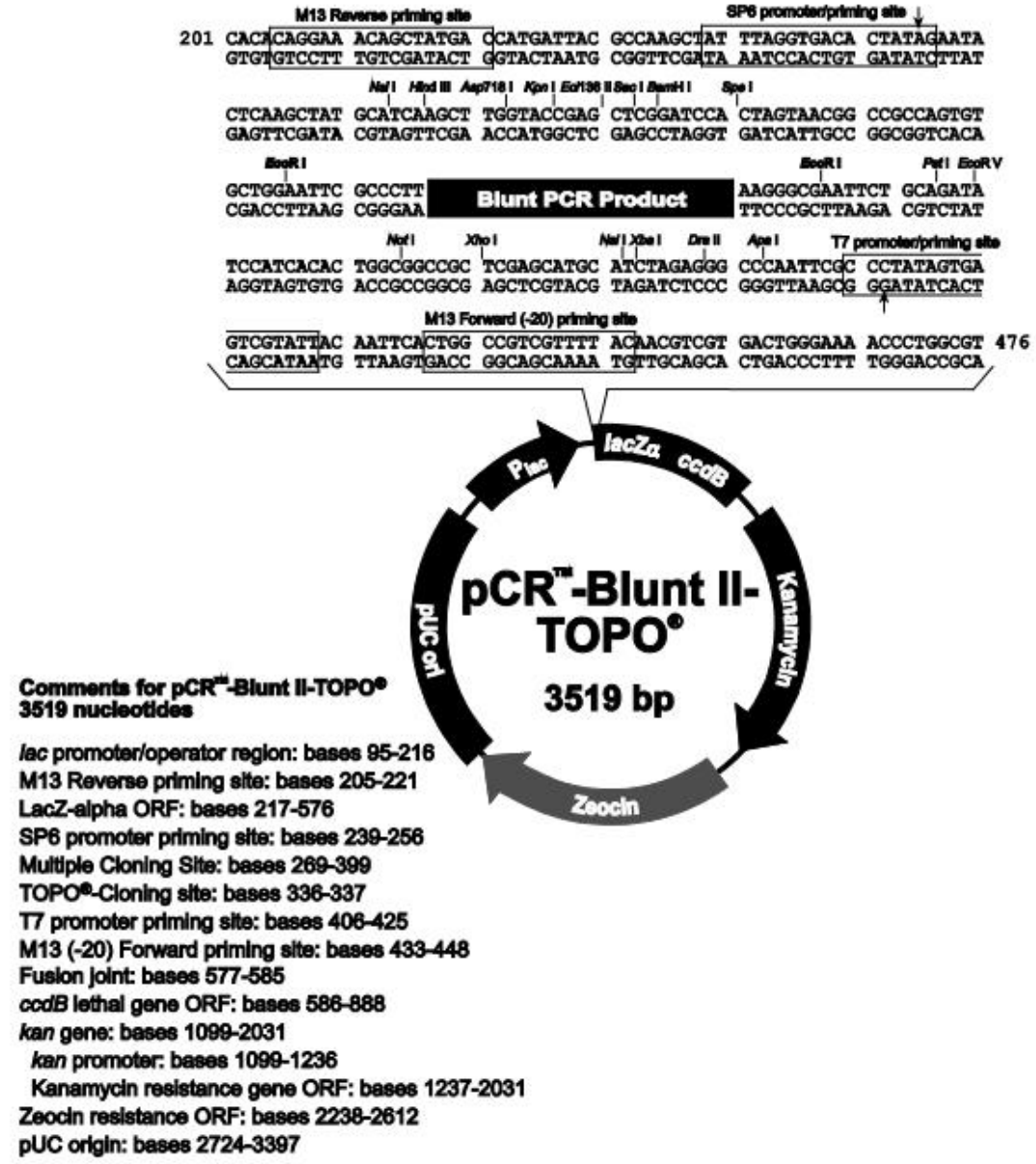

Supplemental Figure 1 - Representation of pCR™-Blunt II- TOPO® plasmid map and corresponding cloning region. It is presented pCR™-Blunt II- TOPO® plasmid map with sequence landmarks. (Retrieved from: https://assets.thermofisher.com/TFS-Assets/LSG/manuals/zeroblunttopo_man.pdf - accessed in November 2016)

Supplemental material 2

Supplemental Table 1 – pET system host *E. coli* BL21(DE3) strain characteristics. It is presented the genotype of the selected expression strain with a brief description of possible applications. Retrieved from Novagen pET system manual.

Strain	Deriv.	Genotype	Description/Application	Antibiotic Resistance
BL21(DE3)	B	F⁻ *ompT hsdS*$_B$(r_B^- m_B^-) *gal dcm* (DE3)	general purpose expression host	none

Supplemental material 3

pET-30a(+) sequence landmarks	
T7 promoter	419-435
T7 transcription start	418
His·Tag coding sequence	327-344
S·Tag coding sequence	249-293
Multiple cloning sites	
(*Nco*I - *Xho*I)	158-217
His·Tag coding sequence	140-157
T7 terminator	26-72
lacI coding sequence	826-1905
pBR322 origin	3339
Kan coding sequence	4048-4860
f1 origin	4956-5411

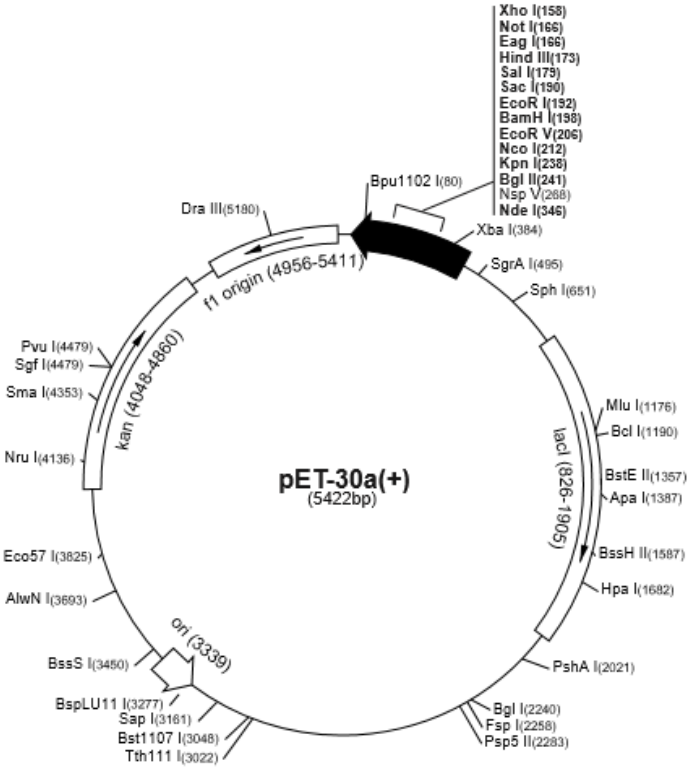

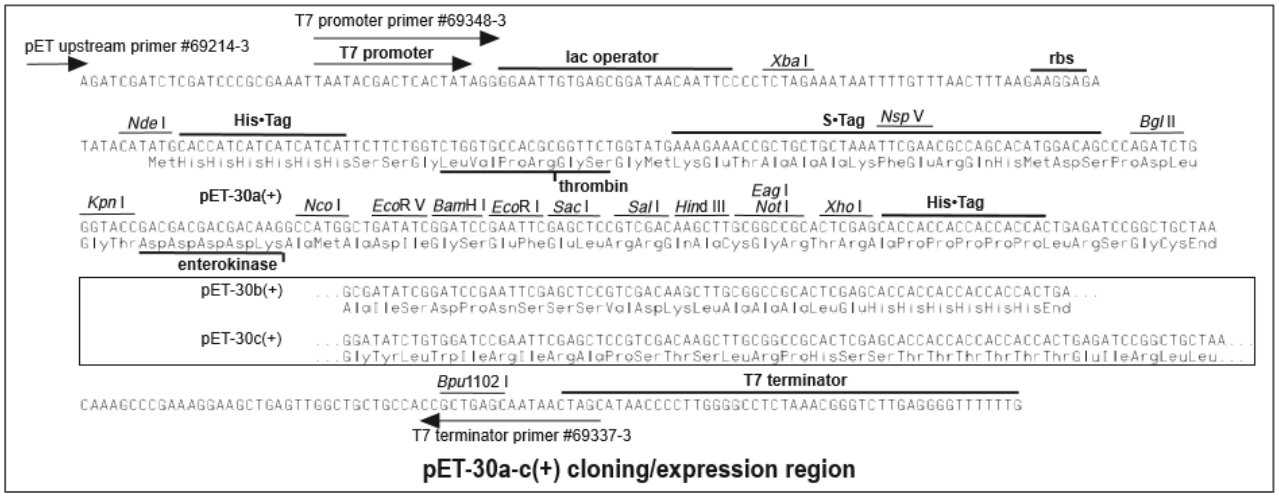

Supplemental Figure 2 – Representation of pET-30a (+) plasmid map and corresponding cloning/expression region. It is presented pET-30a (+) plasmid map with sequence landmarks. PfCRT was previously cloned between *Nde*I and *Xho*I restriction sites in frame with the His-Tag. (Retrieved from: http://www.synthesisgene.com/vector/pET-30a.pdf - accessed in January 2017)